

Probabilistic Approach for Q-based Ground Support Design

by

Ryan A. Ziebarth

Submitted in partial fulfilment of the requirements
for the degree of Masters of Applied Science

at

Dalhousie University

Halifax, Nova Scotia, Canada

August 2020

© Copyright by Ryan A. Ziebarth, 2020

Table of Contents

Table of Contents	ii
List of Tables	v
List of Figures	vi
Abstract	viii
List of Abbreviations and Symbols Used	ix
Acknowledgements	xii
Chapter 1 Introduction.....	1
1.1 Probabilistic Ground Support Design	1
1.2 Overview of Research Project	2
1.3 Organization of Dissertation	3
Chapter 2 Literature Review.....	5
2.1 Geological Uncertainty	5
2.2 Review of Q	7
2.2.1 Rock Quality Designation.....	8
2.2.2 Joint Number (J_n).....	8
2.2.3 Joint Roughness (J_r).....	8
2.2.4 Joint Alteration (J_a).....	9
2.2.5 Joint Water Reduction (J_w)	9
2.2.6 Strength Reduction Factor (SRF).....	9
2.2.7 Support Recommendation Chart.....	10
2.3 Limitations of Q.....	11
2.4 Probabilistic analysis methods in ground support design	12
2.5 Numerical Modelling of Jointed Rock Mass	13

2.6	Background of Relevant Case Studies	14
2.6.1	Overview of Norwegian Underground Olympic Stadium	14
2.6.2	Overview of Nathpa Jhakri Hydro Project.....	19
Chapter 3	Probabilistic Approach for Q-based Ground Support Design	23
3.1	Introduction.....	23
3.2	Q and the Variability in Estimating Rock Quality.....	26
3.3	Probabilistic Design Approach for Q.....	27
3.3.1	Variability in Q Input Parameters	27
3.3.2	Estimation of Distribution Types for Q Input Parameters	28
3.3.3	The MCS Method	29
3.3.4	Methodology	29
3.3.5	Q and Empirical Ground Support Requirements	31
3.4	Case Study Application of MCS for Q	31
3.4.1	Norway Underground Olympic Stadium	32
3.4.2	Nathpa Jhakri Hydro Project.....	39
3.5	FEM Analysis to Validation Ground Support Design Criterion.....	42
3.5.1	Modelling Methodology	42
3.5.2	Boundary Conditions	43
3.5.3	Rock Mass Strength Parameters	45
3.5.4	Properties of Discontinuities.....	47
3.5.5	Q_{μ} -Based Ground Support Design.....	50
3.5.6	Validation of Modelling Method	54
3.5.7	Results and Discussion	56
3.6	Conclusion	63

Chapter 4 Conclusion and Recommendations.....	65
References.....	68
Appendix A: 2019 Annual CGS Conference Paper.....	71
Appendix B: <i>MATLAB</i> Code for MCS	81

List of Tables

Table 2-1. Logged data from a geotechnical investigation of NJHP (Bhasin et al. 1995)	21
Table 3-1. Lower (LL) and upper limits (UL) for Q system rock parameters (NGI, 2015)	30
Table 3-2. Statistical data and limits for measured Q input parameters at NUOS.....	32
Table 3-3. Comparison of probabilistic and deterministic design approach calculation of Q design limits at the NUOS geological site	34
Table 3-4. Rock support recommendations based on Q_{LB} , Q_{μ} , and Q_{UB} ratings from the MCS of the NUOS site data.....	37
Table 3-5. Statistical data and limits for measured Q input parameters at NJHP	39
Table 3-6. Q input parameters for Q_{LB} , Q_{μ} , and Q_{UB} models based on results from MCS of NUOS site data	45
Table 3-7. Rock mass properties for ECR.....	46
Table 3-8. Rock mass properties for intact rock blocks in EJR	47
Table 3-9. Joint properties for EJR	50
Table 3-10. Properties for ground support elements	50
Table 3-11. Expected P_i/P_0 and u_i/u_{max} located 2 m behind tunnel face before installing of ground support	52
Table 3-12. Summary of maximum and average axial force acting on rock bolts plus a count of axial events exceeding 25% and 50% rock bolt capacity for Q_{μ} rock support in Q_{LB} , Q_{μ} , and Q_{UB} models	61

List of Figures

Fig 2-1. Tunnel behaviour chart illustrating the relationship between RMR and the in-situ stress condition to estimate the dominant mode of failure (Martin et al. 1999)	7
Fig 2-2. Q support recommendation chart with annotations to illustrate how to estimate ground support requirements (modified NGI, 2015).	11
Fig 2-3. Geotechnical logging chart for joint parameters at NUOS geological site (Bhasin, 1993).....	17
Fig 2-4. Recorded Q input parameter data for NUOS geological site (Bhasin, 1993).....	18
Fig 2-5. Excavation sequence and bolting pattern for NUOS (Bhasin, 1993)	19
Fig 3-1. Histograms of the actual measured data (inset figures) and simulated data from MCS of NUOS case history for: (a) RQD; (b) J_n ; (c) J_r ; and (d) J_a	33
Fig 3-2. PDF and CDF of Q calculated from MCS of NUOS case history data with the Q_μ (dotted line), Q_{LB} (left dashed line), and Q_{UB} (right dashed line) superimposed on rock classification zones	34
Fig 3-3. Potential failure mechanism for NUOS Q_μ and Q_{LB} rock quality based on the tunneling behaviour chart (modified Kaiser et al. 2000)	36
Fig 3-4. Q_μ (solid red line), Q_{LB} (left dashed blue line), and Q_{UB} (right dashed blue line) superimposed on the Q support recommendation chart and the PDF and CDF from the MCS of NUOS site data on top (modified from NGI, 2015).....	38
Fig 3-5. Histograms of the actual measured (inset figures) and simulated data from MCS of NJHP case history for (a) RQD; (b) J_r ; (c) J_w ; (d) J_n ; (e) J_a ; and (f) SRF	40
Fig 3-6. PDF and CDF of Q calculated from MCS of NJHP case history data with the Q_μ (dotted line), Q_{LB} (left dashed line), and Q_{UB} (right dashed line) superimposed on rock classification zones	41
Fig 3-7. Potential failure mechanism for NJHP Q_μ and Q_{LB} rock quality based on the tunneling behaviour chart (modified Kaiser et al. 2000)	41
Fig 3-8. Illustration of model mesh and boundary conditions with a theoretical horse-shoe shaped tunnel (all dimensions are in meters).....	44
Fig 3-9. Behaviour of G/G_i as s_i increases, where a rock mass with a large s_i is assumed to resemble intact rock (modified Fossum, 1985)	49
Fig 3-10. Q_μ rock support design with shotcrete liner (dashed line) and rock bolts (solid lines) (all dimensions are in meters)	51

Fig 3-11. GRC for Q_{LB} , Q_{μ} , and Q_{UB} rock masses measuring the amount of u_i experienced on the excavation boundary as internal pressure on the tunnel walls is reduced.....	52
Fig 3-12. Size of the plastic zone (bold dash line) in Q_{LB} , Q_{μ} , and Q_{UB} rock masses using the concentration of yielded joints (bold red lines)	53
Fig 3-13. Comparison of the distribution of σ_I when the model is: (a) elastic continuum – entirely ECR with Q_{μ} rock properties; (b) elastic discontinuum - EJR with high cohesion and tension; (c) elastoplastic discontinuum – EJR with Q_{μ} rock properties (dimensions are in meters)	55
Fig 3-14. Absolute horizontal and vertical u_i measured along a 40 m long <i>RS2</i> query line in the direction of the arrow (inset figures) with Q_{μ} rock support.....	57
Fig 3-15. Absolute horizontal and vertical u_i measured along a 40 m long <i>RS2</i> query line in the direction of the arrow (inset figures) without Q_{μ} rock support.....	58
Fig 3-16. Graphical representation of P (solid white bars along bolts) along rock bolts with Q_{μ} rock support in Q_{LB} , Q_{μ} , and Q_{UB} rock masses ($P_{max} = 50.2$ kN).....	60
Fig 3-17. Moment-Thrust diagram of Q_{μ} shotcrete response in Q_{LB} , Q_{μ} , and Q_{UB} rock mass with an $F = 1$ design envelope	62

Abstract

For tunnel, cavern, and shaft design, the inherent variability in a given rock mass domain makes accurately estimating rock quality and support requirements difficult. The Q system developed by Barton provides a method of quantifiably classifying rock quality. However, the input parameters are somewhat subjective and variable within a rock mass, thus introducing uncertainty. A methodology was developed incorporating a statistical analysis of measured Q input parameters and Monte Carlo Simulation (MCS) to perform a probabilistic ground support design with a measure of quantifiable uncertainty. In the statistical analysis, histograms of logged field data were used to estimate the distribution type and calculate the mean and standard deviation for each parameter, becoming the inputs for the MCS. Using the mathematical program *MATLAB*, probability and cumulative density functions were developed and used to perform a probabilistic assessment of Q and subsequent ground support. The method was applied to two case studies, illustrating the approach to estimate rock quality considering uncertainty within a given rock mass domain. Finite Element Modelling (FEM) was used to evaluate the mean Q rock support performance in a range of rock conditions for a specific case study. The Discrete Fracture Network concept was used to model the interaction of individual blocks in the rock mass, with a direct correlation to Q. The approach presents a methodology for analyzing the variability and uncertainty in a rock mass and provide insight into the design criteria for ground support in underground excavations.

List of Abbreviations and Symbols Used

CDF	Cumulative Density Function
COV	Coefficient of Variation
DFN	Discrete Fracture Network
ECM	Equivalent Continuum Model
EJM	Explicitly Jointed Model
ECR	Equivalent Continuum Region
EJR	Explicit Joint Region
ESR	Excavation Support Ratio
FEM	Finite Element Model
GRC	Ground Reaction Curve
GSI	Geological Strength Index
JCS	Joint wall compressive strength
JRC	Joint roughness condition
LDP	Longitudinal Displacement Profile
LL	Lower Limit
MCS	Monte Carlo simulation
NJHP	Nathpa Jhakri Hydro Project
NUOS	Norwegian Underground Olympic Stadium
PDF	Probability Density Function
RQD	Rock Quality Designation
SRF	Strength Reduction Factor (Q parameter)
UCS	Unconfined Compressive Strength (test name)
UL	Upper Limit

F	Factor of safety
μ	Mean
sd	Standard Deviation
Q_{LB}	Lower Bound limit of Q
Q_{μ}	Mean value of Q
Q_{UB}	Upper Bound limit of Q
D_e	Equivalent dimension (Q system)
J_n	Joint number (Q parameter)
J_r	Joint roughness (Q parameter)
J_a	Joint alteration (Q parameter)
J_w	Joint water (Q parameter)
E_i	Young's modulus of intact rock
E_{rm}	Young's modulus of rock mass
σ_c	Unconfined Compressive Strength (test value)
ν	Poisson's ratio
a	Rock mass constant (Hoek Brown constant)
D	Disturbance factor (Hoek Brown constant)
m_i	Intact rock constant (Hoek Brown constant)
m_b	Rock mass constant (Hoek Brown constant)
s	Rock mass constant (Hoek Brown constant)
β	Block shape factor
G	Rock mass shear modulus
G_i	Intact shear modulus
J_i	Joint persistence ratio

J_v	Volumetric joint count
K_n	Joint normal stiffness
K_s	Joint shear stiffness
L_i	Joint trace length
φ_j	Joint friction angle (peak)
φ_{jr}	Residual joint friction angle
φ_{jmax}	Maximum joint friction angle
s_i	Joint spacing
V_b	Block volume
σ_{1-3}	Differential stress
σ_1	Maximum principal stress
σ_2	Intermediate principal stress
σ_3	Minimum principal stress
V_p	P-wave velocity
u_i	Tunnel boundary displacement
u_{max}	Maximum tunnel boundary displacement
R_p	Radius of plastic zone

Acknowledgements

The author would like to express his sincere gratitude to the individuals that provided support and guidance throughout the project.

To Dr Andrew Corkum, it was a privilege to be under the tutelage of a supervisor with your knowledge and infectious enthusiasm. Thank you to my committee members Dr Navid Bahrani and Dr Cristian Caceres, and my colleagues Mehdi Ghodrat and Brock Jeans for their valuable input. Finally, much thanks to my wife Roan for her continued support in my pursuit of knowledge.

Chapter 1 Introduction

For decades, multiple empirical classification systems (e.g. Q, RMR, GSI) have given engineers and geologists a method to quantify the quality of a rock mass. While these methods allow an engineer to associate a single value, or narrow range, to determine the quality of a rock mass, does this accurately represent the inherent variability that exists in a rock mass domain? The relationship between the Rock Mass Rating (RMR) and in-situ stress condition presents a tool to estimate the potential failure modes (Martin et al. 1999). Furthermore, historical case study data facilitates engineers in the design process for ground support, where a current project with ground conditions and excavation dimensions similar to a past project should require similar rock support. However, while two cases may have the same rating, unique geological structures can drastically affect the productivity of the ground support. For this reason, it is essential to understand not only the entire range of possible rock qualities but what value should be considered when selecting suitable ground support. Due to the inherent uncertainty in a rock mass, applying a probabilistic design approach will more accurately estimate the ground condition and rock support requirements, based on an acceptable level of risk.

This dissertation presents a method to estimating ground support for an underground excavation using the probabilistic design approach of Q. A brief review of the probabilistic design approach for ground support, the research project, and organization of the dissertation will be discussed.

1.1 Probabilistic Ground Support Design

In a tunnel, cavern, and shaft designs, identifying the rock mass quality is essential for estimating both the dominant mode of failure and adequate ground support to manage it. Analytical design approaches (e.g. limit equilibrium) presents a deterministic method to determine support based on general estimates or a single factor of safety (F). However, the method only analyzes the stability of a single potential hazard, such as a wedge, and does not correctly represent the active reinforcement a rock bolt and shotcrete pattern create to stabilize an excavation. Empirical classification systems present a quantifiable representation of the rock mass which recommends ground support measures. Although is it advisable to place a single value that classifies the quality of an entire rock mass?

Due to the complex and varied mechanisms related to ground interaction, inherent uncertainty exists in a rock mass. If the rock structure is massive, one can expect the ground condition to be relatively consistent over the length of an excavation; however, in a jointed rock mass, this is not the case. A cluster of random discontinuities could become a systematic set of joints throughout a rock mass, or rock wall condition between joints can improve or deteriorate, effecting the rock quality. Also, certain types of rock support are more suitable than others depending on the expected failure mode. This concept highlights the importance of understanding uncertainty in a rock mass domain and all potential ground conditions.

Assessing the statistical variability of individual input parameters, an engineer can see the extreme measured values and variation of the entire dataset. Furthermore, by considering the values to be independently random, the rock quality can be calculated considering all possible combinations of input parameters. Subsequently, if multiple rock qualities are calculated, the likelihood of a particular ground condition can be determined, and an acceptable degree of risk can be associated with a design.

1.2 Overview of Research Project

To properly support an excavation, understanding the overall ground condition is essential. While rock engineering tools, such as numerical modelling software, are becoming more prevalent in the design process, empirical rock mass classification methods and ‘rule-of-thumbs’ approaches are vital to the design process. Of these classification systems, the two most widely used methods are Q (Barton et al. 1974) and RMR (Bieniawski, 1989). Both methods broadly quantify the quality of a rock mass, but inherent variability and uncertainty in the estimation of input parameters presenting the issue of incorrectly classifying the ground condition. Due to the uncertainty, a designer may select an overly conservative/costly design to reduce the potential of having inadequate support, even though a less redundant design may be sufficient to stabilize the rock mass. The idea of a stochastic approach, so that an engineer can examine uncertainty in the measured input parameters in a rock mass domain has been an area of interest. Mazzoccola et al. (1997) discussed information theory of site investigation data for RMR. Panthi (2006) studied water leakage and tunnel strain in four headrace tunnels in Nepal

using Monte Carlo Simulation (MCS). Cai (2011) presented a probabilistic design approach for GSI to analyze support performance and cavern stability. Hui et al. (2019) investigated the importance of Q input parameters and their effect on the probability density function (PDF).

This dissertation presents the use of MCS to perform a probabilistic design approach of Q to determine rock support for a tunnel, cavern, or shaft. Furthermore, it is suggested that the mean Q rating (Q_μ) should sufficiently support the entire range of possible rock qualities over the rock mass domain, and ultimately considered the design limit. Instead of a single deterministic value representing each Q input parameter, through a statistical analysis of site investigation data, an engineer can determine the statistical distribution of each parameter. From the statistical analysis, initial analysis of which parameters have the highest variability, and subsequently, the most significant effect on the overall rock quality, can be studied. The result from the statistical analysis can be used to randomly generate values in an MCS, producing the PDF and cumulative density function (CDF). The PDF and CDF present a range of all possible outcomes and the likelihood of experiencing a specific rating over the rock mass domain. Instead of designing based on conservative estimates of each input parameter, uncertainty can be considered, and the degree of risk is based on Q_μ or the probability of exceedance.

In the study, case history data from the Norwegian Underground Olympic Stadium (NUOS) and Nathpa Jhakri Hydel Project (NJHP) were used to illustrate the use of a probabilistic design approach to quantify the range of Q. Numerical modelling was implemented to validate the suggested design limits, where a discrete fracture network (DFN) was constructed to replicate the joint network at NUOS. A hypothetical tunnel with Q_μ rock support, using the results from the MCS of NUOS site data were used to determine rock strength properties, and the responses of rock support in different potential rock mass qualities (Q_μ , Q_{LB} , and Q_{UB}) was evaluated.

1.3 Organization of Dissertation

The dissertation consists of four chapters, where the bulk of the thesis content has been submitted as an article to a peer reviewed journal Rock Mechanics and Rock Engineering. Chapter 2 consists of a literature review that discusses uncertainty in a rock

mass domain and the elements that determine the Q rating and ground support recommendations. Further discussion will be on the limitations of Q, probabilistic methods in ground support design, numerical modelling of jointed rock masses, and a review of the case studies that provided data for the dissertation.

Chapter 3 presents the methodology developed to perform a probabilistic design approach to Q. The MCS was performed using the mathematical program *MATLAB*, developing PDF and CDF curves for the range of Q values at the NUOS and NJHP geological sites. The results from NUOS were used to suggest rock support requirements and numerical modelling, using the finite element model (FEM) software *RS2*, analyzed the ground support response to validate the use of Q_{μ} as a design limit.

Chapter 4 presents a conclusion of the key findings in the dissertation and recommendations for future work. Appendix A consists of the paper that was presented at the 2019 Canadian Geotechnical Society Annual Conference, which discussed the preliminary work regarding the probabilistic design approach of Q. Appendix B is a printout of the MCS code for the study, presenting the commands and general logic to perform the MCS.

Chapter 2 Literature Review

While methods are developed to characterize the quality of a rock mass, construction presents challenges due to the variability that exists. Unlike a piece of manufactured steel which meets specific load capacities, this is not the case for a rock mass, and what you see is what you get. In this section of the dissertation, the concept and past work on uncertainty and probabilistic analysis of empirical classification systems are discussed. On top of this, an overview of Q and numerical modelling of jointed rock mass will be reviewed, and an overview of two relevant case studies are presented. The topics show the key concepts discussed in the thesis, providing a piece of essential background information to accompany the thesis.

2.1 Geological Uncertainty

In subterranean projects, limited data can make identifying the ground condition before excavation difficult. Studying air photos, geological maps, and reports from adjacent sites facilitate the design process; however, until an individual is underground, it is difficult to estimate how a rock mass will react due to the high degree of uncertainty that exists. Furthermore, core samples and overcoring techniques, provide detailed information on rock characteristics and the general stress condition, but this is expensive, and at best, limited sampling can be performed.

In rock engineering, ‘data-limited’ problems make it challenging to accurately estimate the quality and composition of complex geological formations (Starfield and Cundall, 1988). Empirical rock mass classification systems (e.g. Q, RMR, GSI) broadly classify the ground condition, assuming a rock mass consists of random discontinuities producing a homogeneous rock mass (Hadjigeorgiou, 2012). Nevertheless, uncertainty exists due to the subjective nature of field investigation and the inherent variability of a rock mass domain. While an estimation of rock quality considering the rock mass to be homogeneous provides a framework to design ground support, it is advised the uncertainty in a rock mass be analyzed.

The concept of uncertainty in estimating rock mass quality using empirical classification systems has been an area of interest. The discussion of applying information theory to site data to develop probability distribution curves of RMR value

was researched by Mazzoccola et al. (1997). Not only does this present a means to analyze uncertainty in the RMR rating, but also the expected mode of failure. Fig 2-1 presents the tunnel behaviour chart developed by Martin et al. (1999), which illustrates the relationship that exists between RMR and the in-situ stress condition to estimate the dominant mode of failure. By knowing the range of possible rock quality ratings, an engineer can identify if only one dominate mode of failure is expected or multiple, which can have a drastic effect on the suggested type of rock support. The relationship between these two studies introduces the importance of stochastic analysis of empirical classification systems to select ground support more accurately. By understanding the range of possible failure modes, the most suitable support recommendation can be chosen.

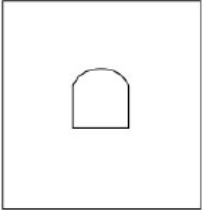
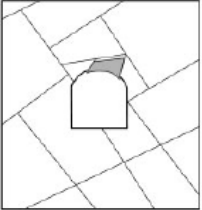
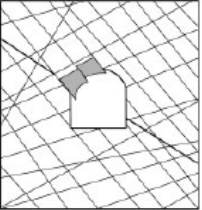

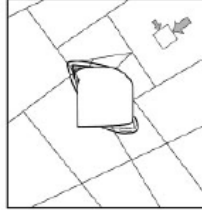
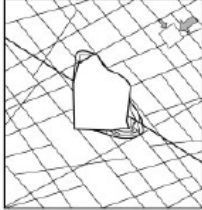

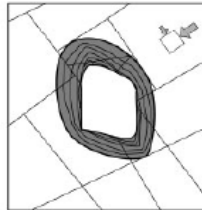
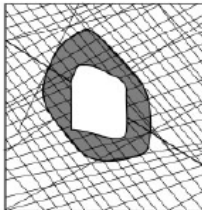
	Massive ($RMR > 75$)	Moderately Fractured ($50 > RMR > 75$)	Highly Fractured ($RMR < 50$)
Low In-Situ Stress ($\sigma_1 / \sigma_c < 0.15$)	 <p>Linear elastic response.</p>	 <p>Falling or sliding of blocks and wedges.</p>	 <p>Unravelling of blocks from the excavation surface.</p>
Intermediate In-Situ Stress ($0.15 > \sigma_1 / \sigma_c < 0.4$)	 <p>Brittle failure adjacent to excavation boundary.</p>	 <p>Localized brittle failure of intact rock and movement of blocks.</p>	 <p>Localized brittle failure of intact rock and unravelling along discontinuities.</p>
High In-Situ Stress ($\sigma_1 / \sigma_c > 0.4$)	 <p>Failure Zone Brittle failure around the excavation.</p>	 <p>Brittle failure of intact rock around the excavation and movement of blocks.</p>	 <p>Squeezing and swelling rocks. Elastic/plastic continuum.</p>

Fig 2-1. Tunnel behaviour chart illustrating the relationship between RMR and the in-situ stress condition to estimate the dominant mode of failure (Martin et al. 1999)

2.2 Review of Q

The Q system presents a means to estimate the quantity and type of ground support required. Consisting of six factors grouped into three components, Q provides a generalization of the block interaction and stress condition for a rock mass (NGI, 2015), measuring the:

- Block Size (RQD/J_n)
- Joint Condition (J_r/J_a)
- Effective Stress (J_w/SRF)

Each subgroup presents essential information required to classify the overall quality of a rock mass. Block size provides insight into how fractured the rock mass is, which has a direct relation to the potential failure modes. The joint condition represents the surface properties of the discontinuities (e.g. joint aperture, roughness, wall strength and infilling material) that increase or decrease the frictional resistance to joint shearing. Effective stress represents the stress condition, with relation to intact rock strength, including the adverse effects when water is present. With the measured input parameters Eq. 2-1 calculates the Q rating, where the rock quality, on a logarithmic scale, ranges from exceptionally poor (0.001) to exceptionally good (1000).

$$Q = \frac{RQD}{J_n} \cdot \frac{J_r}{J_a} \cdot \frac{J_w}{SRF} \quad (2-1)$$

2.2.1 Rock Quality Designation

Developed by Deere (1963), the RQD is a crude measurement of the degree of jointing in a rock mass. The RQD is a percentage ranging between 0 and 100, although an RQD of zero would cause the Q to be same; therefore, all values between 0 and 10 are set to 10 (NGI, 2015). RQD is determined by summing the lengths of the intact core, exceeding 10 cm or twice the diameter of the core sample and dividing by the total run. The size of the blocks provides a fundamental understanding of the expected mode of failure, but one must also understand joint interaction.

2.2.2 Joint Number (J_n)

RQD provides a rough estimate of the frequency of jointing occurring in a rock mass, but it is crucial to understand if these joints are random or have a general trend. J_n is a measurement of the number of occurrences where joints trend in a similar orientation, with systematic spacing, yet if a large spacing exists between the joints, they should be considered random. The measured J_n is not identical to the number of joint sets since multiple joint sets have a more significant effect on the rock mass than a single (NGI, 2015).

2.2.3 Joint Roughness (J_r)

The size of the blocks provides a fundamental understanding of the expected mode of failure, but one must also understand joint interaction. The surface structure, e.g. joint

aperture, and infilling material lying between joints has a significant effect on the frictional interaction and overall shear strength between joint contacts. The J_r is measured based on both small-scale joint waviness (rough, smooth, and slickenside), large-scale roughness (stepped, undulating, and planar), and rock wall contact during shearing. The ideal situation is discontinuous joints with rock wall contact before shear, and the least favourable is a slickenside/planar surface. In cases where infill material impedes rock wall contact, the J_r does not affect the Q rating.

2.2.4 Joint Alteration (J_a)

Reducing shear movement along the joints, due to increased friction, improves the likelihood of blocks not dislodging from the network. The presence of weaker infill material creates a less than ideal condition, allowing shearing between joint surfaces. The J_a quantifies the effects of infill material on the rock quality, where no infill material between joints is preferred; however, a coating of quartz or epidote can actually improve the ground condition (NGI, 2015).

2.2.5 Joint Water Reduction (J_w)

The existence of high and low-stress conditions in connection with pore pressure can have a positive or negative effect on stability, making it impossible to allocate inter-block effective stress (Hoek, 2007); on the other hand, a general estimation of the stress condition can be made. The inflow of water has two significant effects on the stability of a rock mass, (1) inflow can reduce the normal stress by pushing the joints apart, and (2) removal of infill material which was providing frictional resistance. It is essential to understand the potential of inflow, and not merely the current state; since water may be stored in aquifers or occur seasonally. In most cases, inflow is not a significant factor; however, in the presence of extreme inflow, the Q can be as low as 5% of the rock mass quality when in dry conditions.

2.2.6 Strength Reduction Factor (SRF)

The SRF is a comparison between the stresses acting on the rock mass and the rock strength. Four categories define the possible stress conditions, which are weak zones, competent rock with stress issues, squeezing rock, and swelling rock (NGI, 2015).

The quotient of the uniaxial compressive strength (σ_c) and the maximum principal stress (σ_1) or the maximum tangential stress (σ_θ) and σ_c , provides a way to estimate the SRF for competent rock with stress problems. The reduction value for squeezing rock similarly compares σ_θ/σ_c . While this may be true, it is time-dependent presenting issues that require experience and analysis (Palmström and Broch, 2006). On the other hand, the existence of weak zones and squeezing rock are determined based on visual evaluation. Weak zones can be identified from drilling data or by examining existing excavations to determine the size and frequency of problematic zones, which affects the overall rock quality. Swelling rock is a process related to the addition of water within the rock structure; therefore, laboratory testing is sometimes utilised to estimate the magnitude of swelling.

2.2.7 Support Recommendation Chart

The Q provides a quantitative estimation of the rock quality, based on the six rock parameters, overall providing suggestions for ground support requirements. The equivalent dimension (D_e) of the excavation is plotted against Q to provide an empirical estimate of ground support requirements. The D_e represents the relationship between the excavation size, in meters, and the Excavation Support Ratio (ESR), which is analogous to the inverse of the factor of safety (F) accounting for the design life/importance of the excavation. Comparing the Q vs ESR, a graphical ‘point’ on the chart, as seen in Fig 2-2, recommends bolt length and spacing, as well as shotcrete thickness. The bolt length and spacing are measured off the top and right axis, while the shotcrete is a zone which translates the reinforcement and thickness requirements.

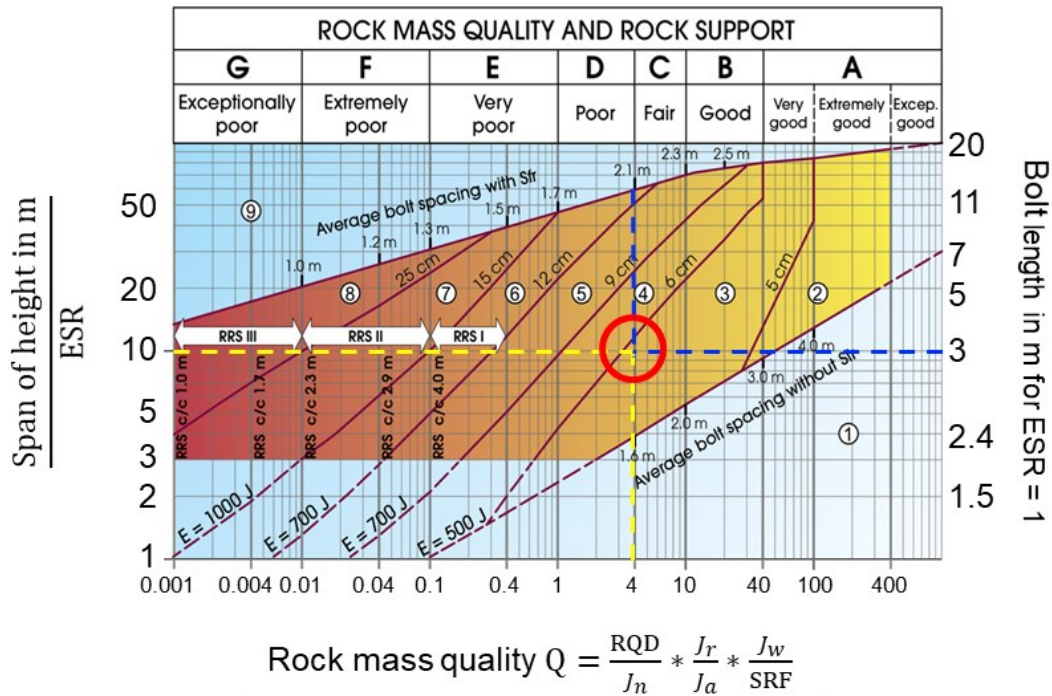


Fig 2-2. Q support recommendation chart with annotations to illustrate how to estimate ground support requirements (modified NGI, 2015).

2.3 Limitations of Q

Q introduces a method to quantify the quality of a rock mass and recommend support to stabilize an excavation, but it has been noted that limitations exist. While excavations with similar ground conditions and dimensions to a degree should be productive for both cases, this is not always true. Structurally unique situations, such as horizontally bedded Hawkesbury Sandstone, can affect the interactions of blocks. Pells (2002) discusses a case where two roof collapse events, where Q recommended support was installed, forced the design to increase the density and capacity of bolts for a cavern project. Similarly, columnar basalt in Iceland has three joint sets creating a hexagonal shape; however, failure can only occur along the axis, and it is suggested a J_n of four instead of nine should be considered, improving the Q rating (NGI, 2015). In both cases, the experience of the individual performing the site investigation is of importance. While a seasoned veteran will understand there are exceptions to the rules, an inexperienced user can produce a conservative estimate on the rock quality.

The measurement of Q input parameters is subjective and hinges both on the experience of the engineer or geologist, and how risk-adverse the individual is. Palmström and Broch (2006) noted that RQD, J_n , J_r and J_a , are prone to inaccurate estimation, which can be directly related to the experience of the user. Milne et al. (1998) comment on the advantage of Q, due to its sensitivity to minor variations in the rock properties, but inexperienced users can have a difficult time properly classifying different Q input parameters. It was noted an inexperienced user might require a long scanline to assess J_n leading to an individual to suggest a group of random joints are a joint set, reducing the Q rating. Pells (2017) discussed RQD, stating the definition of what constitutes a piece of ‘intact’ core is often interpreted differently by different practitioners, which has a direct effect on Q. Overall, inaccurate estimation of a single input parameter can have a drastic effect on the rating of a rock mass, leading to an overly conservative estimate of the ground condition, and the subsequent recommendations of ground support.

2.4 Probabilistic analysis methods in ground support design

While empirical classification systems broadly define the ground condition, the inherent variability in a rock mass domain is not quantifiable. An alternative is a probabilistic approach, where the statistical distribution of input parameters is incorporated in the design process. Cai (2011) researched the distribution of joint parameters to perform a Monte Carlo Simulation (MCS) to calculate the probability density distribution of GSI, and the point estimate method was used to analyze both the yield zone and tunnel wall deformation. Tiwari et al. (2017) further studied the probabilistic approach for GSI researching the effects of uncertainty on the post-peak strength parameters. Incorporating a probabilistic design approach to identifying the GSI can derive rock strength parameters in a finite element model improves the confidence in a ground support design.

Stochastic analysis of Q has been a topic of interest to improve the estimation of rock quality, considering uncertainty in input parameters. A statistical analysis of Q input parameters was performed by Panthi (2006) on headrace tunnels in Nepal examining water leakage and tunnel strain compared to the probability density function (PDF) calculated from an MCS of Q. Similarly, to the work of Cai (2011), both Hui et al. (2019)

and Ziebarth and Corkum (2019) discussed the application of a probabilistic design approach to Q. Hui et al. (2019) investigated the importance of the Q input parameters in relation to the PDF of Q, while Ziebarth and Corkum (2019) examined the selection process for ground support recommendations.

In the studies, it is showcased the importance of understanding the inherent uncertainty that exists in a rock mass. Both the estimate of ground condition and rock support should incorporate a stochastic assessment of the rock characteristics to perform a probabilistic design approach. By estimating the shape of the statistical distribution and calculating the mean (μ) and standard deviation (sd) with Eq. 2-2 and 2-3 instead of merely selecting a single deterministic value for each input parameter, the entire range of possible Q ratings can be assessed.

$$\mu = \frac{1}{n} \sum_{i=1}^n x_i \quad (2-2)$$

$$sd = \sqrt{\frac{\sum_{i=1}^n (x_i - \mu)^2}{n-1}} \quad (2-3)$$

2.5 Numerical Modelling of Jointed Rock Mass

In rock mechanics, numerical modelling has become increasingly common in the design process for geotechnical projects. Continuum models incorporate the Hoek-Brown, Mohr-Coulomb, or another failure criterion to ‘smooth/smear’ the rock properties to act as a continuous material equivalent to the overall jointed rock mass. The results of a continuum model provide insight into the way a rock mass will react. However, this type of model does not accurately simulate the block interaction, which is a critical factor of a jointed rock mass. Joints can reduce the overall strength of a rock mass, and it is essential to understand how the orientation of joints affect the stability of a rock mass. As was seen with columnar basalt in Iceland, three joint sets are present, but the direction of the joints suggest the third joint set is not overly problematic. Instead of a simple continuum model, the discrete fracture network (DFN) concept introduces a method to simulate a jointed rock mass more accurately.

The concept of constructing a fracture network has been discussed by multiple researchers, including Andersson et al. (1984), He et al. (2018), Farahmand et al. (2018),

Grenon and Hadjigeorgiou (2003), and Mas Ivars et al. (2011). In a DFN, the statistical data of the joint orientation, persistence, and spacing from a geological survey creates a fictitious fracture network. By modelling a network of discontinuities, a plethora of information can be gathered, such as the average block size which has a direct relation to the spacing of rock bolts (Hoek, 2007).

The DFN creates a framework of discrete fractures; however, joint strength parameters are required to simulate the interaction of blocks. While Q quantifies the quality of a rock mass, this value is not a strength or stiffness parameter, but a relationship does exist between Q input parameters and GSI, seen in Eq. 2-4. Calculating the GSI from Q , rock mass strength parameters can be calculated from the Hoek-Brown failure criterion. Additionally, the joint strength and stiffness parameters can be related to the J_r and RQD calculated in the MCS. Understanding how blocks interact allows an engineer to analyze problematic areas where wedges can develop, and the rock mass can be modelled as an elastoplastic material where the joints can fail.

$$GSI = \frac{52 J_r / J_a}{(1 + J_r / J_a)} + RQD / 2 \quad (2-4)$$

2.6 Background of Relevant Case Studies

For the study, data from two case histories were examined to illustrate the use of the probabilistic design approach for Q . Palmström and Broch (2006) noted the ideal conditions for Q are a moderately jointed rock mass. For this reason, the Norwegian Underground Olympic Stadium (NUOS) was selected. The second case was the Nathpa Jhakri Hydro Project (NJHP), which is a jointed rock mass. However, it is anisotropic, introducing different issues, which must be examined.

2.6.1 Overview of Norwegian Underground Olympic Stadium

Located 25 km south of Lillehammer in Gjøvik city, Norway, the ice hockey cavern was constructed in 1993. The design consisted of a two-phase site investigation that facilitated the construction of a cavern spanning 62 m, with a length of 91 m and a height of 24 m, making it the largest cavern for public use at its time.

The initial site investigation was analyzing the adjacent rock caverns and access tunnels. The Precambrian gneiss, from the nearby caverns that shared the same hill,

determined the rock mass to have a high frequency of jointing. However, the discontinuities were identified to be irregular with rough-walls, and the dip and strike were quite variable. Concerning the persistence of joints, more extended continuous joints had large spacing, and for the most part, the discontinuities were determined to have low persistence, and the joint walls were rough with little clay infill. Based on the findings, it was noted that the geological conditions were potentially favourable for a large spanning cavern (Bhasin, 1993). While the initial study presented positive initial findings, a more in-depth analysis of the actual geological site was required.

In the second phase of the investigation, four core samples were drilled by the consulting firm NOTEBY, based out of Oslo, Norway. From the core samples, five different joint sets were identified; however, these were not all in the same location and identified as sporadic at best. The cores found the typical coating was rust stains, epidote, and quartz, and the surface was usually rough and undulating. Concerning the RQD, the samples ranged between 70-85%. Overall, the poorest Q rating was measured to be 1.1, while the weighted average was 12, and the best case was 30, seeing the potential rock qualities to range from poor to good.

During construction, geotechnical data were collected from 35 areas, and the histograms of measured Q input parameters and joint properties are illustrated in Fig 2-1 and 2-2. From the analysis, it was found that the joint spacing (s_j) was 0.2 m and joint length ranged between 2-5 m. The joint roughness coefficient (JRC) ranged between 6 and 8, and the joint compressive strength (JCS) was between 50 and 100 MPa. It was noted in the study, the collection of the data from different areas introduces the ability to manipulate the data and considered different combinations of Q input parameters. From the 35 test locations, the mean RQD was between 60-70%, and it was measured, three joint sets were expected, producing a J_n of 9. For the joints, they were identified to be smooth to rough and undulating with no infill, with an expected J_r of 2 to 3 and a J_a of 1. Ultimately, for the site, the mean Q rating was determined to be 9.4, classifying the rock mass as fair to good.

Following the classification of the rock quality, other geotechnical investigation techniques were implemented. SINTEF (the Foundation for Scientific and Industrial

Research in Trondheim, Norway) and NGI (Norwegian Geotechnical Institute) performed overcoring and hydraulic fracturing to measure the in-situ stresses. From the analysis, the σ_1 , intermediate principal stress (σ_2), and minimum principal stress (σ_3) were measured to be 3.5 MPa, 2 MPa, and 1 MPa, where σ_1 was oriented north-south, σ_2 was east-west, and σ_3 was vertical. On top of the in-situ stresses, Bhasin (1993) introduced a relationship to calculate the rock mass modulus (E_{rm}) and P-wave velocity (V_p) from Q using Eq. 2-5 and Eq. 2-6.

$$V_p = 1000 \log Q + 3500 \text{ (m/s)} \quad (2-5)$$

$$E_{rm} = \left(\frac{V_p - 3500}{40} \right) \text{ (GPa)} \quad (2-6)$$

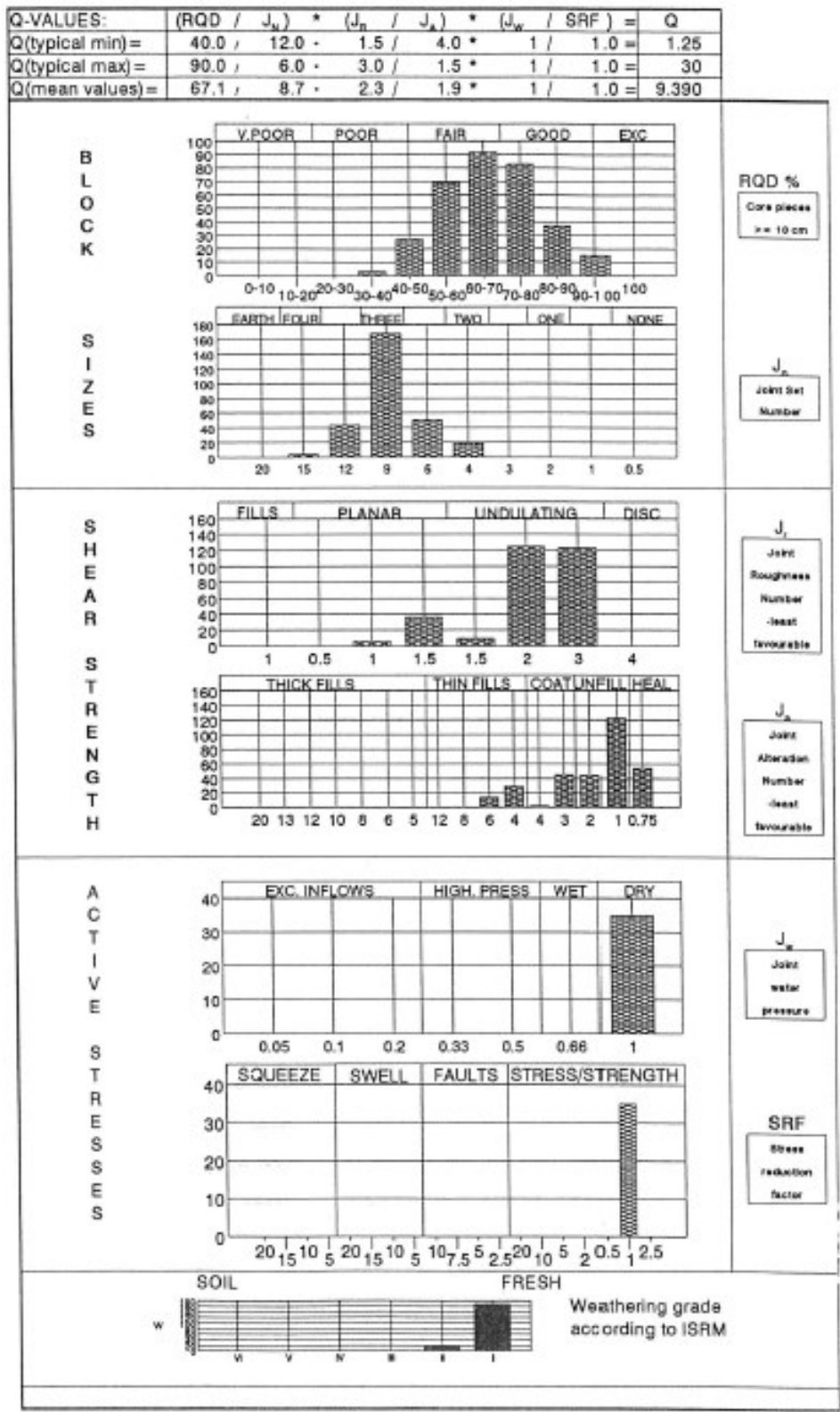


Fig 2-4. Recorded Q input parameter data for NUOS geological site (Bhasin, 1993)

For construction, drilling and blasting techniques were implemented, and occasionally presplitting techniques were used to control damage to the adjacent rock. Due to the sheer size of the excavation, the nearest support category for Q was 1.5 m to 2 m bolt spacing with 100 mm of fibre-reinforced shotcrete. For the design, a combination of untensioned fully grouted rebar and cable bolts were installed. The bolt pattern selected was a combination of 25 mm thick 6 m long rebar bolts in a 2.5 m by 2.5 m pattern and 12 m long twin-stranded 12.5 mm cable bolts in a 5 m by 5 m pattern. Fig 2-3 illustrates both the bolt pattern and the excavation sequence for the design.

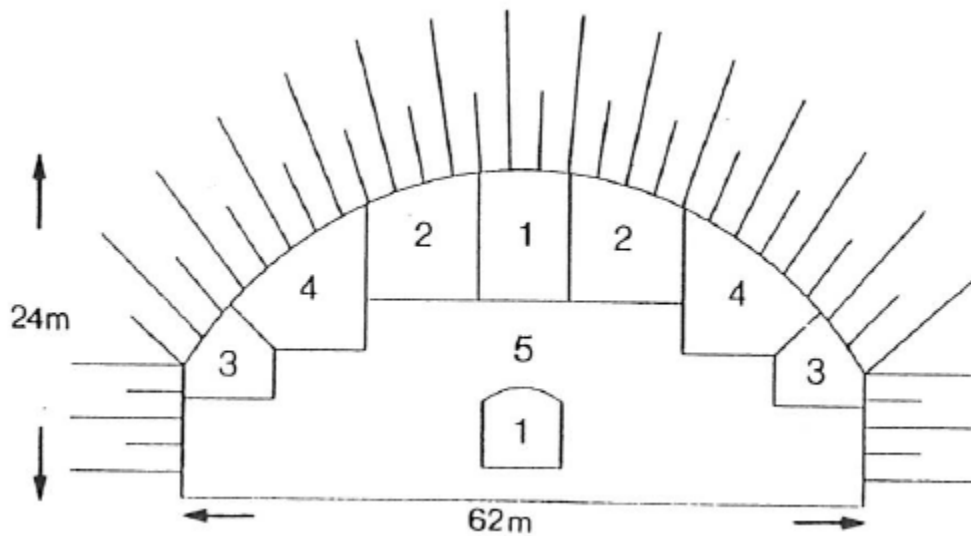


Fig 2-5. Excavation sequence and bolting pattern for NUOS (Bhasin, 1993)

Extensometers were installed in the roof to measure displacement. The instruments measured a maximum displacement of 8.2 mm at the centre of the cavern, which matches well with the results from numerical modelling ranging from 4 to 8 mm. The design illustrates the use of Q to determine support requirements; however, in this case, due to the size of the cavern, engineering judgement was used instead of the recommended Q support.

2.6.2 Overview of Nathpa Jhakri Hydro Project

Located in the Himalayan regions of northern India between 77° and 78° longitude and 31° and 32° latitude, NJHP is a massive 27.3 km long headrace tunnel with a 10.15 m diameter, a 942,000 m³ underground desilting complex, and a 20 m by 49 m by 216 m

powerhouse. Not only the size of the project but also be situated in low strength anisotropic rock introduced difficulties in the design.

For the study, laboratory testing was used to measure rock mass properties, and the Q system was implemented to classify the rock mass quality and estimate ground support requirements. The site consists of jointed Precambrian metamorphic rocks including gneisses, schists, gneissose schists, amphibolites, granite and pegmatites. In the investigation, in the weaker rock (predominately schist), five different joint sets were encountered; however, only three or three plus some random joints were present at a single location. For the granite material, the rock mass was massive with little jointing.

For the classification of the anisotropic rock, a micro-petrographic description was implemented. In the analysis, high clay/mica content was found, ranging from 19% to 44%, which played a significant role in the reduced strength of the rock mass. Furthermore, scanning electron micrographs found features of fracture planes and mineral grains in the schists, having some bearing on the strength of the rock mass.

An EPE Helium Expansion Porosimeter was used to measure specific gravity, density, water absorption, and porosity of core samples. A uniaxial compression test measured the σ_c of a core sample with oven-dried samples ranging between 17-35 MPa and saturate samples seeing a σ_c half that of the dry specimen.

For the classification of rock quality using Q, the focus was placed on the powerhouse cavern. In the assessment, the Q rating ranged from 0.15 (very poor) to 10 (fair/good). A geotechnical site investigation was performed, based on five core drill holes and a 7 m by 7 m by 216 m pilot tunnel. From the core samples, two joint sets were identified with rough undulating surfaces. The RQD measured from the cores ranged from 20% to 100%, where the most typical measurement was 70%. For the infill, most joints had a coating of rust stains, chlorite, and quartz. In the pilot tunnel, the exposed rock was dark grey schist with biotite rich regions. The assessment of Q input parameters was based on a 10 m stretch of tunnel. The Q rating ranged from 0.73 (very poor) to 32 (good), with a weighted average of 2.7. The analysis shows the rock mass is of poor quality, and it was suggested that support installation is required after each excavation

step. Table 2-1 presents all the logged data from the site investigation for both the measured Q input parameters and the joint properties.

Table 2-1. Logged data from a geotechnical investigation of NJHP (Bhasin et al. 1995)

Parameter	Unit	Range	Mean/wt average
RQD	-	50 - 80	69.5
J_n	-	3 - 6	5.2
J_r	-	2 - 3	2.6
J_a	-	1 - 3	2.6
J_w	-	0.66 - 1.0	0.96
SRF	-	2.5 - 5.0	4.9
Q	-	0.73 - 32.0	2.7
s_j	m	0.1 - 0.2	0.19
L_i	m	5 - 10	7.22
J_v	-	3 - 10	8.7
JRC	-	2 - 8	5.7
ϕ_{jr}	°	22 - 26	24.5
JCS	MPa	25 - 50	37.85
σ_c	MPa	20 - 50	35
σ_l	MPa	5 - 10	7.15

The in-situ stress for the project was measured using a combination of overcoring and hydraulic fracture testing. From the hydraulic fracture test, the σ_1 and σ_3 were the maximum and minimum horizontal stresses with σ_1 measured to be 7.14 MPa with an azimuth of N 30° E, and σ_3 was 3.93 MPa with an orientation N 60° W. The vertical stress was σ_2 measured to be 5.89 MPa. The results from the overcoring techniques saw higher readings with a σ_1 of 13.15 MPa (N-S), a vertical σ_2 of 8.00 MPa, and a σ_3 of

4.36 MPa (E-W). Due to the overcoring results being reliant on the assumption of a linear elastic and isotropic rock mass, the results from the hydraulic fracturing were considered for the design (Bhasin, 1995).

Bhasin (1995) developed a numerical model utilizing the results from the geotechnical investigation to gain insight into how the rock mass will react to construction. Prior to bolt installation, the wall displacement was measured, and it was found that the maximum displacement of 43.5 mm was experienced on the left wall. In the model, both 6 m and 12 m bolts with 3 m spacing were in the ground support design, but the fibre-reinforced shotcrete was not included in the model, which will help stabilize smaller blocks at the tunnel boundary. In the analysis, bolts in the crown and lower wall reach the maximum yield limit, and in the case study, it is suggested higher capacity bolts or tighter bolt spacing was required. Overall, the study illustrates the use of Q to provide support recommendations for an excavation; however, as suggested by Palmström and Broch (2006), there is a sweet spot for Q which to a degree makes the estimations less than ideal for large caverns.

Chapter 3 Probabilistic Approach for Q-based Ground Support Design¹

3.1 Introduction

Although rock engineering tools, such as computer modelling simulations, are becoming increasingly common in rock engineering design, empirical rock mass classification and ‘rules-of-thumb’ approaches still play an essential part in the design process. In rock mechanics, ‘data-limited’ problems exist, presenting difficulty in accurately estimating the quality and composition of complex geological formations (Starfield and Cundall, 1988). Empirical classification systems (e.g. GSI, RMR and Q) broadly quantify the quality of the rock mass; however, deterministic design approaches do not always correctly identify the inherent variability and uncertainty that exists within a given rock mass domain (a region of similar rock mass conditions). The use of conservatively selected input parameters is a subjective means of addressing this issue. One challenge of this approach is that it has long been recognized that using conservative estimates of multiple individual input parameters in combination can create the potential for excessively conservative parameters and the overestimation of ground support requirements. Moreover, it can be difficult to truly assess how conservative such estimates might really be.

In the preliminary stage of ground support design for underground excavations, classification systems such as Q (Barton et al. 1974) present a means to quantify the quality of a rock mass. While a helpful tool, it is acknowledged that inherent uncertainty exists in empirical design methods, both due to the subjective nature of field mapping, and the intrinsic variability in rock properties. Allocating a single value to characterize a Q input parameter has the potential to produce a misleading classification of the entire rock domain and affect the overall rock quality and recommended ground support. Instead, using a probabilistic approach could address some of the uncertainty that exists, allowing design considerations to be based on a quantifiable and holistic view of the rock mass.

¹ A version of this chapter has been submitted to Rock Mech Rock Eng.

Q is a powerful tool, but it has its limitations. In structurally unique situations, such as horizontally bedded Hawkesbury Sandstone, Pells (2002) notes a case where an increase in the density and capacity of bolts for a cavern project was required due to two roof collapse events with the recommended Q rock support. Palmström and Broch (2006) noted the input parameters representing block interaction, RQD, J_n , J_r and J_a , are particularly prone to inaccurate estimation, which can be directly related to the experience of the user and the difficulty in classifying different Q input parameters (Milne et al. 1998). Furthermore, an inaccurate estimation can be related to how the Q parameters are measured, such as RQD, where the definition of what constitutes a piece of 'intact' core is often interpreted differently by different practitioners, affecting the rating (Pells, 2017). An empirical analysis is somewhat subjective and reliant on the capabilities of the investigator, and the validity of the subsequent recommendations is only as good as the data collected.

Mazzoccola et al. (1997) discussed information theory of site investigation data, where PDF curves illustrate the distribution of RMR, introducing the concept of uncertainty in a rock mass, and the means to evaluate it in an underground excavation design. Panthi (2006) implemented a probabilistic analysis of Q by performing Monte Carlo Simulation (MCS) on data from four headrace tunnels in Nepal to estimate water leakage and tunnel strain. Cai (2011) presented the use of probabilistic design for GSI, combined with numerical modelling to analyze support performance and cavern stability. Hui et al. (2019) applied MCS to Q to investigate the importance of input parameters and their effect on the PDF of Q. However, to date, a standard has not been suggested for the statistical level of risk that should be applied for ground support design using Q. Rock quality affects support requirements, but when a single value quantifies the quality of the rock mass, should the mean (μ), or a different statistical value of Q or its input parameters, be used as the design criteria?

This paper, a continuation of the work by Ziebarth and Corkum (2019), presents a methodology of more accurately estimating Q through the statistical analysis of measured input parameters and a probabilistic design approach to determine rock quality and ground support requirements. In problems where randomness exists in input parameters, the MCS is a viable method to calculate the probability (PDF) and cumulative density

functions (CDF). In the methodology presented in this study, histograms of the logged Q input parameter data from a field study were analyzed to estimate the distribution and calculate the mean (μ) and standard deviation (sd). The information from the statistical analysis was used to perform MCS using the mathematical program *MATLAB*. The PDF and CDF calculated from the MCS allow an engineer to utilize a probabilistic design approach to determine the most suitable ground support. Specific point estimate values from the PDF were considered for the design, ultimately selecting the mean Q (Q_μ) rock support as the design criterion.

Implementing Q_μ rock support reduces the chance of an overly conservative estimate for ground control. However, the suitability of ground support type (e.g., rock bolt type) required is dictated by the expected mode of failure (e.g., wedge instability or weak rock shearing), and if the Q_μ rock support is not capable of supporting or reinforcing the poorer rock mass a more conservative estimation may be required. While, suggesting a more conservative design ensures all failure modes are supported, increasing the quantity of rock support provides no accurate measurement of its effectiveness. Numerical modelling was used to analyze the ground support response in different ground conditions, presenting a means to validate the use of Q_μ rock support as the design criterion. Similarly, to work by He et al. (2018), the Discrete Fracture Network (DFN) concept was used to provide a framework for modelling of the discontinuities. Three different rock masses were modelled representing Q_μ and upper (Q_{UB}) and lower (Q_{LB}) bounds comparing the response of ground support to a wide range of potential rock qualities. Joint strength parameters for the rock mass were calculated from Q, and the Finite Element Model (FEM) program *RS2* was used to simulate tunnel wall displacement (u_i) and rock support response in different ground conditions. Data from the Norwegian Underground Olympic Stadium (NUOS) and Nathpa Jhakri Hydel Project (NJHP) was used to illustrate the use of a probabilistic design approach to quantify the range of Q. The results from the MCS of NUOS were applied to a hypothetical tunnel to evaluate the response of the recommended ground support in different potential rock mass qualities (Q_μ , Q_{LB} , and Q_{UB}). Through this method, the raw measured geotechnical data provides a means to properly consider the uncertainty in individual rock properties and improve the estimation of ground support design.

3.2 Q and the Variability in Estimating Rock Quality

The Q system presents a means to estimate the quantity and type of ground support required. Consisting of six factors grouped into three components, Q provides a generalization of the block interaction and stress condition for a rock mass (NGI, 2015). Each subgroup presents essential information required to classify the overall quality of a rock mass. Block size (RQD/J_n) provides insight into how fractured the rock mass is and its potential failure modes. The joint condition (J_r/J_a) represents the surface properties of the discontinuities (e.g. joint aperture, roughness, wall strength and infilling material) that increase or decrease the frictional resistance to joint shearing. Effective stress (J_w/SRF) represents the stress condition, with relation to intact rock strength, including the adverse effects when water is present. Using Eq. 3-1, Q rates the rock quality on a log scale, ranging from exceptionally poor (0.001) to exceptionally good (1000). The equivalent dimension (D_e) of the excavation is plotted against Q to provide an empirical estimate of ground support requirements. The graphical ‘point’ on the Q chart recommends bolt length and spacing, as well as shotcrete thickness. The D_e represents the relationship between the excavation size, in meters, and the Excavation Support Ratio (ESR), which is analogous to the inverse of factor of safety (F) accounting for the design life/importance of the excavation.

$$Q = \frac{RQD}{J_n} \cdot \frac{J_r}{J_a} \cdot \frac{J_w}{SRF} \quad (3-1)$$

In cases where the stress condition or block framework resemble excavations on which the empirical basis was developed, the assumption of similar support requirements holds merit. Although no two cases are identical, and many elements can create uncertainty in the estimation of rock quality including, inadequate geological investigation, complex geology at depth with limited access, and the level of experience of the investigator (Panthi, 2006). Additionally, a degree of variability exists within the case histories database on which the Q ground support design is based, but this aspect is unquantifiable. In the empirical method, scaling the design for ground support to the D_e (akin to F) creates an unclear relationship to Q, and to some degree accounts for uncertainty.

Since Q was introduced in 1974, two revisions have been presented, with the addition of ground support data from almost 2000 case histories in Norway, Switzerland and India (NGI, 2015). The introduction of this data increases confidence in the recommended support and application of new support methods that were not commonly used in past versions. When calculating Q, multiple conservative estimations of an input parameter can lead to the mischaracterization of rock quality. While an extreme measurement, poor or favourable, can exist for an input parameter, the range of possible data is not infinite. For this reason, upper (UL) and lower limits (LL), from the Norwegian Geotechnical Institution (NGI) handbook, set the range for the Q input parameters during the geotechnical investigation. While limiting the spread of the input values reduces the chance of estimating an extreme unrealistic value, it is vital to know the statistical distribution of the data obtained from field mapping. A normal distribution has a symmetrical shape, while a skewed normal or lognormal distribution results in data concentrated to one side of the distribution. Selecting the most suitable distribution for each input parameter ensures an accurate estimation of the field data in a random number generation and the overall Q.

3.3 Probabilistic Design Approach for Q

In any location along the length of a tunnel, cavern or shaft, variability exists in the properties that define the rock mass. A designer can select a specific value to quantify a Q input parameter, but does this accurately estimate that characteristic over the entire rock mass domain? A statistical analysis of the individual input parameters presents the spread of data, and the statistical distribution, μ and sd build the framework for an MCS to perform a probabilistic design approach.

3.3.1 Variability in Q Input Parameters

To analyze the variability that exists in rock properties, a statistical analysis of the Q input parameters presents valuable information on the distributive shape of field data. In this method, the estimated distribution type for each input parameter is determined by analyzing the histograms of the logged data from the geotechnical investigation, and the μ and sd , are calculated using Eq. 3-2 and Eq. 3-3. With the μ , sd , and distributive shape, the PDF can be simulated for each Q input parameter, to perform MCS for Q.

$$\mu = \frac{1}{n} \sum_{i=1}^n x_i \quad (3-2)$$

$$sd = \sqrt{\frac{\sum_{i=1}^n (x_i - \mu)^2}{n-1}} \quad (3-3)$$

Panthi (2006) applied this statistical method to Q input data from four headrace tunnel cases in Nepal, and it was found that the shape of the distribution for each input parameter was not the same from case to case. For this reason, a statistical analysis of field data should be developed and scrutinized for each case, and the most suitable distribution type (e.g., normal, lognormal) for each input parameter must be identified.

3.3.2 Estimation of Distribution Types for Q Input Parameters

While the distributive shape of the data for an input parameter can vary from case to case, to a certain degree, a specific ‘type’ of distribution can be expected. A relationship exists between the spacing of discontinuities and the RQD, and research by Priest and Hudson (1976) and Sen and Kazi (1984) suggests that joint spacing follows a negative exponential distribution, which translates to the characteristics of the RQD distribution. Onsel et al. (2011) found the RQD to follow a lognormal and negative exponential distribution from collected core data, while the distribution was estimated to be normal in most cases and lognormal in poor rock conditions by Panthi (2006). Logged field data measurements from studies by Panthi (2006), Bedi (2013), and Panthi and Nilsen (2010) suggested J_n follows a triangular distribution. Cai (2011) discussed the distribution of the joint condition and commented that J_r and J_a could be assumed to be normally distributed. This ideology was also suggested by Panthi (2006) and Panthi and Nilsen (2010), while Panthi (2006) measured at cases where both J_r and J_a follow a lognormal distribution. Beer et al. (2002) studied the joint roughness condition (JRC) which has a direct relationship to the J_r , finding the JRC follows a normal distribution, while Bedi (2013) estimated both joint condition input parameters to follow a triangular distribution. Both J_w and SRF were suggested to have a truncated triangular distribution (Panthi, 2006). However, it should be noted measured principal stress data from the Canadian Shield (Kaiser and Maloney, 2005) followed a normal distribution. Since the major principal stress (σ_1) has a direct relation to the SRF , a normal distribution should be considered over a truncated triangular. It should be noted that SRF is more challenging to

measure than the other Q parameters, and perhaps uncertainty in measurement is a more significant factor than is its true variability within a rock mass domain. The assumptions discussed are considered for the application of the method to the case studies; however, it is still imperative to analyze the data measured to ensure the most suitable distribution is selected for each input parameter.

3.3.3 The MCS Method

When variability exists in input parameters for a specific problem, MCS presents a means to evaluate randomness in design parameters. MCS is a computational statistical method that produces numerical results from repeatedly generating random values. The set of data points from the simulation produces PDF and CDF curves, illustrating all potential outcomes and the likelihood of an individual event. The possibility of an event can be analyzed using the PDF, and a subsequent design can be based on point estimate values, such as the μ (Q_μ) and $\mu \pm 1 \text{ } sd$ (Q_{UB} and Q_{LB}). Alternatively, the CDF can be related to the probability associated with a range of values, ensuring the estimation is above or below a specific portion of all possible results. Applying MCS, in place of the deterministic approach, an estimate of Q considering the randomness in the rock mass can be calculated.

3.3.4 Methodology

MCS was performed using the mathematical software *MATLAB*. The distributions for each Q input parameter were determined from the histograms of the statistical data collected in the geotechnical investigation for a given case. For the simulation, input parameters were assumed to be independent random variables, bounded by the LL and UL (lowest and highest permitted values, respectively). In most cases, a universal LL and UL are prescribed for the categories set by the NGI handbook, presented in Table 3-1. However, in special cases, such as a triangular distribution for the *SRF*, the limits may be altered due to the extreme range in certain stress conditions.

Table 3-1. Lower (LL) and upper limits (UL) for Q system rock parameters (NGI, 2015)

Q Parameter	Cat.	Description	LL	UL
RQD	-	-	10	100
J_n	-	-	0.5	20
J_r	a	Rock-wall contact (no mineral fillings, only coatings)	0.5	4
	b	Rock-wall contact before 10 cm shear (thin mineral fillings)	0.5	4
	c	No rock-wall contact when sheared (thick mineral fillings)	1	1
J_a	a	Rock-wall contact (no mineral fillings, only coatings)	0.75	4
	b	Rock-wall contact before 10 cm shear (thin mineral fillings)	4	12
	c	No rock-wall contact when sheared (thick mineral fillings)	6	20
J_w	-	-	0.05	1
SRF	a	Weak zones	2.5	10
	b	Competent rock with stress issues	0.5	400
	c	Squeezing Rock	5	20
	d	Swelling Rock	5	15

For the MCS, multiple randomized iterations were performed to calculate a dataset of Q values. The PDF and CDF are created from the data points produced, and a certain number of iterations are required to be confident in the results. If too few data points are simulated, the PDF and CDF will be less consistent and have reduced clarity. In this study, initially, the MCS was programmed to run 10,000 iterations; however, this value was increased to 100,000 to improve the resolution of the simulation and produced more consistent results without excessively long run times. An ‘if’ statement was written in *MATLAB* to allocate the appropriate UL and LL to truncate each Q parameter. To set the shape of the distribution, e.g. normal or lognormal, and ensure no data was generated outside the LL and UL, a combination of the ‘*random*’, ‘*makedist*’, and ‘*truncate*’ *MATLAB* commands were used. The ‘*random*’ command created individual values for

each input parameter, calculating a single Q value. The *'truncate'* command deemed values outside the range of the LL and UL non-permissible and regenerated the data until all conditions are met for the iteration. Limiting the range of the data has the potential to induce minor distortion of the PDF, raising the question, should the distribution be truncated? However, the sample size is quite large, and the potential for values outside the LL and UL is negligible and unlikely to affect the validity of the analysis. With 100,000 data points, the PDF and CDF curves of Q can be developed with the *'fitdist'*, *'pdf'*, and *'plotcdf'* *MATLAB* commands.

3.3.5 Q and Empirical Ground Support Requirements

Ground support recommendations with Q are directly related to the quality of the rock mass and D_e , which relates excavation size to the ESR. Based on the PDF and CDF of Q, a probabilistic analysis was used to determine the design criterion for ground support. While the ESR acts as an analogous to the inverse F , the value does not account for uncertainty in the rock mass. A more appropriate method is to associate an acceptable level of risk to the estimation of rock quality. Whether it is the probability of exceedance, where only a portion of possible rock qualities is less than the estimate, or the Q_μ , Q_{LB} , or Q_{UB} , an engineer can decide how conservative the design should be. In the proposed method, Q_{LB} (defined: $\mu - 1 sd$), Q_μ and Q_{UB} (defined: $\mu + 1 sd$) were points selected in the PDF, representing design suggestions for ground support. A conservative engineer may characterize the rock mass as Q_{LB} , recommending Q_{LB} rock support that theoretically stabilizes a vast majority of all possible rock qualities. However, it is unclear if Q_μ rock support can still provide adequate reinforcement for the anticipated range of rock mass conditions within the domain (e.g., even when Q_{LB} conditions are encountered).

3.4 Case Study Application of MCS for Q

Field data from two case projects were analyzed to illustrate the probabilistic design approach for Q. In both cases, the PDF and CDF present the full range of potential Q, and suggestions for design limits (i.e. Q_{LB} , Q_μ , and Q_{UB}). In this study, the focus was placed on the NUOS site data, illustrating the application of the method for ground support design, and the NJHP data was used as an additional, second demonstration for the MCS of Q.

3.4.1 Norway Underground Olympic Stadium

Located in Gjøvik city, Norway, the NUOS site comprises of Precambrian gneiss, with highly variable jointing (Bhasin et al. 1993). The area for the proposed cavern excavation was at a depth of 45 m, and the initial investigation found the rock mass quality was generally low. The geotechnical study found the range of Q to be substantial, with a typical minimum of 1.25, a typical maximum of 30 and a weighted average of 9.39. Table 3-2 presents the statistical μ and sd for each Q parameter calculated from the logged field data and the LL and UL for each parameter. For this specific case, the J_w and SRF were assumed to be constant and have no bearing on the overall quality of the rock mass. The joint condition ranged between class (a) and (b) overall, indicating minimal infilling existed between joints.

Table 3-2. Statistical data and limits for measured Q input parameters at NUOS

Q Parameter	μ	sd	LL	UL	Distribution
RQD	67.0	13.2	10	100	Truncated Normal
J_n	8.7	2.3	0.5	20	Truncated Normal
J_r	2.3	0.6	0.5	4	Truncated Normal
J_a	1.9	1.4	0.75	12	Truncated Normal
J_w	1	0	N/A	N/A	NA
SRF	1	0	N/A	N/A	NA

Before probabilistic analysis was performed on the PDF and CDF, the simulated data for each Q input parameter was compared to the measured data. Fig 3-1 shows the simulated Q parameters matched well with the measured data (shown in figure inset), except for J_r , suggesting an alternative distribution, such as a lognormal distribution, may be a more suitable alternative. For the MCS, RQD, J_n , J_r , and J_a were represented by a truncated normal distribution, while J_w and SRF are a constant of 1, as determined in the site investigation data, and for this reason, not presented in Fig 3-1. Using Eq. 3-1 in the MCS, the randomized Q parameters produce a lognormal distribution of Q, presented in the PDF and CDF for the NUOS rock mass illustrated in Fig 3-2. The lognormal distribution is experienced due to the multiplication of multiple independent random variables based on the central limit theorem (Limpert and Stahel, 2011). For this

particular case, the effective stress is not considered a factor in the design; however, when variability exists, a decrease in the the overall Q rating is possible, as seen in NJHP. Based on the simulated Q values, Q_{LB} , Q_{μ} , and Q_{UB} were calculated to be 2.17, 9.94, and 17.71.

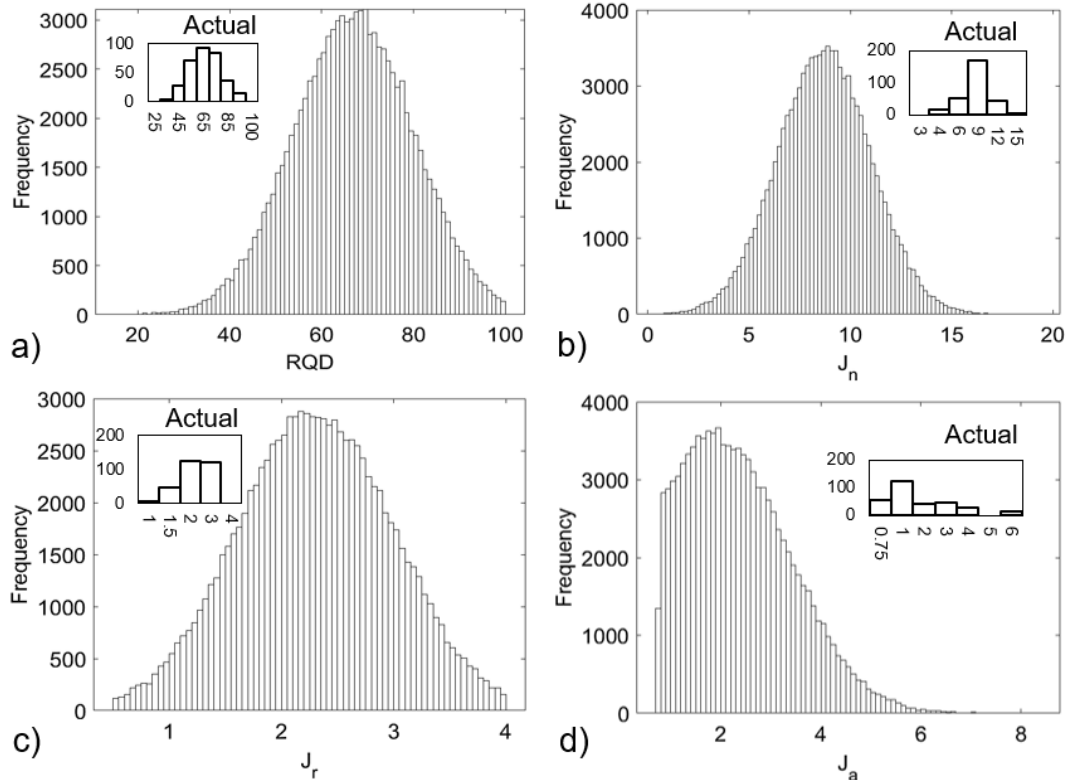


Fig 3-1. Histograms of the actual measured data (inset figures) and simulated data from MCS of NUOS case history for: (a) RQD; (b) J_n ; (c) J_r ; and (d) J_a

In Table 3-3, the results from the probabilistic design approach were compared to the deterministic method. For the deterministic approach, Q_{μ} was calculated with the μ of each Q parameter, while Q_{LB} and Q_{UB} were calculated with the $\mu \pm 1 sd$ values. The calculated Q_{μ} does not produce the same results for both methods, suggesting a distributive range should be considered instead of a single value for each input parameter. This is most noticeable for Q_{UB} in Table 3-3, where the deterministic value is substantially higher, due to the multiple under-conservative values being multiplied together producing an unrealistic value for the upper bound. In the probabilistic approach, the $\mu + 1 sd$ values is based only on the simulated Q values and is not affected as easy by the extreme values of each individual input parameter.

Table 3-3. Comparison of probabilistic and deterministic design approach calculation of Q design limits at the NUOS geological site

	Q_{LB}	Q_{μ}	Q_{UB}
Probabilistic	2.2	9.9	17.7
Deterministic	2.4	9.3	72.8

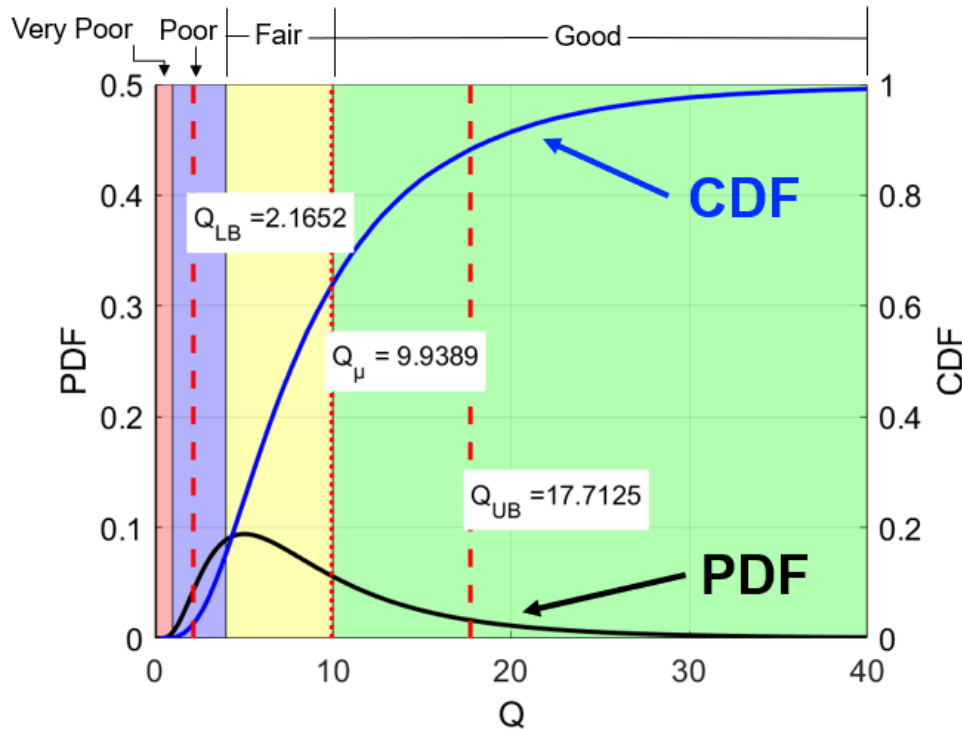


Fig 3-2. PDF and CDF of Q calculated from MCS of NUOS case history data with the Q_{μ} (dotted line), Q_{LB} (left dashed line), and Q_{UB} (right dashed line) superimposed on rock classification zones

The probabilistic design approach offers a holistic view of the rock mass, improving the overall accuracy of the quality estimation. Still, the extreme range of values from the MCS affects the μ and sd . Q_{LB} , Q_{μ} , and Q_{UB} provide points to base a design on, but with a high coefficient of variation (COV), Q_{LB} can be considerably lower than Q_{μ} . Though these concerns exist, the method does consider the uncertainty in the measurement and inherent variability in rock structures. The bigger question is, which value should be regarded as the design criterion for ground support? Should the value be Q_{LB} , Q_{μ} , Q_{UB} , or some other value for that matter? Furthermore, a probabilistic design

approach can improve the accuracy of estimating the ground condition, but confidence in a statistical analysis is only as strong as the data. Ensuring the correct distribution for each Q input parameter is vital in the MCS, and in the current simulation, J_r may be better represented by a lognormal distribution.

Additionally, if a relationship does exist between input parameters, the randomized results of one parameter can be mutually affected by the other and cannot be assumed to be fully independent. For this reason, further analysis should be performed to measure if a correlation exists between input parameters, both in general and case by case. Furthermore, because of the broad range in Q, instead of associating the design criterion on Q_μ , the probability of exceedance of Q values based on the CDF may be a more suitable design option.

The dominant failure mode (e.g., squeezing, gravity-driven, spalling) has a direct relation to the quality of the rock mass and stress condition (Martin et al. 1999), affecting the type of ground support required to stabilize it effectively. While the quantitative rating of Q is related to a qualitative description of the rock quality, it does not identify the expected mode of failure. By understanding the potential mode of failure in all likely ground conditions in a rock domain, an engineer can gauge how risk-averse the design should be. If the mode of failure is the same for Q_{LB} and Q_μ , one can expect the type of support to be useful in all cases. However, if the mode is entirely different, a more conservative estimate may be required. The tunneling behaviour chart (Kaiser et al. 2000) presents a means to compare the rock quality to the in-situ stress condition, although the ground condition is measured with the RMR. To relate this back to Q, the RMR was calculated using Eq. 3-4 (Bieniawski, 1976). Through the calculation, the estimated Q can be compared to the in-situ stress condition to determine the expected mode of failure for Q_{LB} , Q_μ , and Q_{UB} . From the equation, the RMR was calculated to be 50.9, 64.7, and 69.9 (Q_{LB} , Q_μ , and Q_{UB}) for the NUOS geological site. With a σ_c of 60 MPa and a σ_l of 3.5 MPa, the NOUS rock mass was in a low in-situ stress condition, where Q_μ was moderately fractured, and Q_{LB} was moderate to almost highly fractured. Fig 3-3 illustrates the MCS results and how they translate to the tunneling behaviour chart, showing the expected mode of failure for the NUOS rock mass to be falling and sliding of blocks, with the potential to experience some unravelling of blocks.

$$RMR = 9 \ln Q + 44$$

(3-4)

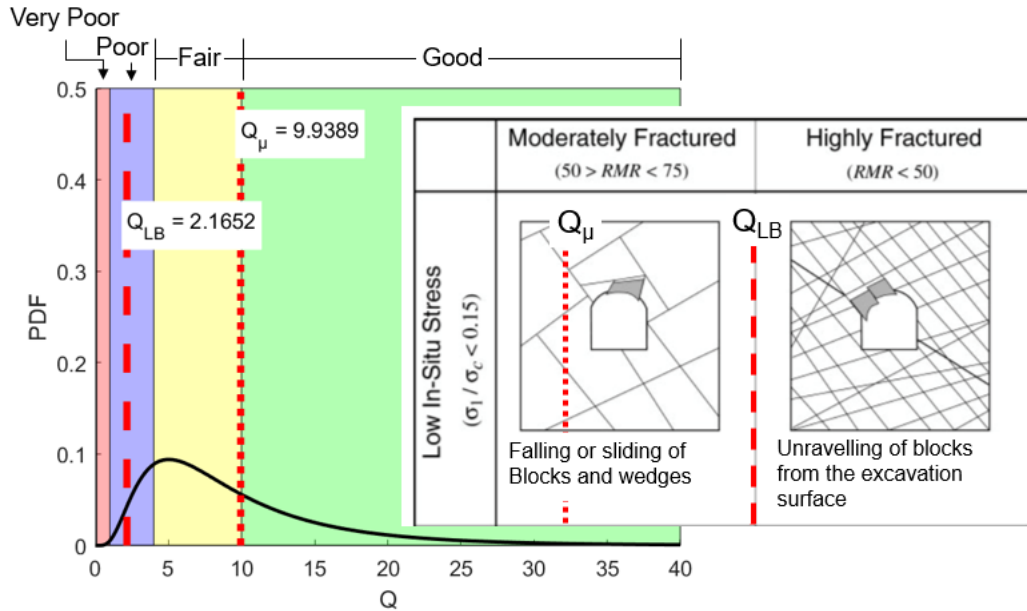


Fig 3-3. Potential failure mechanism for NUOS Q_{μ} and Q_{LB} rock quality based on the tunneling behaviour chart (modified Kaiser et al. 2000)

The PDF and CDF developed from the MCS can be superimposed on the support recommendation chart, to illustrate the use of probabilistic design to determine ground support requirements. For the cavern at NUOS, with a span of 62 m and ESR of 0.8, the D_e is 77.5, requiring special evaluation as suggested by the NGI handbook. For this reason, a theoretical horseshoe-shaped tunnel was analyzed to illustrate the use of the probabilistic design approach for ground support, in the ‘sweet spot’ of the Q recommendation chart (Palmström and Broch, 2006). The dimensions of the horseshoe-shaped tunnel are 4 m wide and 5 m high. The span was assumed to be 5 m, and the ESR was 1, overall calculating a D_e of 5. In the recommendation chart, both shotcrete thickness and bolt spacing is measured based on Q, while bolt length is determined from D_e (NGI, 2015). It can be seen in Fig 3-4, the difference in recommended bolt spacing is significantly less between Q_{μ} and Q_{UB} , compared to Q_{LB} , and the same relationship existed for the shotcrete thickness. From the chart, bolt length is based on D_e , suggesting the same bolt length for Q_{μ} , Q_{LB} , and Q_{UB} , but it has been suggested in unfavourable jointed rock, that longer bolts be installed when a lower Q is measured. Overall, in less

desirable rock, a more significant increase in bolt density or length is required between Q_μ and Q_{LB} rock support.

Based on a Q_μ of 9.94 and a D_e of 5, the top and right axis of Fig 3-4 suggested a 2.4 m bolt spacing and 2.5 m bolt length for the excavation. In addition to rock bolts, the rock quality and D_e placing the excavation in zone 3 of the chart, suggesting 5-6 cm of fibre-reinforced shotcrete. It is important to note, the recommendation chart is only a suggestion, and for the tunnel in question, the 2.4 m bolt spacing is too large for a 2.5 m rock bolt. The rules-of-thumb for maximum bolt spacing is half the length of the rock bolt (Lang et al. 1982); therefore, bolt spacing was set to 1.25 m for the Q_μ rock support. For the Q_{LB} rock support, the minimum bolt spacing, based on the same rules-of-thumb, was set to 0.9 m, which is presented in Table 3-4. In all three designs, a 4 mm wire mesh was included with the shotcrete.

Table 3-4. Rock support recommendations based on Q_{LB} , Q_μ , and Q_{UB} ratings from the MCS of the NUOS site data

	Q_{LB}	Q_μ	Q_{UB}
Bolt Length (m)	2.5	2.5	2.5
Bolt Spacing (m)	0.9	1.25	1.25
Shotcrete Thickness (cm)	6	5.5	5.25

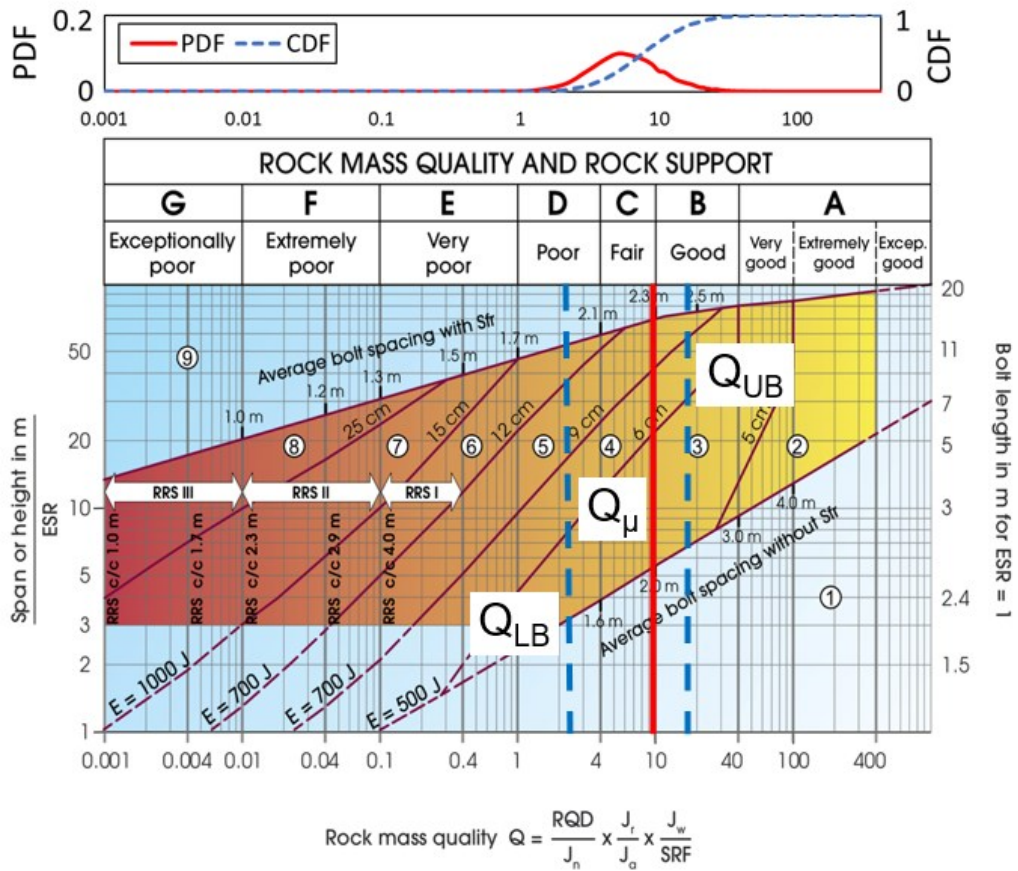


Fig 3-4. Q_{μ} (solid red line), Q_{LB} (left dashed blue line), and Q_{UB} (right dashed blue line) superimposed on the Q support recommendation chart and the PDF and CDF from the MCS of NUOS site data on top (modified from NGI, 2015)

In poor rock conditions, the potential for stability issues is a concern, although simply designing support to the worst case is not always practical or viable economically. The support recommendation chart is based on what was installed in historical sites, and it is unlikely that excavations are designed just short of failure, so some level of conservatism can be assumed to exist. In the preliminary stages of design, the Q_{μ} rock condition better represents the overall rock mass, and the author suggests it as a more suitable design criterion. The Q_{μ} rock support has the potential to provide enough reinforcement for poorer ground, and numerical analysis of the response of rock support to poor conditions can validate this ideology.

3.4.2 Nathpa Jhakri Hydro Project

A second demonstration of the method was performed with the geological data from the NJHP site. Located in the Kinnaur and Simla district of India, the site is comprised of a low strength anisotropic rock mass (Bhasin et al. 1995). The rock mass consists of gneiss, schists and amphibolite, with a weighted average Q of 2.7, measured from a pilot tunnel. RQD, J_n , J_r , and J_a were assumed to have a truncated normal distribution, while J_w and SRF followed a truncated triangular distribution, with a μ , sd , LL, and UL listed in Table 3-5. The LL and UL for the triangular distributions were based on the maximum and minimum values measured instead of the limits set by the NGI handbook. The reason for the different limits is the extreme values, especially for the SRF , which can distort the distribution and would not match what is to be expected. Comparing the simulated to the actual data, the distributions selected for the MCS match well with the field measurements illustrated in Fig 3-5.

Table 3-5. Statistical data and limits for measured Q input parameters at NJHP

Q Parameter	μ	Sd	LL	UL	Distribution
RQD	69.5	16.3	10	100	Truncated Normal
J_n	5.2	2.1	0.5	20	Truncated Normal
J_r	2.7	0.6	0.5	4	Truncated Normal
J_a	2.6	1.9	0.75	12	Truncated Normal
J_w	NA	NA	0.66	1	Truncated Triangular
SRF	NA	NA	2.5	10	Truncated Triangular

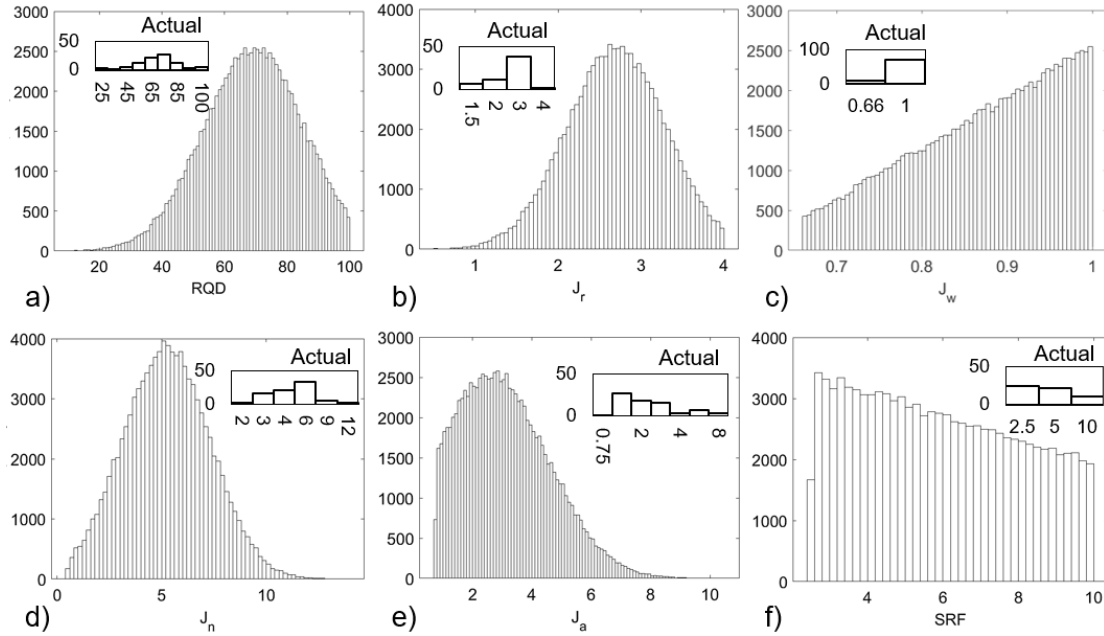


Fig 3-5. Histograms of the actual measured (inset figures) and simulated data from MCS of NJHP case history for (a) RQD; (b) J_r ; (c) J_w ; (d) J_n ; (e) J_a ; and (f) SRF

The probabilistic design methodology was applied to NJHP field data, illustrated in Fig 3-6, and the Q_{LB} , Q_{μ} , and Q_{UB} were calculated to be 0.001, 3.08, and 6.92. Using Eq. 3-4, the RMR rating for Q_{LB} was calculated to be less than zero, which is not possible with the lowest value being 8 (Hoek, 2007), and Q_{μ} had an RMR of 54.1. Overall, Q_{LB} estimated the rock mass to be highly fractured while Q_{μ} is moderately fractured, and both are in an intermediate in-situ stress field (depicted by the tunneling behaviour chart) with a σ_1 of 7.14 MPa and a σ_c of 35 MPa producing a σ_1/σ_c of 0.2. Based on the results, Fig 3-7 illustrates the potential modes of failure for Q_{LB} and Q_{μ} , ranging from localized brittle failure in intact rock and a range of sliding/movement to the unravelling of blocks. In this case, Q_{LB} was calculated to be the worst possible quality, presenting the issue of considering Q_{LB} as the design criterion when the coefficient of variation is high for the simulated Q . However, when the Q_{LB} ground condition is present, the Q_{μ} rock support may not be adequate due to the two completely different expected modes of failure, which should be considered when selecting an acceptable level of risk for the design, such as designing rock support for all but 10% of all possible ground conditions.

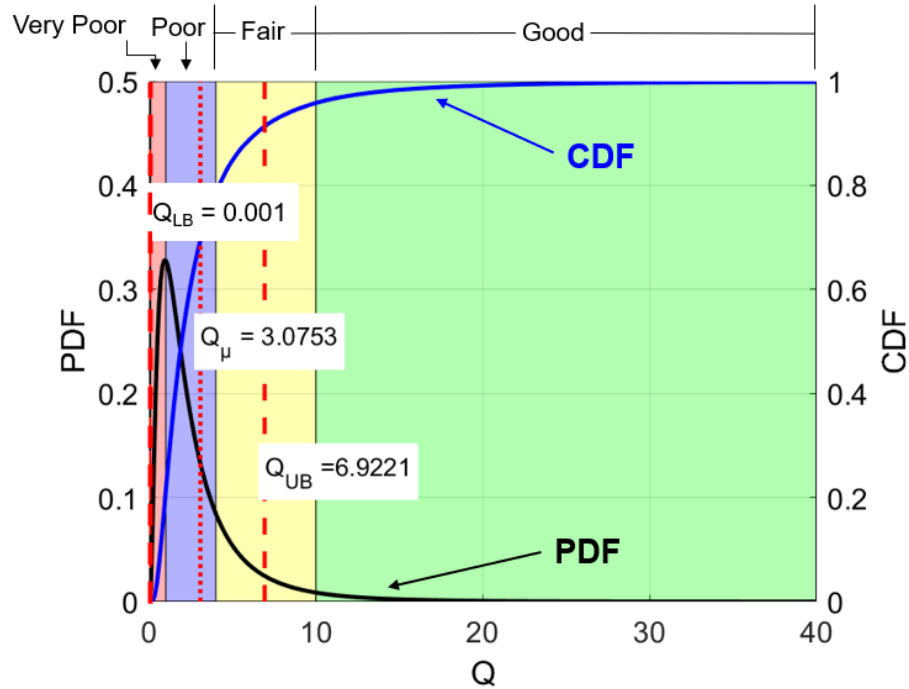


Fig 3-6. PDF and CDF of Q calculated from MCS of NJHP case history data with the Q_μ (dotted line), Q_{LB} (left dashed line), and Q_{UB} (right dashed line) superimposed on rock classification zones

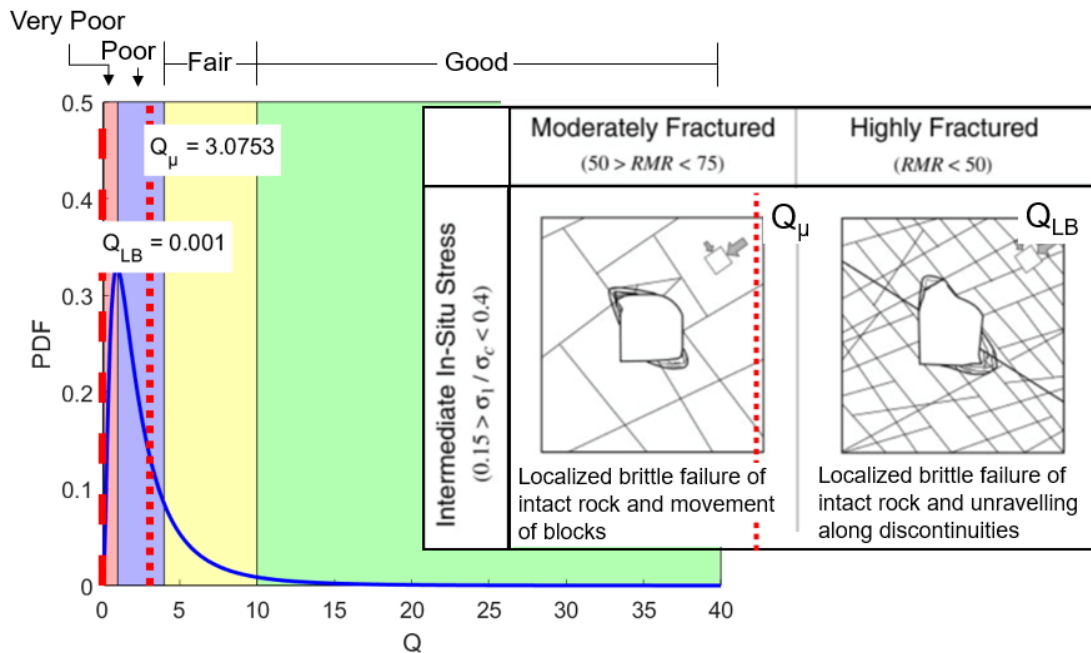


Fig 3-7. Potential failure mechanism for NJHP Q_μ and Q_{LB} rock quality based on the tunneling behaviour chart (modified Kaiser et al. 2000)

3.5 FEM Analysis to Validation Ground Support Design Criterion

Numerical modelling of the NUOS rock mass was performed to analyze the response of suggested ground support for a range of potential rock mass qualities (Q_{LB} , Q_{μ} , and Q_{UB}). From the probabilistic design approach, Q_{μ} rock support was selected from the design chart (Fig 3-4). Still, the question is whether the recommended support is suitable in the range of potential ground conditions, and for that reason, the method must be validated. This issue was explored by conducting numerical model simulations with the jointed rock mass explicitly represented using the two-dimensional finite element software code *RS2*. A hypothetical tunnel was simulated using the rock mass conditions from the NUOS case study. Creating three separate models resembling the rock mass framework of Q_{LB} , Q_{μ} , and Q_{UB} , the response of support elements can be measured to determine the effectiveness of the Q_{μ} rock support in the range of ground conditions. While Q_{LB} rock support is expected to be useful for the full range of ground conditions (Q_{LB} to Q_{UB}), if a numerical model proves Q_{μ} rock support produces adequate results for the majority of the range of anticipated conditions, the option to install Q_{μ} instead of Q_{LB} rock support is validated.

3.5.1 Modelling Methodology

Three separate models were developed in *RS2* with the same boundary conditions, ground support, and excavation dimensions, where the only difference was the rock mass properties, based on the Q_{LB} , Q_{μ} , and Q_{UB} estimates from the MCS. Rock mass classification systems, such as Q, classify the rock quality but do not provide the rock mass strength and stiffness parameters directly, which are required for analyzing ground behaviour in a numerical model. While Q cannot be directly incorporated in the *RS2* model, previous work has provided relationships between the Geological Strength Index (GSI) and Q (Hoek et al. 2013). With a GSI value, rock strength and stiffness parameters can be calculated with the Hoek-Brown failure criterion.

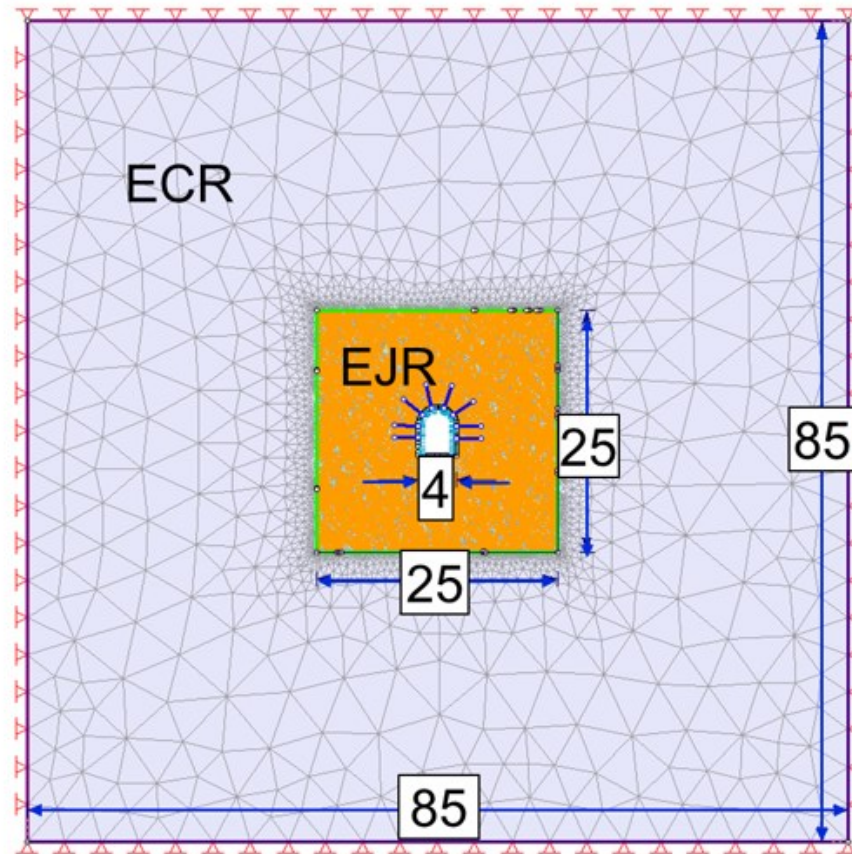
The rock mass could be simulated using an Equivalent Continuum Model (ECM), based on continuum mechanics, where the Hoek-Brown failure criterion ‘smooths/smears’ the rock properties to act as a continuous material equivalent to the overall jointed rock mass. While an ECM provides a means to analyze the effects an

excavation has on a rock mass, the question is whether the model correctly considers the movement of individual blocks in the joint network. To properly analyze the effects of discontinuities on the stability of the excavation, an Explicitly Jointed Model (EJM) was developed for this modelling program. The DFN concept was used to create the framework of the EJM, where the statistical data from a geological survey creates a fictitious fracture network based on the orientation, persistence, and spacing of joints. With the explicit joint network, the EJM captures the nature of the joint interaction for different ground conditions, modelling the rock mass as an elastoplastic material, where the stability is affected by both the joint and intact rock properties.

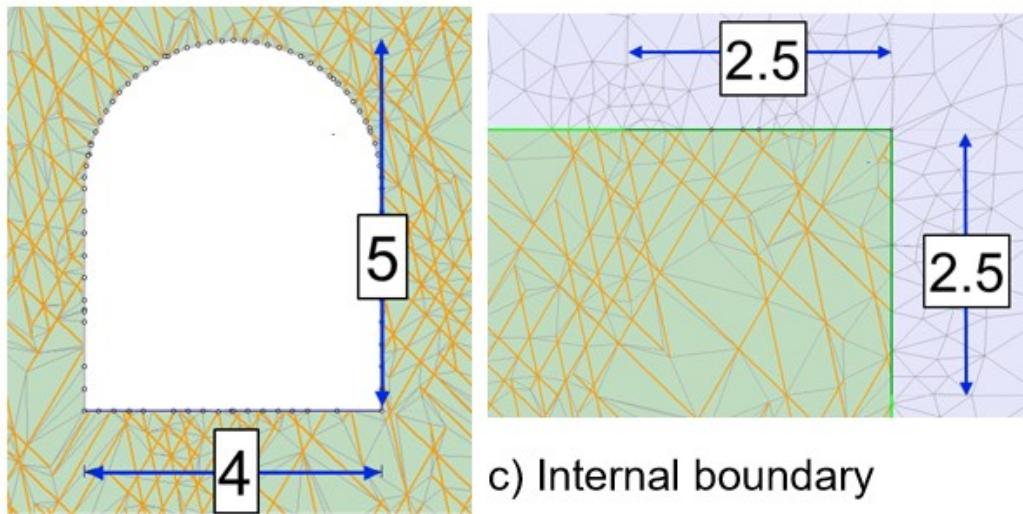
3.5.2 Boundary Conditions

The model consisted of a hypothetical horse-shoe shaped excavation, with a width of 4 m and a height of 5 m. Surrounding the excavation a 25 m by 25 m Explicit Joint Region (EJR) was modelled to simulate the rock mass behaviour when explicit joints were present. Encapsulating the EJR was an 85 m by 85 m Equivalent Continuum Region (ECR), illustrated in Fig 3-8. The dimensions of the EJR were set to be approximately two times the tunnel span from the excavation, where at this internal model boundary the stress redistribution is minor and the use of an ECR would have little influence on the simulation results while allowing for quicker simulation times. The external boundary was fixed, assuming negligible rock mass movement occurred on the extremities of the FEM, due to the distance from the tunnel. The mesh framework is a graded three-node triangulation, and mesh size was based on a gradation factor of 0.1 and a default of 110 nodes of the excavation boundary.

At the NUOS site, the $\sigma_1:\sigma_2:\sigma_3$ ratio was measured to be 3.5:2:1 from hydraulic fracturing and overcoring techniques. The principal stresses are oriented N-S for σ_1 , E-W for σ_2 , and vertical for σ_3 (Bhasin, 1993). From the paper, the azimuth of the tunnel was N65°E; therefore, the horizontal in-plane to out-of-plane stress ratio was 2.3 to 3.2 for the model, due to the fact the azimuth of the tunnel was not parallel to σ_2 . Furthermore, instead of a constant stress field, gravity loading at a tunnel depth of 45 m was used to calculate the vertical stress while assuming the unit weight of the overlying rock mass to be 25 kN/m³.



a) Entire model mesh



b) Tunnel boundary

c) Internal boundary

Fig 3-8. Illustration of model mesh and boundary conditions with a theoretical horse-shoe shaped tunnel (all dimensions are in meters)

3.5.3 Rock Mass Strength Parameters

For this study, the Q input parameters are used to calculate the strength parameters of the rock mass. For this reason, three iterations from the MCS that provided Q_{LB} , Q_{μ} , and Q_{UB} were used to estimate the rock strength parameters for each model, as shown in Table 3-6. The Q input parameters were applied to Eq. 3-5 (Hoek et al. 2013) to calculate the GSI, which was used to estimate the elastic rock mass properties for the ECR and EJR.

Table 3-6. Q input parameters for Q_{LB} , Q_{μ} , and Q_{UB} models based on results from MCS of NUOS site data

	Q_{LB}	Q_{μ}	Q_{UB}
RQD	56.0	69.0	74.5
J_n	10.8	9.0	7.4
J_r	1.3	2.5	2.8
J_a	3.1	1.9	1.6

$$GSI = \frac{52 J_r / J_a}{(1 + J_r / J_a)} + RQD / 2 \quad (3-5)$$

The rock type that exists at NUOS is Precambrian gneiss. For the model, the average value for gneiss from the database in the program *RocData* was used to estimate the Hoek-Brown intact rock constant (m_i) and the modulus ratio (MR) to be 28 and 525. The Disturbance Factor (D) was set to 0.5, assuming no significant damage from blasting, and the Unconfined Compressive Strength (UCS) was measured to be 60 MPa (Bhasin et al. 1993). Eq. 3-6 to Eq. 3-8 were used to calculate the Hoek-Brown constant (m_b) and rock mass constants (s) and (a) for Q_{LB} , Q_{μ} , and Q_{UB} . While Eq. 3-9 and Eq. 3-10 were used to calculate the intact modulus (E_i) and rock mass modulus (E_{rm}), with all assumed and calculated material properties for the ECR presented in Table 3-7.

$$m_b = m_i \exp\left(\frac{GSI-100}{28-14D}\right) \quad (3-6)$$

$$s = \exp\left(\frac{GSI-100}{9-3D}\right) \quad (3-7)$$

$$a = \frac{1}{2} + \frac{1}{6} (e^{-GSI/15} - e^{-20/3}) \quad (3-8)$$

$$E_i = MR \cdot \sigma_c \quad (3-9)$$

$$E_{rm} = E_i \left(0.2 + \frac{1-D/2}{1+e^{((60+15D-GSI)/11)}} \right) \quad (3-10)$$

Table 3-7. Rock mass properties for ECR

Parameter	Q_{LB}	Q_{μ}	Q_{UB}
E_i (GPa)	31.5	31.5	31.5
E_{rm} (GPa)	3.0	10.5	14.0
ν	0.22	0.22	0.22
σ_c (MPa)	60	60	60
GSI	44	64	70
D	0.5	0.5	0.5
s	0.0005	0.0081	0.0193
a	0.509	0.502	0.501
m_i	28	28	28
m_b	1.900	5.014	6.838

A typical tunnel experiences blast damage for a radius of up to approximately 2 m which can be modelled assuming various concentric zones of rock mass properties corresponding to different D (blast damage) factors: high near the tunnel boundary and decreasing with distance away from the tunnel boundary. Given that this is a hypothetical tunnel analysis exercise, overly complex assumptions were not made concerning the zone of damage and resulting D . Instead, an intermediate value of $D = 0.5$ was assumed for the ECM rock mass uniformly. Given that the focus of the study is the elastoplastic analysis, the rock mass yielding, displacement, and ground support loading near the tunnel boundary would be adequately captured by this simplified approach. The $D = 0.5$ assumption for the rock mass at a distance from the tunnel has a negligible impact on the results. This assumption was evaluated by running comparative models with $D = 0$ in the ECM region of the model, and the results verified negligible impact from this simplifying assumption.

The core diameter has a direct effect on the UCS, where Hoek (2004) showed that laboratory tests conducted on 200 mm diameter specimens had a UCS that was 80% of 50 mm diameter cores (Hoek, 2007). There was no data for specimens greater than 200

mm diameter. This is due to the larger number of microfractures present in the larger volume of rock. This concept can be applied to the intact rock blocks within the EJR, where we assumed the intact rock blocks had a UCS of 80% of the reported laboratory test values.

Table 3-8. Rock mass properties for intact rock blocks in EJR

Parameter	Value	Parameter	Value
σ_c (MPa)	48	m_b	28
GSI	100	E_i (GPa)	25.2
D	0	E_{rm} (GPa)	25.0
s	1	ν	0.22
a	0.5		

3.5.4 Properties of Discontinuities

In a jointed rock mass, multiple factors affect the excavation stability, such as the joint spacing (s_i), joint friction angle (ϕ_j), joint normal stiffness (K_n), and joint shear stiffness (K_s). The intersection of joints in a rock mass produces a network of rock segments with a block volume (V_b) directly related to the RQD (Palmström, 2017). With the RQD known, Eq. 3-11 can be used to back-calculate the volumetric joint count (J_v), and the V_b has a direct relationship between J_v and the block shape factor (β), as seen in Eq. 3-12. The rock mass has three joint sets that are cubical, and based on the characterization set by Palmström (2017) the β was assumed to be 27, and the cubic root of the V_b is used to calculate an estimate of s_i in meters (Eq. 3-13).

$$RQD = 115 - 3.3J_v \quad (3-11)$$

$$V_b = \beta J_v^{-3} \quad (3-12)$$

$$s_i = \sqrt[3]{V_b} \quad (3-13)$$

In the model, the parallel deterministic joint network model was selected in *RS2* to develop the DFN, where the orientation, s_i , joint length (L_j), and joint persistence ratio (P_j) are assumed to be constant. In *RS2*, instead of the conventional joint length to measure persistence, a combination of the L_j and P_j is used instead. The P_j ultimately sets

the distance from where a joint terminates and another begin measuring L_j to total length along the plane, i.e. P_j of 1 means the joints are infinitely persistent. The persistence of the joints was measured to ranged between 2 m and 5 m (Bhasin, 1993), and for the model, L_j was set to be 3.5 m. For the Q_{LB} , Q_{μ} , and Q_{UB} cases, the P_j was assumed to be 0.6, 0.5, and 0.45. All joints in the EJR were ‘closed’, meaning a single node represents the end of the joint and relative movement does not occur at the joint end. For the three joint sets, one was almost vertical striking with a dip/dip direction of $85^{\circ}/90^{\circ}$, while the other two sets were $50^{\circ}/190^{\circ}$ and $60^{\circ}/340^{\circ}$. The tunnel azimuth was $N65^{\circ}E$, and a trace plane angle of 155° was applied to the DFN to ensure the tunnel properly intersected the joint sets.

Through an extensive literature survey, Kulhawy (1975) studied the properties of discontinuities for different rock masses. For this study, data from rock masses resembling the NUOS geological site were considered for the model. From the findings, a non-foliated metamorphic rock on average has a φ_j of 36.6° , and the Torino Gran Paradiso Massiccio (Granitic gneiss fractures) has a maximum joint friction angle (φ_{jmax}) and residual joint friction angle (φ_{jr}) of 40° , and cohesion of zero. The rock mass at NUOS is a poorly foliated, Precambrian gneiss; therefore, the φ_j for Q_{μ} was assumed to be 36° , and Q_{UB} was the maximum value found for granitic gneiss fractures at 40° . With the Q rating for Q_{LB} significantly less than Q_{μ} , the φ_j was assumed to be 30° .

As noted earlier, Q does not provide an estimate of the rock mass strength; however, the φ_{jr} and Barton-Bandis shear strength criterion have a connection to the frictional strength (Bretuzzi, 2019), and was used as the slip criterion for the EJM. The joint compressive strength (JCS) was estimated to be 48 MPa, (equal to the UCS for the intact blocks in the EJM), and the JRC estimation compared the J_r to the JRC values for an undulating surface with a joint length of 1 m (Bretuzzi, 2019). The φ_j in all cases was assumed to equal φ_{jr} .

In connection with the Barton-Bandis slip criterion, the K_s and K_n determined the strength of the joint surface. Fossum (1985), developed the relationship between the s_i , K_n , K_s , Poisson ratio (ν) and E_{rm} , seen in Eq. 3-14, to determine the Bulk modulus (G). As s_i increases, the G becomes the intact Bulk modulus (G_i) seen in Eq. 3-15. Fig 3-9

illustrates the relationship between s_i and the ratio of the G/G_i , and by calculating G_i with the estimated E_{rm} and ν , the “goal seek” function in *Microsoft Excel* can be used to perform an iterative method of back-calculate K_s and K_n using Eq. 3-14, 3-15, and 3-16. A list of all joint properties is listed in Table 3-9.

$$G = \frac{1}{30} \left[\frac{E_{rm}}{(1+\nu)} \frac{9(1+\nu)(1-2\nu)s_i K_n + (7-5\nu)E_{rm}}{(1+\nu)(1-2\nu)s_i K_n + (1-\nu)E_{rm}} \right] + \frac{2}{5} \frac{E_{rm} s_i K_s}{2(1+\nu)s_i K_s + E_{rm}} \quad (3-14)$$

$$G_i = \frac{E_{rm}}{2(1+\nu)} \quad (3-15)$$

$$K_s = \frac{k_n}{2(1+\nu)} \quad (3-16)$$

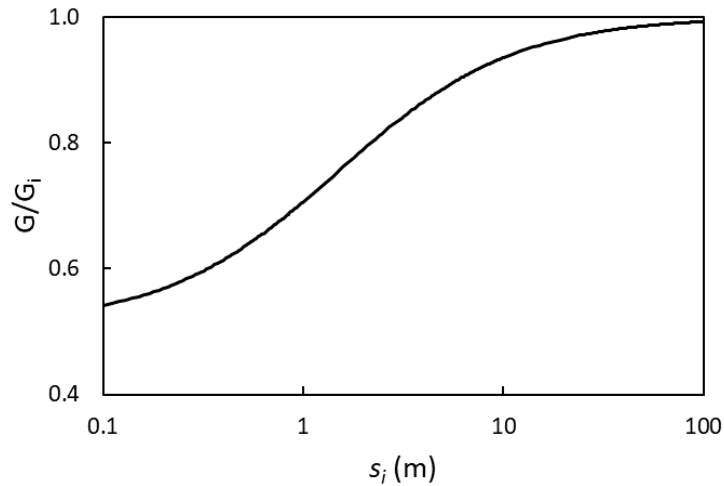


Fig 3-9. Behaviour of G/G_i as s_i increases, where a rock mass with a large s_i is assumed to resemble intact rock (modified Fossum, 1985)

Table 3-9. Joint properties for EJR

Parameter	LB	μ	UB
φ_j (°)	30.0	36.0	40.0
s_j (m)	0.17	0.22	0.24
L_j (m)	3.5	3.5	3.5
J_i	0.6	0.5	0.45
K_n (MN/m ³)	2,266	7,835	10,368
K_s (MN/m ³)	929	3,211	4,249
JCS (MPa)	48	48	48
JRC	6	8	9

3.5.5 Q_μ -Based Ground Support Design

Based on a Q_μ of 9.94 and a D_e of 5, the recommended rock support design was 2.5 m long bolts spaced 1.25 m apart with 5.5 cm of shotcrete reinforced with a 4 mm wire mesh. For the bolt pattern, installation began halfway up the sidewall and shotcrete was applied to the roof and walls of the excavation, presented in Fig 3-10. The properties for each element are from the *RS2* database and listed in Table 3-10.

Table 3-10. Properties for ground support elements

	Diameter (mm)	Spacing (mm)	E (MPa)	ν	σ_c (MPa)	Tensile Capacity (kN)	Tensile Strength (MPa)
Rock bolts	19	-	200000	-	-	100	-
Shotcrete	-	-	30000	0.15	40	-	3
Wire Mesh	4	100	200000	0.25	400	-	400

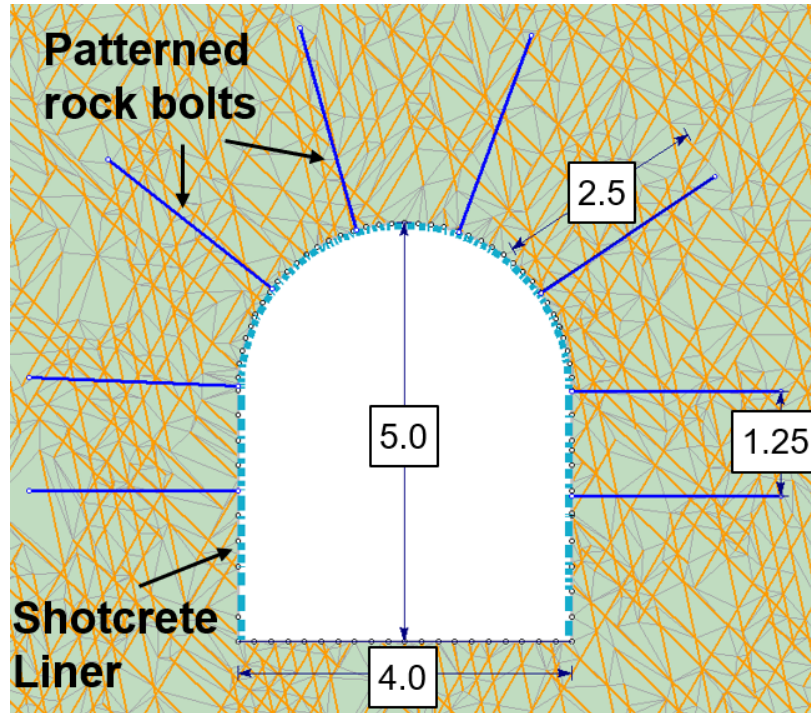


Fig 3-10. Q_{μ} rock support design with shotcrete liner (dashed line) and rock bolts (solid lines) (all dimensions are in meters)

For all three cases, Q_{LB} , Q_{μ} , and Q_{UB} , the DFN simulates the typical joint interaction; however, in practice installing the ground support without experiencing any resistance from the face is unlikely. As an excavation face advances, resistance from the face decreases and tunnel wall displacement (u_i) increases, until the expected maximum tunnel wall displacement (u_{max}) is reached at approximately three tunnel diameters from the face (Vlachopoulos and Diederichs, 2009). Based on this theory, some internal pressure (P_i) acting on the tunnel walls must be determined and applied to the model during installation of rock support.

Ground Reaction Curves (GRC) were developed by progressively reducing the P_i and measuring the largest u_i at each stage of the model. The three GRCs in Fig 3-11 illustrated the simulated u_{max} as the P_i incrementally decreases against the tunnel boundary. Using the GRC combined with the Longitudinal Displacement Profile (LDP) allows an individual to estimate the P_i applied to the model during the installation of the ground support. For this analysis, support was designed to be installed 2 m behind the face, which is half the tunnel width.

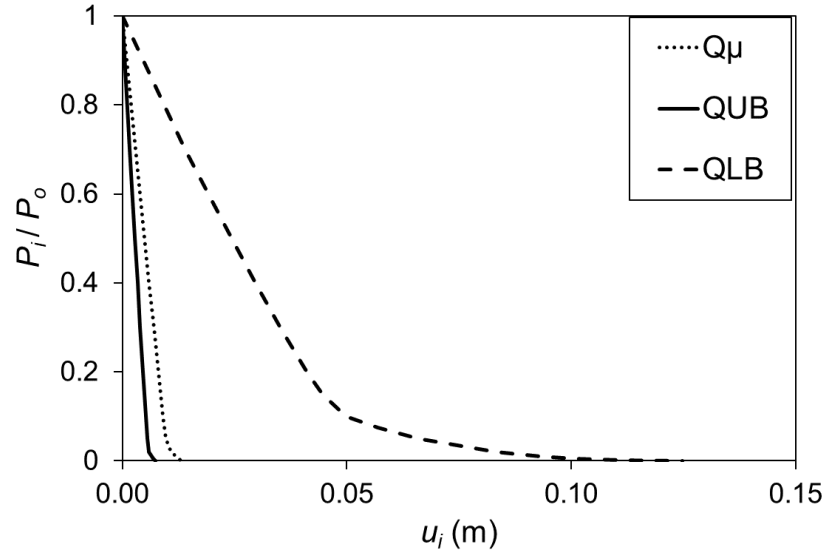


Fig 3-11. GRC for Q_{LB} , Q_{μ} , and Q_{UB} rock masses measuring the amount of u_i experienced on the excavation boundary as internal pressure on the tunnel walls is reduced

In Fig 3-12, the bold lines (red in colour image) represent joints that yielded, and the concentration of yielded joints represents the plastic zone in the rock mass, outlined by the dashed (black) line. The radius of the plastic zone (R_p) was measured from the centre of the excavation to the point where it was observed that the concentration of failed joints is sparse, estimating the average plastic zone. The ratio of the R_p and the tunnel radius (R_T) were applied to the Vlachopoulos and Diederichs (2009) chart to determine the u_i/u_{max} , where u_{max} was the u_i measured when P_i/P_0 equals zero, providing an estimate of the P_i from the GRC. The P_i for support installation one R_T from the face is presented in Table 3-11 and applied to the model for each case.

Table 3-11. Expected P_i/P_0 and u_i/u_{max} located 2 m behind tunnel face before installing of ground support

	R_p / R_T	u_i / u_{max}	P_i / P_0
Q_{LB}	2	0.65	0.024
Q_{μ}	1.5	0.74	0.051
Q_{UB}	1.25	0.77	0.041

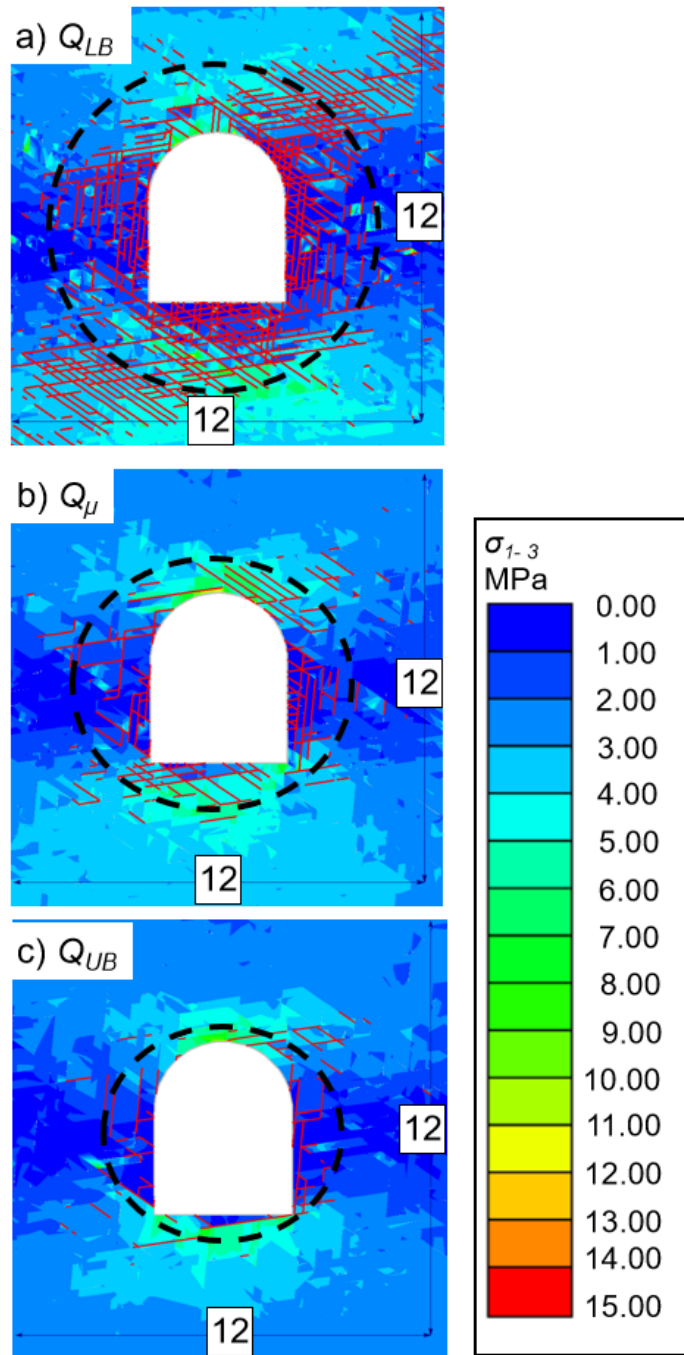


Fig 3-12. Size of the plastic zone (bold dash line) in Q_{LB} , Q_{μ} , and Q_{UB} rock masses using the concentration of yielded joints (bold red lines)

3.5.6 Validation of Modelling Method

The presence of joints in the EJR affects the redistribution of stresses compared to a model that is composed entirely of an ECR (continuum model), because joints can yield, resembling an elastoplastic rock mass. While the stress redistribution around the excavation in a discontinuum model, with explicit joints, will not perfectly replicate an ECM, the contours of the principal stresses should be similar. To prove the validity of the concept, models of an elastic continuum, elastic discontinuum, and elastoplastic discontinuum with Q_μ rock properties were compared. The elastic continuum model was entirely an ECR (Fig 3-13a), while both the elastic (Fig 3-13b) and elastoplastic (Fig 13-13c) discontinuum models were a combination of an EJR and ECR. For the elastic discontinuum, the cohesion and tension were set to extreme values, to ensure no joint movement, while the elastoplastic model is the Q_μ model for the study. The contours of σ_I in all three models hold a similar shape, validating the use of an EJR to model the jointed rock mass.

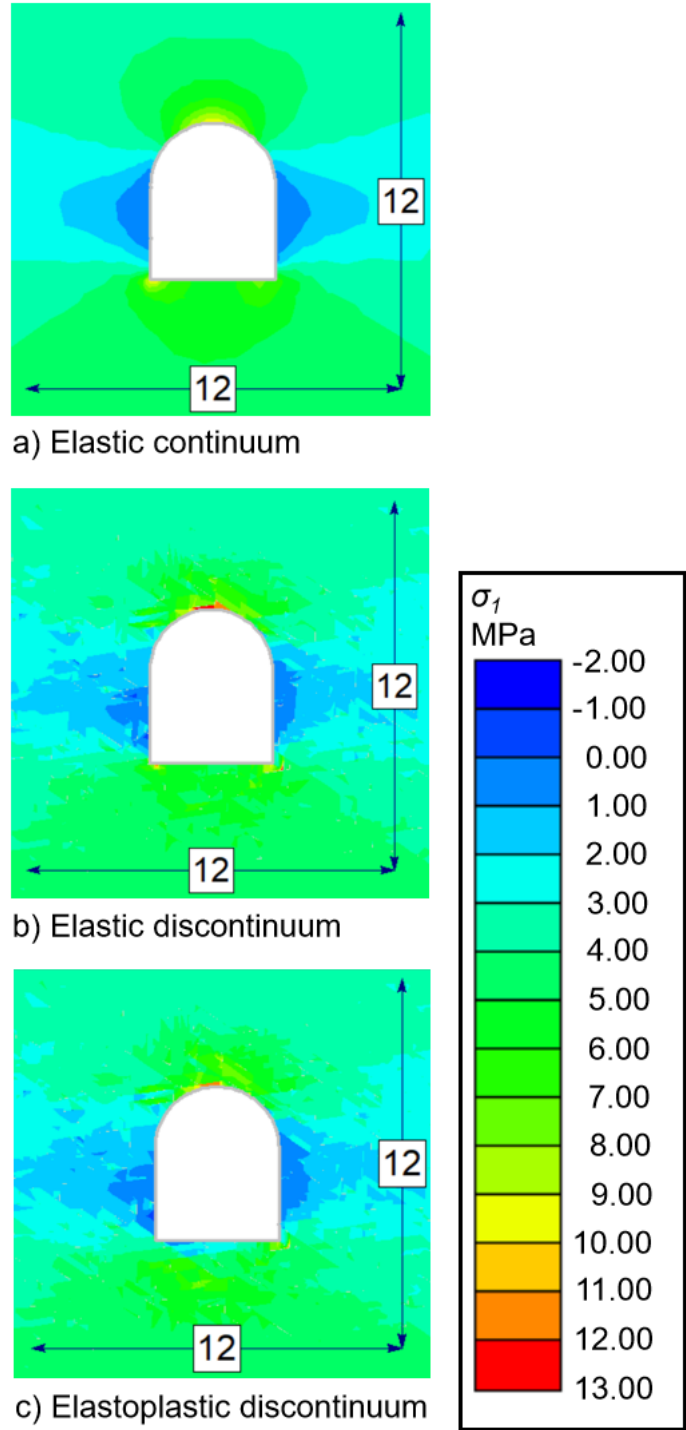


Fig 3-13. Comparison of the distribution of σ_1 when the model is: (a) elastic continuum – entirely ECR with Q_μ rock properties; (b) elastic discontinuum - EJR with high cohesion and tension; (c) elastoplastic discontinuum – EJR with Q_μ rock properties (dimensions are in meters)

3.5.7 Results and Discussion

Analysis of ground support performance under the different conditions was evaluated in three ways: (1) u_i measured at the midpoint of the sidewall and crown; (2) axial force (P) acting on the rock bolts, and; (3) axial thrust and bending moment measured along the length of the shotcrete liner. Three ‘query’ lines (*RS2* model data collection along lines) were created to measure the u_i in the rock mass. Fig 3-14 presents the measured u_i along the query lines when Q_μ rock support is present. The absolute vertical u_i , measured from the crown of the excavation to the model boundary, found the maximum u_i to be 0.27 cm, 0.13 cm, and 0.05 cm in the Q_{LB} , Q_μ , and Q_{UB} models. In contrast, two perpendicular query line from the midpoint of the sidewall to the model boundary found the maximum absolute horizontal u_i to be 6.00 cm, 1.03 cm, and 0.59 cm. Without Q_μ rock support, Fig 3-15 presents a slight increase in both the horizontal and vertical u_i ; however, in this case, tunnel strain is only 3% in the Q_{LB} model, suggesting ground support is required, but Q_μ rock support should suffice. As a test, the concentration of rock bolts and shotcrete thickness was increased and applied to the Q_{LB} rock mass. In the test, the u_i for Q_{LB} and Q_μ rock support was almost identical, showing increased support has some benefits; however, not enough to warrant the substantial increase in cost.

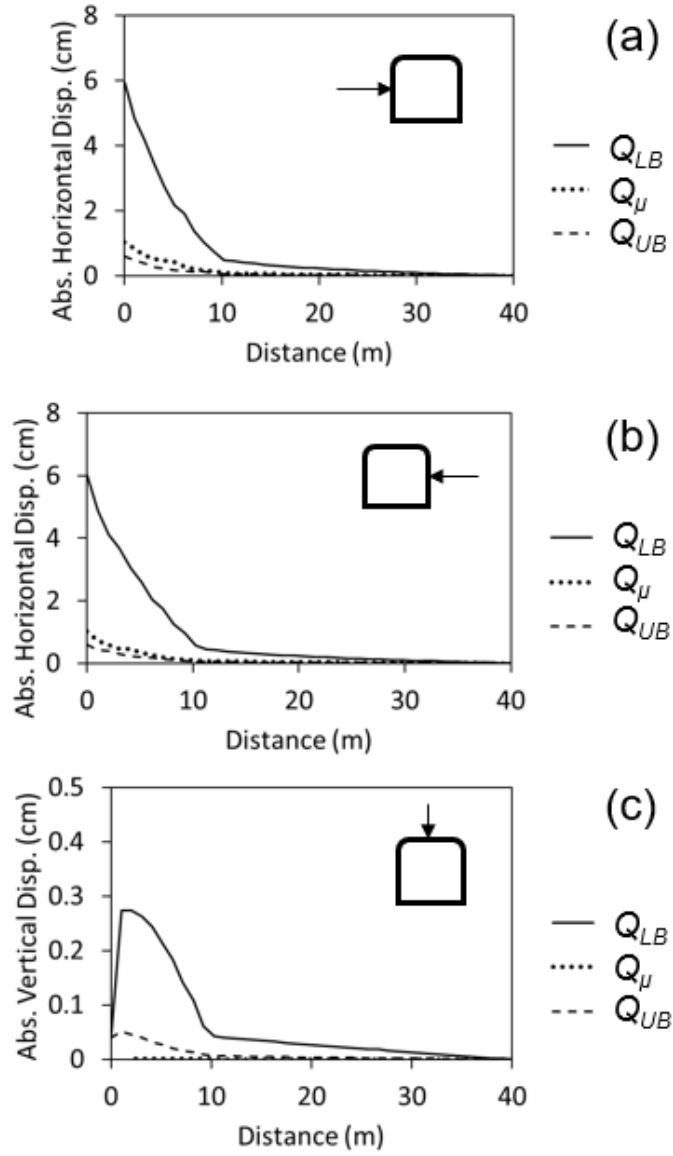


Fig 3-14. Absolute horizontal and vertical u_i measured along a 40 m long *RS2* query line in the direction of the arrow (inset figures) with Q_{μ} rock support

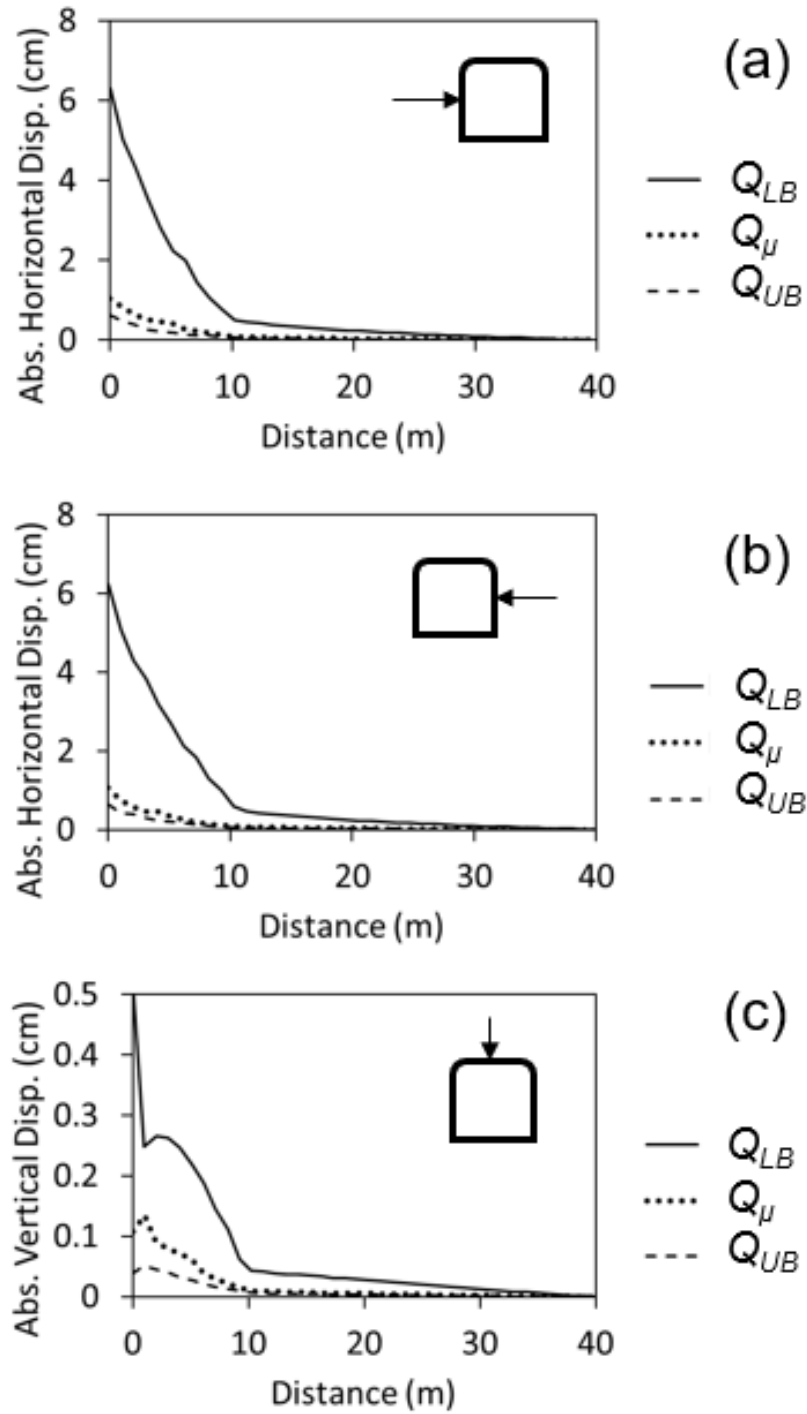


Fig 3-15. Absolute horizontal and vertical u_i measured along a 40 m long RS2 query line in the direction of the arrow (inset figures) without Q_{μ} rock support

Instead of u_i , a better measurement of rock support effectiveness is by analyzing the forces acting on the rock bolts and shotcrete. If there are no signs of rock bolts or the shotcrete reinforcement system is failing, and the u_i is not excessive, a designer can be confident the excavation is stable. Fig 3-16 illustrates the differential stress (σ_{1-3}) contours, and the axial force (P) occurring along the length of the bolt. The P is the solid white shading in Fig 3-16, presenting a graphical illustration of the P , where the maximum axial force (P_{max}) for each case is Q_{LB} (50.2 kN), Q_{μ} (47.6 kN), and Q_{UB} (39.3 kN). The data for all nine bolts for each model were collected to calculate the average axial force (P_{avg}) and P_{max} , plus a count of all events that exceeded 25% and 50% bolt capacity. As expected, significantly more events that exceeded 25% bolt capacity were measured in the Q_{LB} case comparatively to Q_{μ} and Q_{UB} . Table 3-12 presented these findings, and P_{avg} and P_{max} were highest for Q_{LB} , but no bolts experienced yielding in all three cases and only two events reaching 50% bolt capacity.

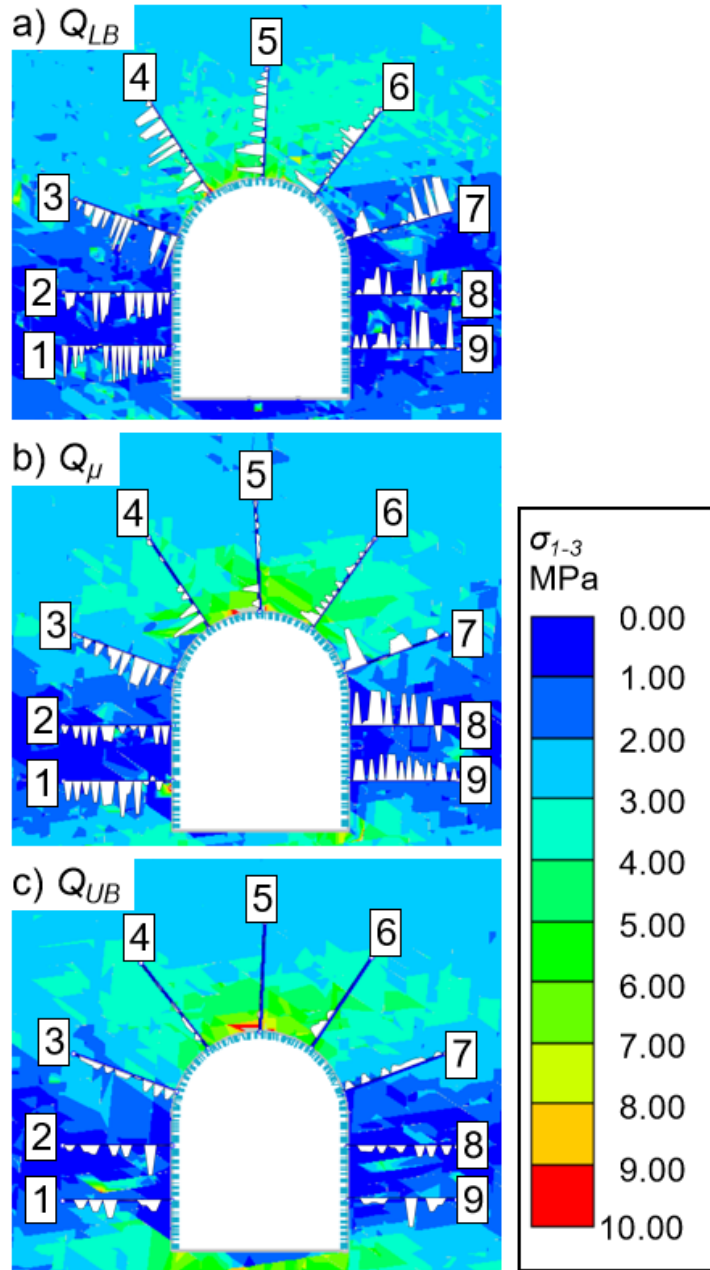


Fig 3-16. Graphical representation of P (solid white bars along bolts) along rock bolts with Q_{μ} rock support in Q_{LB} , Q_{μ} , and Q_{UB} rock masses ($P_{max} = 50.2$ kN)

Table 3-12. Summary of maximum and average axial force acting on rock bolts plus a count of axial events exceeding 25% and 50% rock bolt capacity for Q_μ rock support in Q_{LB} , Q_μ , and Q_{UB} models

	Q_{LB}	Q_μ	Q_{UB}
$\geq 25\%$ capacity events	102	64	4
$\geq 50\%$ capacity events	2	0	0
P_{max} (kN)	50.2	47.6	39.3
P_{avg} (kN)	13.0	10.6	4.4

A moment vs axial thrust diagram was produced to analyze the response of the shotcrete liner. The moment-thrust diagram allows an engineer to see the stresses acting on the shotcrete liner with relation to a specific strength envelope. For the study, the strength envelope for the shotcrete liner was based on the Carranza-Torres and Diederichs (2009) method from the dropdown menu in *RS2* with an $F = 1$, which is calculated based on Eq. 3-17. Fig 3-17 illustrated the moment-thrust diagram for the shotcrete liner, and it can be seen the axial thrust acting on the liner is minimal, due to the low stress field because of the shallow tunnel depth. On the other hand, a few points lie outside the $F = 1$ diamond in the Q_μ liner, expected to be directly related to a larger than anticipated block formed by the larger s_i . Shotcrete has been found in common practice to perform better than expected (Hoek, 2004), with the shotcrete adhering to the rock mass, helping blocks interact and self-support. In *RS2*, shotcrete is modelled as reinforced concrete similar to a standard beam; modelling the shotcrete more as a solid wall that holds back the rock mass, instead of a tool to improve arching. While a few results from the Q_μ and Q_{UB} moment-thrust diagram lie outside the $F = 1$ failure envelope, the overall liner should be considered stable.

$$FS = \frac{\sigma_c}{\sigma_{max}} = \frac{\sigma_t}{\sigma_{min}} \quad (3-17)$$

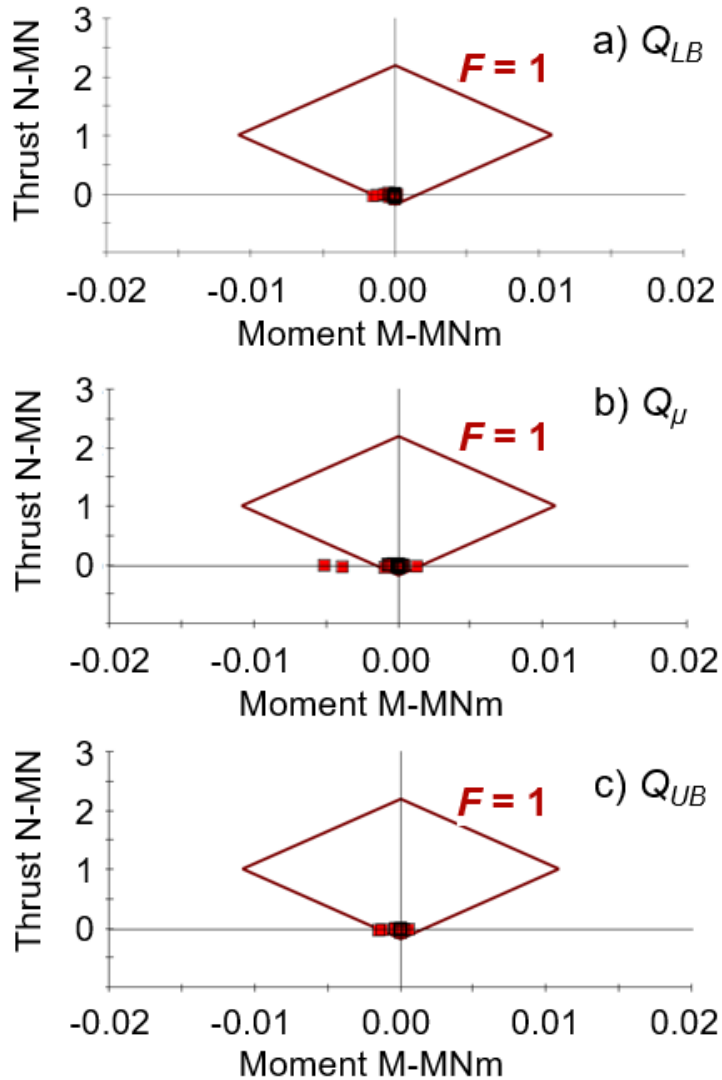


Fig 3-17. Moment-Thrust diagram of Q_{μ} shotcrete response in Q_{LB} , Q_{μ} , and Q_{UB} rock mass with an $F = 1$ design envelope

From the analysis of the NUOS site, it can be said the Q_{μ} rock support provides adequate support for all possible rock conditions. Applying the probabilistic approach to Q improves the accuracy of identifying rock quality and support recommendations at the preliminary design stage. Table 3-12 and Fig 3-17 show the Q_{μ} rock support is sufficient for the entire rock mass, but certain rock strength parameters were back-calculated from correlations with Q , and not based directly on measured field data. Q is a rating of the rock quality and not strength; therefore, a more effective way to analyze the Q_{μ} rock support response would be to create a model with measured rock properties, instead of estimated values from Q_{LB} , Q_{μ} , and Q_{UB} . A statistical analysis of the measured rock

strength properties compared to the Q_μ rock support will more effectively analyze the ground support response in all possible ground conditions.

3.6 Conclusion

Due to the uncertainty and variability that exists in individual rock parameters, simply classifying the quality of a rock mass within a domain using a single value can be inadequate. Deterministic methods do not correctly capture the uncertainty in individual rock parameters. Instead, a probabilistic design approach can improve the accuracy for estimating Q . With the methodology presented, an engineer can associate an acceptable level of risk based on the statistical range of all possible rock qualities and make a decision for ground support based on quantifiable uncertainty in the rock mass domain.

The current paper illustrates the application of a probabilistic design approach to estimate Q and ultimately the rock support for a tunnel, shaft, or cavern. The PDF and CDF of Q were calculated using the MCS method in the program *MATLAB*. Statistical analysis was performed on the geological data, and the μ , sd , and estimated distributive shape were used in the MCS to simulate each Q input parameter. The method was applied to the jointed rock masses at NUOS and NJHP, and it was found the simulated Q input parameters matched well with actual logged data, except for J_r , highlighting the importance of selecting the correct distributive shape. From the PDF and CDF, the point estimate values Q_{LB} , Q_μ , and Q_{UB} , present a range of design limits connected to an acceptable level of risk. The results show a significant difference in Q_{LB} and Q_μ , related to the extreme values that exist in the lognormal distribution Q follows. Q_μ rock support was suggested to be the design criteria; however, the mode of failure plays an important role in selecting ground support. In cases where Q_{LB} and Q_μ are completely different modes, considering a probability of exceedance instead of Q_μ may be a better option. To validate the suggestions made in the first portion of the paper, a FEM was developed in the program *RS2* to analyze the effectiveness of Q_μ rock support in different ground conditions. The model consisted of an EJM in the immediate tunnel vicinity where the explicit joint network was developed based on the DFN concept, and the remaining model was an ECM. In the FEM, the P_{avg} and P_{max} saw the greatest values in the Q_{LB} rock mass; however, no yielding occurred in the rock bolts, with only two events reaching

50% bolt capacity, and no apparent issues with the shotcrete liner. Tunnel strain was measured to be 3% in the Q_{LB} rock mass; however, increasing rock bolt concentration and shotcrete thickness to the Q_{LB} ground support recommendations resulted in no significant reduction in u_i . The results from the case study show Q_{μ} rock support was sufficient for Q_{LB} , Q_{μ} , and Q_{UB} ground conditions and should be used as the design criteria when performing a probabilistic design approach with Q.

Applying statistical analysis to classification systems presents a systematic approach to the design of rock support in underground excavations. Utilizing this method, an engineer can now see how the uncertainty in specific rock properties affects the overall rock quality. The results from the MCS allows an engineer to have confidence Q_{μ} rock support is a suitable design value. The case studies for the paper were jointed rock masses, which are ideal for Q; however, limitations do exist in Q when time-dependent failure is prevalent. Though these limitations exist, applying the current methodology to squeezing or swelling rock can provide more backing to the validity of the process, and potentially create a probabilistic approach to ground support for all failure modes. The tool provides an approach to define the quality of the rock mass more accurately, and the design criteria for rock support, reducing overly conservative/costly designs. Although, it is imperative to understand empirical methods are based on the judgement of the engineer or geologist, and improper data collection or assumptions can harm the overall design.

Chapter 4 Conclusion and Recommendations

Most rock mass domains are not homogeneous, and due to the geological structures, variability exists that affects the ground condition. The empirical classification system Q presents a means to broadly quantify the quality of a rock mass and provide ground support recommendations. However, can a single deterministic value or narrow range, accurately estimate the Q rating? Whether it is a single value representing each input parameter, or a statistical value based on a small dataset of measured Q, the issue of uncertainty and over-conservative estimations of rock quality exist. A better approach to the limited data problem is to perform statistical analysis on the Q input parameters, to perform a probabilistic design approach to estimate rock quality and the recommended ground support more accurately.

In the dissertation, geotechnical investigation data from the NUOS and NJHP case studies illustrated the use of the probabilistic design approach of Q using MCS with the mathematical program *MATLAB*. In the study, a statistical analysis of Q input parameters to determine the distribution and the μ and sd was performed. In both case studies, the RQD, J_n , J_r , and J_a were assumed to have a normal distribution, while the J_w and SRF for NUOS were a constant value of 1, and NJHP followed a triangular distribution. From the simulation, it was found the input parameters matched well with the actual data, except for J_r . Research has shown that particular distributions can be expected for different parameters. To ensure the most suitable distribution is selected to have the most accurate estimation of Q. While a lognormal distribution may be a better fit for J_r in both the NUOS or NJHP case, the author is confident in the estimation of Q for the current study.

In both case studies, Q_{LB} , Q_{μ} , and Q_{UB} were calculated to present the range of possible rock qualities between the bounds of $\mu \pm 1 sd$. The Q_{LB} , Q_{μ} , and Q_{UB} for the MCS of NUOS site data were 2.2, 9.9, and 17.7, while NJHP was 0.001, 3.1, and 6.9. It can be seen that a broad range of possible rock qualities exist, with NUOS measuring poor to good ground conditions and NJHP was exceptionally poor to fair. When compared to the tunnel behaviour chart, the dominant mode of failure for the NUOS case was the same for Q_{LB} and Q_{μ} , suggesting the recommended support has the potential to be effective in both Q_{μ} and Q_{LB} . This was not the case for NJHP, and while two different

modes of failure could exist in the rock mass, due to the high COV in the data, the Q_{LB} does not represent the ground condition over the rock mass domain. The Q_{LB} is a pseudo-worst-case scenario, and the ground support design should stabilize the expected ground condition. Instead of Q_{μ} and Q_{LB} , in cases such as NJHP, it is advisable to consider the probability of exceedance. When Q_{LB} ground conditions are experienced during production, alternative options can be implemented to mitigate the issue.

The results from the probabilistic design approach were compared to the deterministic results for the NUOS case study. The probabilistic approach produced a different Q_{μ} and Q_{LB} compared to the deterministic method. The test illustrates the idea of selecting the μ or $\mu \pm 1sd$ of each Q input parameter is not the same as calculating Q through a probabilistic design approach. Estimating Q , based on the statistical analysis of input parameters allows an engineer to measure uncertainty and variability in a rock mass domain to make an educated decision on the level of acceptable risk for a rock support design. The results were compared to the Q ground support recommendation chart for the NUOS case, basing the ground support design on the construction of a theoretical 5 m high and 4 m wide horse-shoe shaped tunnel. Based on the chart, support recommendations were similar for the Q_{μ} and Q_{UB} cases, while Q_{LB} suggested a higher concentration of rock bolts and thicker shotcrete. Based on a Q_{μ} rock support design, 2.5 m grouted rock bolts with 1.25 m spacing, and 5.5 cm shotcrete with a 4 mm mesh were suggested for the theoretical tunnel.

To validate the suggested design limit, a FEM was developed using the program *RS2* to analyze the response on Q_{μ} rock support over the range of possible rock qualities (Q_{LB} , Q_{μ} and Q_{UB}). The model was separated into two regions, an EJM in the immediate tunnel vicinity consisting of an explicit joint network based on the DFN concept, and the remaining model was an ECM. To analysis ground support response, the P acting along the rock bolts was measured, and the greatest P_{avg} and P_{max} were measured in the Q_{LB} rock mass; however, no yielding occurred in the rock bolts, with only two events reaching 50% bolt capacity. For the shotcrete liner, a moment-thrust diagram was developed, and due to the shallow depth of the excavation minimal axial thrust was experienced. Events of higher bending moment were measured in the liner for Q_{μ} rock mass model, but due to the way a liner is modelled in *RS2* it can be assumed no apparent

issues exist. In the Q_{LB} rock mass, tunnel strain was measured to be 3%, but when the concentration of rock bolt and shotcrete thickness is increased to the Q_{LB} ground support recommendations, no significant reduction in u_i was measured. The thesis presents both a methodology and justification that Q_{μ} rock support is sufficient for Q_{LB} , Q_{μ} , and Q_{UB} ground conditions. In cases where the range of ground conditions have a similar failure mode, Q_{μ} rock support should be used as the design criteria when performing a probabilistic design approach with Q.

The inherent variability that exists in a rock mass domain must be considered when determining rock support requirements. Applying statistical analysis of the measured input parameters to perform an MCS of Q presents a systematic approach to the design of ground support in underground excavations. However, further work can be performed to increase the value of the proposed methodology.

In the thesis, NUOS is a jointed rock mass, which is ideal for Q, and it has been noted that limitations do exist in Q when time-dependent failure is prevalent. In time-dependent failure, i.e. squeezing and swelling, the effects to Q have a strong correlation to the SRF. An in-depth study of the statistical distribution of the SRF for squeezing and swell conditions could increase the confidence in the estimate. Furthermore, performing the proposed method in squeezing and swell rock could validate the process and potentially create a probabilistic approach to ground support for all failure modes.

A second point to consider in the study, was the input parameters were assumed to be independent. While to a degree, this assumption is valid; parallels exist between J_r and J_a . Both ratings are categorized by the amount of shearing before rock contact, which is considered when the UL and LL are set in the simulation; however, on a smaller scale, a correlation may exist. A study on whether J_r and J_a (and other variables) are depended or independent, not only would ensure the most realistic results of produced but also if a relationship exists, the chance of a reduced COV for Q is possible.

References

- Andersson J, Shapiro AM, Bear J (1984) A Stochastic Model of a Fractured Rock Conditioned by Measured Information. *Water Resour Res* 20:79–88
- Barton N, Lien R, Lunde J (1974) Engineering Classification of Rock Masses for the Design of Tunnel Support. *Norg Geotek Inst, Publ 6*
- Bedi A (2013) A proposed framework for characterising uncertainty and variability in rock mechanics and rock engineering. Department of Earth Science and Engineering
- Beer, AJ; Stead, D; Coggan J (2002) Technical Note Estimation of the Joint Roughness Coefficient (JRC) by Visual Comparison. *Rock Mech Rock Eng* 35:65–74
- Bertuzzi R (2019) Revisiting rock classification to estimate rock mass properties. *J Rock Mech Geotech Eng* 11:494–510
- Bhasin R, Barton N, Loset F (1994) Engineering geological investigations and the application of rock mass classification approach in the construction of Norway's underground Olympic stadium. *Publ - Norges Geotek Inst* 194:93–101
- Bhasin R, Barton N, Grimstad E, Chryssanthakis P (1996) Engineering geological characterization of low strength anisotropic rocks in the Himalayan region for assessment of tunnel support. *Publ - Norges Geotek Inst* 197:169–193
- Bieniawski ZT (1989) Engineering rock mass classifications: a complete manual for engineers and geologists in mining, civil, and petroleum engineering. John Wiley & Sons
- Cai M (2011) Rock mass characterization and rock property variability considerations for tunnel and cavern design. *Rock Mech Rock Eng* 44:379–399
- Carranza-Torres C, Diederichs M (2009) Mechanical analysis of circular liners with particular reference to composite supports. For example, liners consisting of shotcrete and steel sets. *Tunn Undergr Sp Technol* 24:506–532
- Farahmand K, Vazaios I, Diederichs MS, Vlachopoulos N (2018) Investigating the scale-dependency of the geometrical and mechanical properties of a moderately jointed rock using a synthetic rock mass (SRM) approach. *Comput Geotech* 95:162–179
- Fossum AF (1985) Effective elastic properties for a randomly jointed rock mass. *Int J Rock Mech Min Sci* 22:467–470
- Grenon M, Hadjigeorgiou J (2003) Drift reinforcement design based on discontinuity network modelling. *Int J Rock Mech Min Sci* 40:833–845

- Hadjigeorgiou J (2012) Where do the data come from? *Trans Institutions Min Metall Sect A Min Technol* 121:236–247
- He S, Li Y, Aydin A (2018) A comparative study of UDEC simulations of an unsupported rock tunnel. *Tunn Undergr Sp Technol* 72:242–249
- Hoek E (2007) *Practical Rock Engineering*. www.rocsience.com
- Hoek E, Carter TG, Diederichs MS (2013) Quantification of the Geological Strength Index chart. 47th US Rock Mech Symp
- Kaiser PK, Maloney S (2005) Supporting Technical Report Review of Ground Stress Database for the Canadian Shield Report No: 06819-REP-01300-10107-R00 December 2005
- Kaiser PK, Diederichs MS, Martin CD, Sharp J, Steiner W (2000) Underground Works in Hard Rock Tunnelling and Mining. In: *GeoEng 2000 - Melbourne Australia*. pp 841–926
- Kulhawy F (1975) Stress Deformation Properties of Rock and Rock Discontinuities. *Eng Geol* 9:327–350
- Lang TA & Bischoff JA (1982) Stabilization of Rock Excavations Using Rock Reinforcement. In *Proceedings 23rd U.S. Symposium on Rock Mechanics* pp. AIME, New York. 935–944
- Limpert E, Stahel WA (2011) Problems with using the normal distribution - and ways to improve quality and efficiency of data analysis. *PLoS One* 6(7)
- Lu H, Kim E, Gutierrez M (2019) Monte Carlo simulation (MCS)-based uncertainty analysis of rock mass quality Q in underground construction. *Tunn Undergr Sp Technol* 94
- MATLAB [Computer software]. (2019) www.mathworks.com
- Martin CD, Kaiser PK, McCreath DR (1999) Hoek-Brown parameters for predicting the depth of brittle failure around tunnels. *Can Geotech J* 36:136–151
- Mas Ivars D, Pierce ME, Darcel C, et al (2011) The synthetic rock mass approach for jointed rock mass modelling. *Int J Rock Mech Min Sci* 48:219–244
- Mazzoccola DF, Millar DL, Hudson JA (1997) Information, uncertainty and decision making in site investigation for rock engineering. *Geotech Geol Eng* 15:145–180
- Milne D, Hadjigeorgiou J, Pakalnis R (1998) Rock mass characterization for underground hard rock mines. *Tunn Undergr Sp Technol* 13:383–391

- Norwegian Geotechnical Institute (2015) Using the Q-system: Rock mass classification and support design (handbook). www.ngi.no/eng
- Onsel IE, Ozturk CA, Ozkan M, Nasuf SE (2011) Software for RQD and rock mass evaluation. 45th US Rock Mech / Geomech Symp
- Palmström A, Broch E (2006) Use and misuse of rock mass classification systems with particular reference to the Q-system. *Tunn Undergr Sp Technol* 21:575–593
- Panthi K (2006) Analysis of Engineering Geological Uncertainties Related to Tunnelling in Himalayan Rock Mass Conditions
- Panthi K, Nilsen B (2010) Uncertainty analysis for assessing leakage through water tunnels: A case from Nepal Himalaya. *Rock Mech Rock Eng* 43:629–639
- Pells PJ, Bieniawski ZT, Hencher SR, Pells SE (2017) Rock quality designation (RQD): Time to rest in peace. *Can Geotech J* 54:825–834
- Pells PJ (2002) Developments in the design of tunnels and caverns in the Triassic rocks of the Sydney region. *Int J Rock Mech Min Sci* 39:569–587
- Potvin Y, Hadjigeorgiou J (2015) Empirical ground support design of mine drives. In: *Proceedings of the International Seminar on Design Methods in Underground Mining*. pp 419–430
- Priest SD, Hudson JA (1976) Discontinuity spacing in rock. *Int J Rock Mech Min Sci* 13:135–148
- RS2 [Computer software] (2019) www.rocscience.com
- Sen Z, Kazi A (1984) Discontinuity spacing and RQD estimates from finite length scanlines. *Int J Rock Mech Min Sci* 21:203–212
- Starfield, AM; Cundall P (1988) Towards a Methodology for Rock Mechanics Modelling. *Int J Rock Mech Min Sci Geomech* 25:99–106
- Tiwari G, Pandit B, Latha GM, Sivakumar Babu GL (2017) Probabilistic analysis of tunnels considering uncertainty in peak and post-peak strength parameters. *Tunn Undergr Sp Technol* 70:375–387
- Vlachopoulos N, Diederichs MS (2009) Improved longitudinal displacement profiles for convergence confinement analysis of deep tunnels. *Rock Mech Rock Eng* 42:131–146
- Ziebarth RA, Corkum AG (2019) Statistical Analysis of the Q-system in Different Tunnelling Conditions. In: *Geo St. John's Conference*. pp 1–7



Appendix A: 2019 Annual CGS Conference Paper

Statistical Analysis of the Q-system in Different Tunnelling Conditions

R.A. Ziebarth & A.G. Corkum

Department of Civil and Resource Engineering – Dalhousie University, Halifax, NS, Canada

ABSTRACT

Understanding of the quality of a rock mass is essential in determining the expected mode of failure and the support requirement for tunnel and cavern designs. The Q-system quantifies the quality of a rock mass, but due to the complex and varied mechanisms related to ground structure interaction, a single value is unlikely to classify the variety in a rock mass correctly. Statistical methods can account for uncertainty to select the suitable design value for Q instead of a deterministic value, based on estimated Q input parameters. In this study, the Monte Carlo simulation (MCS) method is used to apply statistical analysis to the Q-system. The paper describes the basis and methodology, in conjunction with a case study, to present the use of MCS analysis, of the Q-system, to associate a quantitative level of risk with determining ground support needs for tunnel and cavern excavations.

RÉSUMÉ

La compréhension de la qualité d'une masse rocheuse est essentielle pour déterminer le mode de rupture prévu et les exigences de soutien pour la conception des tunnels et des cavernes. Le système Q quantifie la qualité d'une masse rocheuse, mais en raison des mécanismes complexes et variés liés à l'interaction de la structure du roches, il est peu probable qu'une seule valeur puisse classer correctement la variété dans une masse rocheuse. Les méthodes statistiques peuvent tenir compte de l'incertitude pour choisir la valeur de calcul appropriée pour Q au lieu d'une valeur déterministe, en fonction des paramètres d'entrée Q estimés. Dans cette étude, la méthode de simulation de Monte Carlo (MCS) est utilisée pour appliquer l'analyse statistique au système qualité. Le document décrit la base et la méthodologie, en conjonction avec une étude de cas, pour présenter l'utilisation de l'analyse MCS, du système Q, afin d'associer un niveau quantitatif de risque à la détermination des besoins d'appui au sol pour les excavations en tunnel et en caverne.

1. INTRODUCTION

In tunnel and cavern design, identifying the quality of a rock mass is essential to both determining the dominant mode of failure and adequate ground support to manage it. Empirical classification systems present a quantifiable representation of the rock mass which recommends ground support measures; however, is it advisable to place a single value that classifies the quality of an entire rock mass? Multiple conservative estimations of input parameters to determine rock quality can lead to redundancy, and overestimation of support requirements.

Two of the most widely used empirical classification systems are the Rock Mass Quality Index (Q) (Barton et al. 1974) and Rock Mass Rating (RMR) (Bieniawski, 1989). The Q-system considers multiple parameters, such as joint characteristics and stress regime, to classify the overall quality of a rock mass and provide ground support recommendations. A single Q input parameter, such as joint roughness (J_r), does not wholly define an entire rock mass, but it can significantly affect the overall rating. The Q-system relies on visual observation, instead of an analytical calculation or numerical modelling, which introduces greater potential for human error to affect the estimation. Complex and varied mechanisms related to ground interaction make considering a single value for a Q parameter impractical and can lead to over, or under, evaluation of Q. If a design is believed to be conservative, to decrease the quantity of rock support provides no accurate measurement of its effectiveness. Facilitating the planning process of ground support with statistical analysis reduces the potential to under, or over, estimate the quality of the rock mass.

Ground support recommendations, for Q, are directly correlated to the performance of historical case data, and the majority of the existing data for the Q-system are tunnels from the Scandinavia region. Different conditions can significantly affect the performance of ground support, which can be problematic, leading to the question of how conservative a designer should be (Potvin, 2015). Palmstrom and Broch (2006) performed

a detailed review of the limitations of the Q-system, and one major takeaway was that the classification system was most accurate in moderately fractured rock. Specific scenarios can see a substantial alteration in the support installed to recommendations by the Q-system, such as Hawkesbury Sandstone, where Q recommended substantially lower support than what was adopted at five specific sites (Pells, 2002). Overall, empirical analysis is reliant on the capabilities of the investigator. Statistical methods can provide an alternative which can enhance the classification system by allowing a quantifiable level of risk to be estimated instead of relying on judgement alone.

In this paper, the idea of statistical analysis methods to facilitate the planning process of ground support will be discussed. Monte Carlo Simulation (MCS), considering all measured Q input parameters as independent variables, was implemented to develop probability (PDF) and cumulative distribution function (CDF) curves of Q, creating an intuitive method for determining the rock mass quality. A case study on the Norwegian Underground Olympic Stadium (NUOS) demonstrates the process, illustrating how a designer can use the statistical curves. Through this method, the raw measured data provides a means to allocate an acceptable level of risk when determining support requirements for underground excavations.

2. REVIEW OF THE Q-SYSTEM

The Q rating consists of three terms which provide a generalisation of the block interaction and stress condition for tunnelling projects (NGI, 2015), measuring the:

- Block Size (RQD/J_n)
- Joint Condition (J_r/J_a)
- Effective Stress (J_w/SRF)

By calculating the product of the three subgroups, the six rock parameters produce a single value that represents the overall quality of the rock mass as seen in the equation below.

$$Q = (RQD/J_n) * (J_r/J_a) * (J_w/SRF) \quad (1)$$

2.1 Block Size (RQD/J_n)

The quotient of the Rock Quality Designation (RQD) and the joint number (J_n) represents the relative size of the blocks in the rock mass. Understanding the size of the blocks, corresponding to the excavation span, provides insight into the potential failure modes and effects the type of ground support required.

RQD provides a rough estimate of the frequency of jointing occurring in a rock mass, but it is also important to understand whether these joints are random or have a general spatial trend. J_n is a measurement of the number of occurrences where joints trend in a similar orientation, with systematic spacing, yet if a very large spacing exists between the joints they should be considered random. The values for block size can range by a magnitude of 400, with the potential for a massive rock mass to be measured as high as 100/0.5 or as low as 10/20 for crushed rock (Palmstrom and Broch, 2006).

2.2 Joint Condition (J_r /J_a)

The size of the blocks provides a fundamental understanding of the expected mode of failure, but one must also understand the condition of the joint's surface, which affects block interaction. The surface structure (e.g. joint aperture, roughness, wall strength and infilling material) has a significant effect on the frictional interaction and overall, the shear strength between joint contacts. Reducing shear movement along the joints, due to increased friction, improves the compression arch in the block network, and overall stability of an excavation. Based on this, joints with rock-wall contact and a light coating of material on the surface of the discontinuity improve the quality with a joint condition value as high as 4/0.75, while joints with no contact and thick bands of clay can have a joint condition of 1/20.

2.3 Effective Stress (J_w/SRF)

The block size and condition play a significant role in determining the potential mode of failure; however, the stability of an excavation is directly related to the effective stress acting on the rock mass. Block network and stress conditions provide a framework to estimate the potential mode of failure that exists in a rock mass (Martin et al. 1999). The existence of high and low-stress conditions in connection with pore pressure can have a positive or negative effect on stability, making it impossible to allocate inter-block effective stress (Hoek, 2004); on the other hand, a general estimation of the stress condition can be made.

The inflow of water has two significant effects on the stability of a rock mass, (1) inflow can reduce the normal stress by pushing the joints apart, and (2) removal of infill material which provides frictional

resistance. On the other hand, SRF is a relative measure between the stresses acting on the rock mass and the rock strength (NGI, 2015). The stress condition is classified into one of four categories, weak zones, competent rock with stress issues, squeezing rock and swelling rock. In cases, such as competent rock and squeezing rock, the uniaxial compressive strength (σ_c) and the major principle stress (σ_1) or the maximum tangential stress (σ_{max}), provide a framework to estimate the SRF. For weak zones, visual evaluation of the size and frequency of problematic zones provides a means to quantify the effects on the overall rock quality, while swelling rock considers the magnitude of the reaction related to the addition of water within the rock structure.

2.4 Support Recommendation Chart

By comparing the Q to the Equivalent Dimension (D_e), Figure 1 illustrates how a designer can recommend bolt spacing, bolt length and shotcrete for a specific tunnel or cavern. The D_e is the quotient of the span or height of the excavation, in meters, and the Excavation Support Ratio (ESR), a generalised safety factor which accounts for the longevity/importance of the excavation.

3. STATISTICAL VARIABILITY AND DESIGN CONSIDERATIONS FOR THE Q-SYSTEM

The support recommendation chart is based on historical case history data to predict the most suitable ground support. As new data is collected, a more accurate estimation for ground support exists, although inherent variability is present, since an individual can estimate the quality of a rock mass differently than another. Because of this, understanding the standard deviation (SD), and distribution of the data is crucial since a larger SD indicates a substantially higher spread of potential outcomes.

The general trend of the data plays a significant role in any statistical analysis. While a normal distribution is a symmetrical shape, where the vast majority of data lies within two SD, this is not the case for all statistical distributions. Any distribution has the potential to have extreme data points, which can cause an abnormally large SD, raising the question: should the probability of exceedance be considered?

3.1 Variability of Q Parameters

The significant factors that determine the quality of the rock mass are the product of the block size and joint condition, known as Q' . Effective stress, due to the effects of pore pressure, is an essential factor to consider, but it can be challenging to define, and often is regarded as a constant value.

The presence of an aquifer or surface water over specific spans in a longer reach of a tunnel can cause variability in the groundwater condition, although J_w is generally a constant value. Similarly, in most cases for the SRF, unless the rock type drastically changes or water causes swelling, the reduction value is kept constant. At the same time, anisotropic stress conditions present the potential for variability to exist in the maximum tangential stress which is directly related to the orientation of the excavation and the principle stresses, which have been seen to typically follow a normal distribution (Kaiser and Maloney, 2005).

3.2 Monte Carlo Simulation (MCS)

MCS has been implemented in numerous engineering disciplines, presenting a useful approach to analyse distributions with random data inputs. When the statistical data and its distribution of input values are known, and the random variables have a direct relation to the solution, MCS is a viable option.

The geotechnical assessment of a particular site provides valuable statistical data which can be used in conjunction with the mathematical software MATLAB² to develop PDF and CDF curves. Each Q input parameter has an absolute lower limit (LL) and upper limit (UL) that cannot be exceeded; therefore, all random variables are truncated to the values in Table 1, dependent on the existing conditions for the rock mass in question. Truncating the data has the potential to distort the PDF of each Q parameter somewhat; however, to ensure that the LL and UL were not exceeded this was considered valid until alternative methods can be applied.

4. EXAMPLE APPLICATION OF METHOD

Field data from the Norway Underground Olympic Stadium (NUOS) was used to demonstrate the statistical design method for the Q-system. The NUOS is a vast cavern, with a span of 64 m; therefore, all data is

² <https://www.mathworks.com>

experienced on the extremities of the recommendation chart (Bhasin et al. 1993). Instead of directly analysing the existing excavation a theoretical excavation of a 10 m wide roadway, ESR = 1, was considered instead of the actual dimensions of the stadium. An excavation of this size will see the simulated PDF of Q occur in a more central location of the support recommendation chart, providing a better illustration of the statistical analysis of the Q-system.

4.1 Location and Geotechnical Investigation

The NUOS is located in Gjovik city, 25 km south of Lillehammer, Norway. Nearby caverns and access tunnels in the hillsides were investigated as they were expected to have the same geology, and mapping was performed on the Precambrian gneiss. The frequency of jointing in the Precambrian gneiss was determined to have large variability (Bhasin et al. 1993). Overall, the initial investigation determined the rock mass would have lower quality, and the high horizontal stress of 3.5 – 4 MPa at a shallow depth of 45 m presented the potential for stability issues.

Table 1. Lower and upper limits for Q-system rock parameters

Q Parameter	Cat.	Description	LL	UL
RQD	-	-	10	100
J_n	-	-	0.5	20
J_r	a	Rock-wall contact (no mineral fillings, only coatings)	0.5	4
	b	Rock-wall contact before 10 cm shear (thin mineral fillings)	0.5	4
	c	No rock-wall contact when sheared (thick mineral fillings)	1	1
J_a	a	Rock-wall contact (no mineral fillings, only coatings)	0.75	4
	b	Rock-wall contact before 10 cm shear (thin mineral fillings)	4	12
	c	No rock-wall contact when sheared (thick mineral fillings)	6	20
J_w	-	-	0.05	1
SRF	a	Weak zones	2.5	10
	b	Competent rock with stress issues	0.5	400
	c	Squeezing Rock	5	20
	d	Swelling Rock	5	15

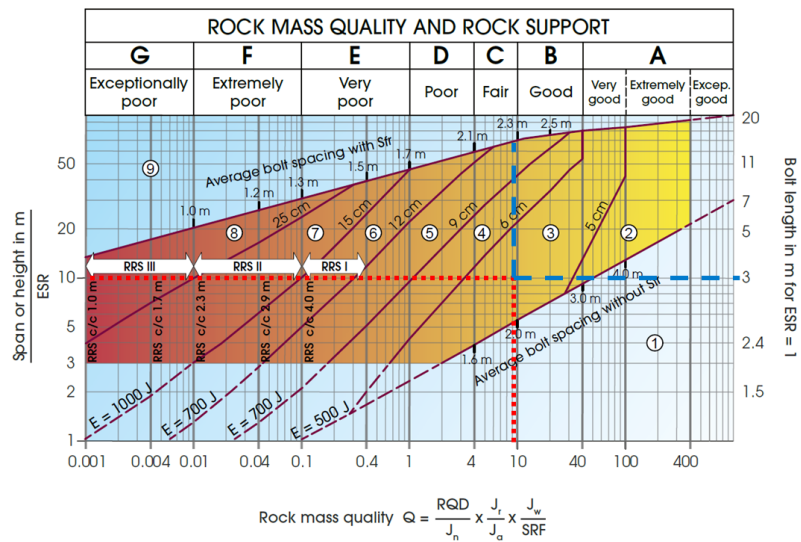


Figure 1. Q-system Support Recommendation Chart with an example, the dotted line is measured values and dashed shows recommended support (revised from NGI, 2015)

4.2 Statistical Data Collection

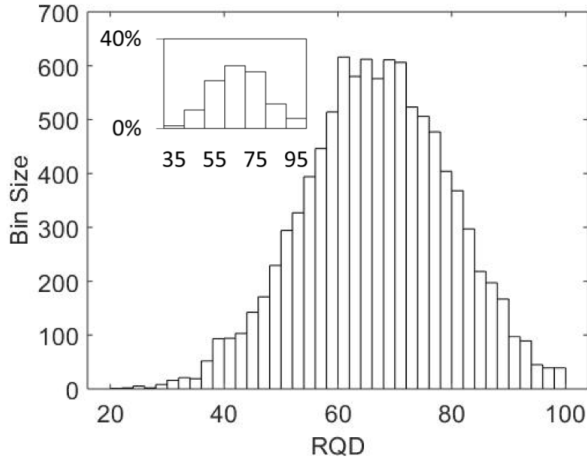
Based on the geotechnical investigation, histograms of the measured data were developed to estimate the Q for the rock mass. The original geotechnical study analysed the extreme low and high values, plus the weighted average for Q, determining the rock mass had a range of 1.1, 9.4 and 30. These values were based on differing block sizes and joint condition; however, the effective stress was considered to be constant with a value of 1. Before implementing MCS the statistical μ and SD for each parameter were calculated from the field data, presented in Table 2.

Table 2. Statistical parameters determined from measured data during the geotechnical investigation of NUOS

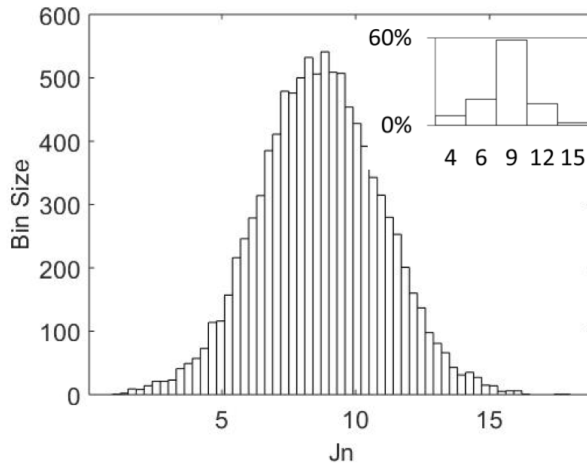
Q Parameter	μ	SD	LL	UL
RQD	67.0	13.2	10	100
J_n	8.7	2.3	0.5	20
J_r	2.3	0.6	0.5	4
J_a	1.9	1.4	0.75	4

4.3 Monte Carlo Simulation Analysis

The statistical distribution of all rock parameters was considered to be normally distributed, and histograms were simulated with the program MATLAB. The input parameters for the MCS can be seen in Table 2, which include the μ and SD from the measured data for each Q input parameter, and LL and UL determined to be in category (a) for the J_r and J_a based on the statistical data. Due to the effective stress being considered a constant value of 1, histograms of the RQD, J_n , J_r and J_a were only developed. Figures 2 and 3 illustrate these simulations, and it can be seen all parameters, except J_r , match almost identically with the measured field data. While the idea of J_r being normally distributed has validity to it, there is the potential for any parameter not to have a perfectly normal distribution and be skewed.



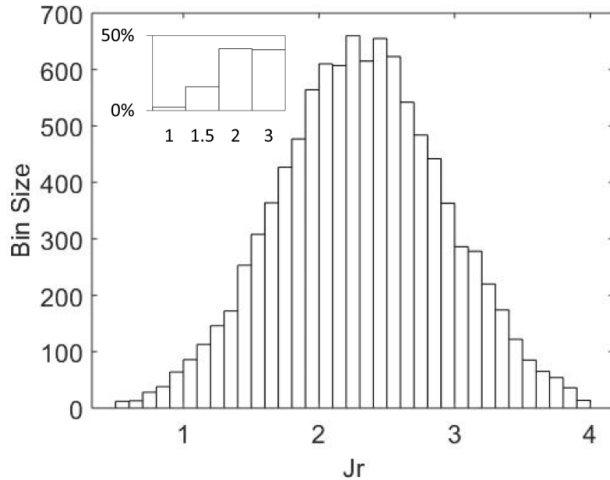
a) Distribution of Measured and Simulated RQD



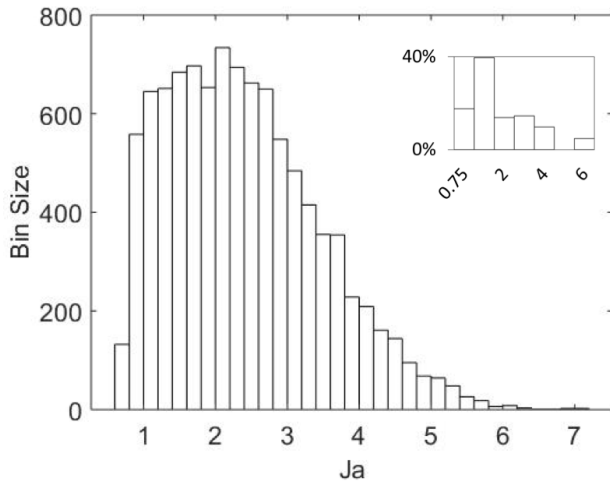
b) Distribution of Measured and Simulated J_n

Figure 2. Distribution of block size parameters using MCS compared to actual measured data (inset figures).

In the MCS, 10,000 iterations were performed with MATLAB to develop the PDF and CDF curves illustrated in Figure 4. An “if” statement was developed to determine UL and LL, considering a single type of rock contact and SRF for the simulation. With the limits set, the “makedist”, “truncate” and “random” commands were implemented, creating an individual value for each Q input parameter in a single iteration. The “makedist” function set the shape of the distribution, e.g. normal, log-normal, etc., while “truncate” ensures no data is generated outside the UL and LL. Based on the shape of the distribution, considering the μ , SD, UL and LL, the “random” command will generate a value for each Q input parameter. In cases where the data generated is outside the UL and LL, the iteration repeats until all conditions are met, which can slightly distort the PDF of a specific Q input parameter. Truncating the data raises the question of whether the simulation causes slight deviation from the intended distribution; however, the number of data points that have the potential to exist outside the UL and LL are negligible compared to the sample size and do not affect the validity of the analysis. At the end of each iteration, Q is calculated with equation 1, overall producing 10,000 Q data points based on the statistical data from each input parameter. For design purposes, the PDF can be compared to either the mean Q (Q_μ) or plus/minus one SD denoted as the lower bound (Q_{LB}) and upper bound (Q_{UB}). Additionally, using the CDF, an acceptable level of risk can be applied as a design parameter.



a) Distribution of Measured and Simulated J_r



b) Distribution of Measured and Simulated J_a

Figure 3. Distribution of joint conditions parameters using Monte Carlo simulation compared to actual measured data (inset figures)

Overall, Figure 4 provides useful insight into the classification of the quality of the rock mass, but the primary reason for the study is to relate this statistical analysis to recommendations for ground support directly. Figure 5 illustrates the PDF and CDF curves superimposed on top of the recommendation chart to allow for statistical analysis to be implemented to determine ground support requirements for an excavation.

Based on the simulation a Q_μ was found to be 10, and the Q_{LB} was 2.5. Both statistical points suggest a bolt length of 3 m; in contrast the significant difference is related to spacing and shotcrete requirements, where a change was experienced for the shotcrete requirements from zone 3 (5-6 cm fibre reinforced shotcrete) to zone 4 (6-9 cm fibre reinforced shotcrete) and a decrease in bolt spacing of 0.3 m.

D_e has a significant effect on the shotcrete requirements, and if the 10 m tunnel were increased to a 20 m cavern the range from the μ_Q to Q_{LB} would increase drastically, ranging from zone 3 to zone 5 (which is 9-12 cm of shotcrete). The Q_μ and Q_{LB} provide a reasonable estimate for a practical Q ; however, comparing the probability of exceedance is another option which could be better due to the fact in many cases the SD of the distribution is quite large compared to the Q_μ .

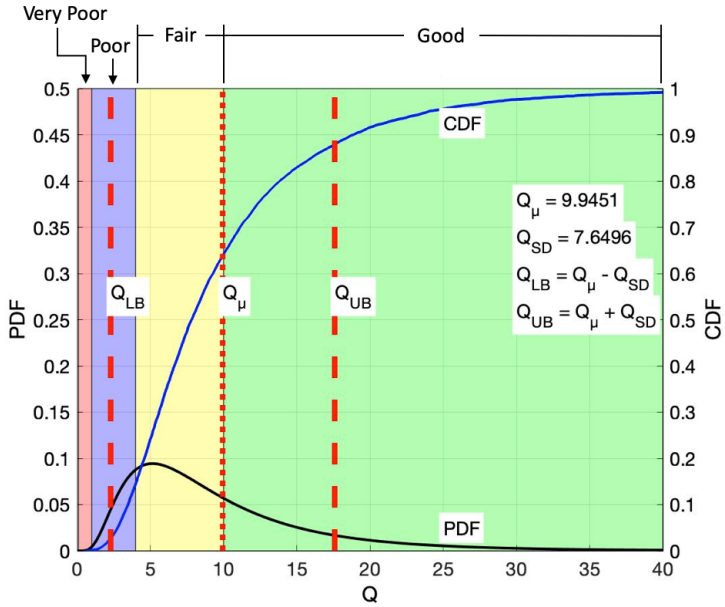


Figure 1. PDF and CDF of Q compared to statistical values Q_μ , Q_{LB} and Q_{UB} , plus the shade rock classification zones

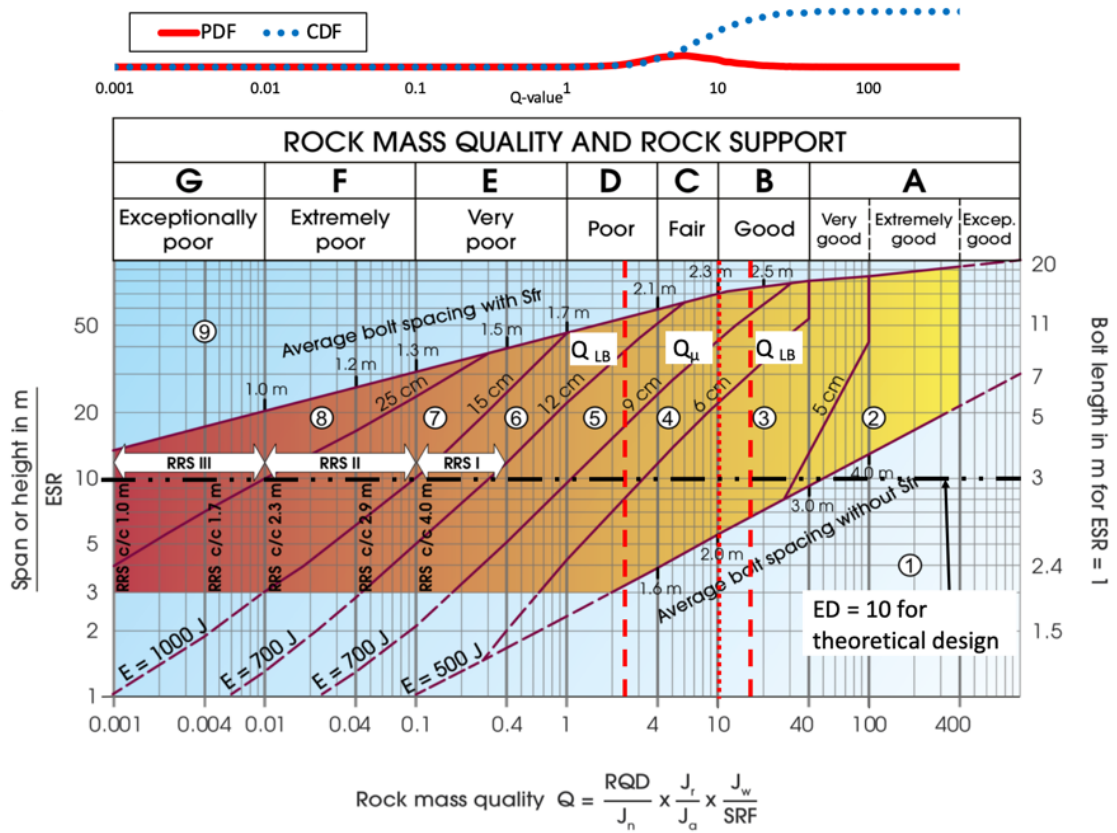


Figure 2. Support recommendation chart for Q with the MCS superimposed on top (revision of NGI, 2015).

5. FUTURE DISCUSSION

The results of MCS are only as reliable as the input parameters, and as shown in Figure 3a, it may not always be normally distributed. Different types of distributions for each Q parameter should be considered to ensure a close match with the measured field data. Further, by forcing all Q parameters to lie within the LL and UL the PDFs can be somewhat distorted, putting into question the validity of the simulation. Instead, placing the data in log-normal space, to ensure no negative values exist, and running the simulation may be a better option.

The Q-system works best in the moderately jointed rock mass, and time-dependent failure such as squeezing or swelling can be challenging to predict ground support measures. Instead, comparing the magnitude of potential tunnel deformation to the estimated Q value, and support recommendation could be beneficial. By correlating tunnel deformation and the Q, support recommendations can be compared to bolt and shotcrete response through numerical modelling to determine if the suggested ground support has the capabilities to manage the expected tunnel deformation.

6. CONCLUSION

Deterministic methods place a significant emphasis on the abilities of the engineer to accurately estimate Q as a single value that defines the entire rock mass. Alternatively, by considering the variability in each Q input parameter, a statistical design approach provides the ability to analyse all likely rock conditions.

This paper illustrated the use of statistical analysis on the Q-system to design ground support for tunnels and caverns. The Q was calculated using MCS with the program MATLAB to develop PDF and CDF curves. The method was applied to a jointed rock mass at the NUOS, considering the geotechnical data with a theoretical tunnel design. Before Q was calculated histograms of each Q parameters were developed with MCS, and it was found the simulated data almost perfectly matched the shape of the measured data, except J_r , validating the assumptions, but presenting the idea of considering different distributions for each specific Q parameters. Figure 5 illustrated by superimposing the PDF and CDF curves on the support recommendation chart substantially difference in support requirements are suggested considering the Q_{μ} and Q_{LB} . A difference in bolt spacing of 0.3 m and 1-3 cm thicker shotcrete for the Q_{μ} and Q_{LB} of a 10 m roadway tunnel was determined, while a 20 m cavern saw an increase of 4-7 cm of shotcrete, in the NUOS rock mass.

Instead of merely making an assumption all Q input parameters are a single estimated value, the Q_{μ} and Q_{LB} considered the dispersion Q. A designer can now review all potential rock conditions and the likelihood that best suits the project in question, to make a sound judgement for the ground support design. The tool provides a new approach to improve an existing system potentially. While this may be correct, empirical methods are based on the judgement of the geologist or engineer, and experience of the individual will be a driving factor to determine how risk-averse the project will be.

REFERENCES

- Barton, N., Lien, R., and Lunde, Z. (1974). Engineering Classification of Rock Masses for the Design of Tunnel Support. *Rock Mechanics*, 6, 189-236.
- Cai, M. (2011). Rock Mass Characterization and Rock Property Variability Considerations for Tunnel and Cavern Design. *Rock Mechanics Rock Engineering*, 44, 379–399.
- Hoek, E. (2004). Rock Mass Classification. Hoek's Corner, rocscience.com, accessed April 2019.
- Kaiser, P. K., & Maloney, S. (2005). Review of ground stress database for the Canadian Shield. Prepared by MIRARCO Mining Innovation. Ontario Power Generation, Nuclear Waste Management Division Report.
- C.D. Martin, P.K. Kaiser, and D.R. McCreath. (1999). Hoek–Brown parameters for predicting the depth of brittle failure around tunnels. *Canadian Geotechnical*. 36, 136–151.
- NGI. (2015). The Q-system Handbook, www.ngi.no, accessed January 30, 2018.
- R. Bhasin, N. Barton and F. Loset. (1993). Engineering geological investigation and the application of rock mass classification approach in the construction of Norway's underground Olympic stadium. *Engineering Geology*, 35, 93-101.
- Palmstrom, A. and Broch, E. (2006). Use and misuse of rock mass classification systems with particular reference to the Q-system. *Tunnelling and Underground Space Technology*, 21, 275-593.
- Palmstrom, A. and Stille, H. (2007). Ground behaviour and rock engineering tools for underground excavations. *Tunnelling and Underground Space Technology*, 22, 2363-376.

Pells, P.J. (2002). Developments in the design of tunnels and caverns in the Triassic rocks of the Sydney region. *International Journal of Rock Mechanics & Mining Sciences*, 39, 569–587.

Potvin, Y., & Hadjigeorgiou, J. (2015, November). Empirical ground support design of mine drives. In *Proceedings of the International Seminar on Design Methods in Underground Mining* (pp. 419-430). Australian Centre for Geomechanics.

Appendix B: *MATLAB* Code for MCS

```
% -----  
% This code performs Monte Carlo simulation to develop  
% the PDF and CDF of Q for the probabilistic design approach  
% based on the statistical analysis of the Q input parameters.  
% -----  
  
% Q input parameters  
% -----  
% RQD = Degree of jointing (Rock Quality Designation)  
% Jn = Joint set number  
% Jr = Joint roughness number  
% Ja = Joint alteration number  
% Jw = Joint water reduction factor  
% SRF = Stress Reduction Factor  
% -----  
  
% Model Terms  
% -----  
% mu = Mean ( $\mu$ )  
% sigma = Standard Deviation (sd)  
% n = Sample Size  
% -----  
  
% Joint and Stress Condition Classifications  
% -----  
% Rock_Contact = 1 (Rock contact)  
% Rock_Contact = 2 (Rock contact before 10 cm shear)  
% Rock_Contact = 3 (No rock contact when sheared)  
  
% Stress_Condition = 1 (Weak zone)  
% Stress_Condition = 2 (Competent w. stress issues)  
% Stress_Condition = 3 (Squeezing rock)  
% Stress_Condition = 4 (Swelling rock)  
% -----  
  
% Model parameters to determine joint condition category,  
% stress category and number of iterations (n).  
% -----  
n = 100000;  
NUOS_Rock_Contact = 12;  
NUOS_Stress_Condition = 2;  
NJHP_Rock_Contact = 12;  
NJHP_Stress_Condition = 2;  
% -----
```

% Field data measurements for Q input parameters at NUOS

```
% -----  
RQD_muNUOS = 67;  
RQD_sigmaNUOS = 13.1;  
Jn_muNUOS = 8.7;  
Jn_sigmaNUOS = 2.3;  
Jr_muNUOS = 2.3;  
Jr_sigmaNUOS = 0.7;  
Ja_muNUOS = 1.9;  
Ja_sigmaNUOS = 1.4;  
Jw_muNUOS = 1;  
Jw_sigmaNUOS = 0;  
SRF_muNUOS = 1;  
SRF_sigmaNUOS = 0;  
% -----
```

% Field data measurements for Q input parameters at NJHP

```
% -----  
RQD_muNJHP = 69.5;  
RQD_sigmaNJHP = 16.3;  
Jn_muNJHP = 5.2;  
Jn_sigmaNJHP = 2.1;  
Jr_muNJHP = 2.7;  
Jr_sigmaNJHP = 0.6;  
Ja_muNJHP = 2.6;  
Ja_sigmaNJHP = 1.9;  
Jw_aNJHP = 0.6;  
Jw_bNJHP = 1;  
Jw_cNJHP = 1;  
SRF_aNJHP = 2.5;  
SRF_bNJHP = 2.5;  
SRF_cNJHP = 20;  
% -----
```

% Setting lower limit (LL) and upper limit (UL) for input parameters

% based on joint condition and stress category for NUOS.

```
% -----  
RQD_LLNUOS = 10;  
RQD_ULNUOS = 100;  
  
Jn_LLNUOS = 0.5;  
Jn_ULNUOS = 20;  
  
Jw_LLNUOS = 0.05;  
Jw_ULNUOS = 1;
```

```
if NUOS_Rock_Contact == 1
  Jr_LLNUOS = 0.5;
elseif NUOS_Rock_Contact == 2
  Jr_LLNUOS = 0.5;
elseif NUOS_Rock_Contact == 12
  Jr_LLNUOS = 0.5;
else NUOS_Rock_Contact == 3;
  Jr_LLNUOS = 1;
end
```

```
if NUOS_Rock_Contact == 1
  Jr_ULNUOS = 4;
elseif NUOS_Rock_Contact == 2
  Jr_ULNUOS = 4;
elseif NUOS_Rock_Contact == 12
  Jr_ULNUOS = 4;
else NUOS_Rock_Contact == 3;
  Jr_ULNUOS = 1;
end
```

```
if NUOS_Rock_Contact == 1
  Ja_LLNUOS = 0.75;
elseif NUOS_Rock_Contact == 2
  Ja_LLNUOS = 4;
elseif NUOS_Rock_Contact == 12
  Ja_LLNUOS = 0.75;
else NUOS_Rock_Contact == 3
  Ja_LLNUOS = 6;
end
```

```
if NUOS_Rock_Contact == 1
  Ja_ULNUOS = 4;
elseif NUOS_Rock_Contact == 2
  Ja_ULNUOS = 12;
elseif NUOS_Rock_Contact == 12
  Ja_ULNUOS = 12;
else NUOS_Rock_Contact == 3
  Ja_ULNUOS = 20;
end
```

```
if NUOS_Stress_Condition == 1
  SRF_LLNUOS = 2.5;
elseif NUOS_Stress_Condition == 2
  SRF_LLNUOS = 0.5;
elseif NUOS_Stress_Condition == 3
  SRF_LLNUOS = 5;
```

```

else NUOS_Stress_Condition == 4
    SRF_LLNUOS = 5;
end

if NUOS_Stress_Condition == 1
    SRF_ULNUOS = 10;
elseif NUOS_Stress_Condition == 2
    SRF_ULNUOS = 400;
elseif NUOS_Stress_Condition == 3
    SRF_ULNUOS = 20;
else NUOS_Stress_Condition == 4
    SRF_ULNUOS = 15;
end
% -----

% Setting lower limit (LL) and upper limit (UL) for input parameters
% based on joint condition and stress category for NJHP.
% -----
RQD_LLJHP = 10;
RQD_ULJHP = 100;

Jn_LLJHP = 0.5;
Jn_ULJHP = 20;

Jw_LLJHP = 0.05;
Jw_ULJHP = 1;

if NJHP_Rock_Contact == 1
    Jr_LLJHP = 0.5;
elseif NJHP_Rock_Contact == 2
    Jr_LLJHP = 0.5;
elseif NJHP_Rock_Contact == 12
    Jr_LLJHP = 0.5;
else NJHP_Rock_Contact == 3;
    Jr_LLJHP = 1;
end

if NJHP_Rock_Contact == 1
    Jr_ULJHP = 4;
elseif NJHP_Rock_Contact == 2
    Jr_ULJHP = 4;
elseif NJHP_Rock_Contact == 12
    Jr_ULJHP = 4;
else NJHP_Rock_Contact == 3;
    Jr_ULJHP = 1;
end

```



```

if NJHP_Rock_Contact == 1
  Ja_LLJHP = 0.75;
elseif NJHP_Rock_Contact == 2
  Ja_LLJHP = 4;
elseif NJHP_Rock_Contact == 12
  Ja_LLJHP = 0.75;
else NJHP_Rock_Contact == 3
  Ja_LLJHP = 6;
end

```

```

if NJHP_Rock_Contact == 1
  Ja_ULJHP = 4;
elseif NJHP_Rock_Contact == 2
  Ja_ULJHP = 12;
elseif NJHP_Rock_Contact == 12
  Ja_ULJHP = 12;
else NJHP_Rock_Contact == 3
  Ja_ULJHP = 20;
end

```

```

if NJHP_Stress_Condition == 1
  SRF_LLJHP = 2.5;
elseif NJHP_Stress_Condition == 2
  SRF_LLJHP = 0.5;
elseif NJHP_Stress_Condition == 3
  SRF_LLJHP = 5;
else NJHP_Stress_Condition == 4
  SRF_LLJHP = 5;
end

```

```

if NJHP_Stress_Condition == 1
  SRF_ULJHP = 10;
elseif NJHP_Stress_Condition == 2
  SRF_ULJHP = 400;
elseif NJHP_Stress_Condition == 3
  SRF_ULJHP = 20;
else NJHP_Stress_Condition == 4
  SRF_ULJHP = 15;
end

```

```

% -----

```

```

% Statistical analysis of Q input parameter based on assumed distribution
% and UL and LL truncation limits for NUOS.

```

```

% -----

```

```

if RQD_sigmaNUOS == 0

```

```

RQD_NUOS = RQD_muNUOS;
else pd_RQDNUOS = makedist('Normal', 'mu', RQD_muNUOS, 'sigma',
RQD_sigmaNUOS);
t_RQDNUOS = truncate(pd_RQDNUOS, RQD_LLNUOS, RQD_ULNUOS);
RQD_NUOS = random(t_RQDNUOS, n, 1);
end

if Jn_sigmaNUOS == 0
Jn_NUOS = Jn_muNUOS;
else pd_JnNUOS = makedist('Normal', 'mu', Jn_muNUOS, 'sigma', Jn_sigmaNUOS);
t_JnNUOS = truncate(pd_JnNUOS, Jn_LLNUOS, Jn_ULNUOS);
Jn_NUOS = random(t_JnNUOS, n, 1);
end

if Jr_sigmaNUOS == 0
Jr_NUOS = Jr_muNUOS;
else pd_JrNUOS = makedist('Normal', 'mu', Jr_muNUOS, 'sigma', Jr_sigmaNUOS);
t_JrNUOS = truncate(pd_JrNUOS, Jr_LLNUOS, Jr_ULNUOS);
Jr_NUOS = random(t_JrNUOS, n, 1);
end

if Ja_sigmaNUOS == 0
Ja_NUOS = Ja_muNUOS;
else pd_JaNUOS = makedist('Normal', 'mu', Ja_muNUOS, 'sigma', Ja_sigmaNUOS);
t_JaNUOS = truncate(pd_JaNUOS, Ja_LLNUOS, Ja_ULNUOS);
Ja_NUOS = random(t_JaNUOS, n, 1);
end

if Jw_sigmaNUOS == 0
Jw_NUOS = Jw_muNUOS;
else pd_JwNUOS = makedist('Normal', 'mu', Jw_muNUOS, 'sigma', Jw_sigmaNUOS);
t_JwNUOS = truncate(pd_JwNUOS, Jw_LLNUOS, Jw_ULNUOS);
Jw_NUOS = random(t_JwNUOS, n, 1);
end

if SRF_sigmaNUOS == 0
SRF_NUOS = SRF_muNUOS;
else pd_SRFNUOS = makedist('Normal', 'mu', SRF_muNUOS, 'sigma',
SRF_sigmaNUOS);
t_SRFNUOS = truncate(pd_SRFNUOS, SRF_LLNUOS, SRF_ULNUOS);
SRF_NUOS = random(t_SRFNUOS, n, 1);
end
% -----

```

```

% Statistical analysis of Q input parameter based on assumed distribution
% and UL and LL truncation limits for NJHP.

```

```

% -----
if RQD_sigmaNJHP == 0
    RQD_NJHP = RQD_muNJHP;
else pd_RQDNJHP = makedist('Normal', 'mu', RQD_muNJHP, 'sigma',
RQD_sigmaNJHP);
    t_RQDNJHP = truncate(pd_RQDNJHP, RQD_LLJHP, RQD_ULJHP);
    RQD_NJHP = random(t_RQDNJHP, n, 1);
end

if Jn_sigmaNJHP == 0
    Jn_NJHP = Jn_muNJHP;
else pd_JnNJHP = makedist('Normal', 'mu', Jn_muNJHP, 'sigma', Jn_sigmaNJHP);
    t_JnNJHP = truncate(pd_JnNJHP, Jn_LLJHP, Jn_ULJHP);
    Jn_NJHP = random(t_JnNJHP, n, 1);
end

if Jr_sigmaNJHP == 0
    Jr_NJHP = Jr_muNJHP;
else pd_JrNJHP = makedist('Normal', 'mu', Jr_muNJHP, 'sigma', Jr_sigmaNJHP);
    t_JrNJHP = truncate(pd_JrNJHP, Jr_LLJHP, Jr_ULJHP);
    Jr_NJHP = random(t_JrNJHP, n, 1);
end

if Ja_sigmaNJHP == 0
    Ja_NJHP = Ja_muNJHP;
else pd_JaNJHP = makedist('Normal', 'mu', Ja_muNJHP, 'sigma', Ja_sigmaNJHP);
    t_JaNJHP = truncate(pd_JaNJHP, Ja_LLJHP, Ja_ULJHP);
    Ja_NJHP = random(t_JaNJHP, n, 1);
end

pd_JwNJHP = makedist('Triangular','a', Jw_aNJHP,'b', Jw_bNJHP,'c',Jw_cNJHP);
t_JwNJHP = truncate(pd_JwNJHP,0.66,1);
Jw_NJHP = random(t_JwNJHP, n, 1);

pd_SRFNJHP = makedist('Triangular','a', SRF_aNJHP,'b', SRF_bNJHP,'c',SRF_cNJHP);
t_SRFNJHP = truncate(pd_SRFNJHP,2.5,10);
SRF_NJHP = random(t_SRFNJHP, n, 1);
% -----

% Monte Carlo simulation of Q for NUOS and calculation
% to determine Qμ, QLB, and QUB.
% -----
QPNUOS = (RQD_NUOS./Jn_NUOS).*(Jr_NUOS./Ja_NUOS);
QNUOS = QPNUOS.*(Jw_NUOS./SRF_NUOS);
QNUOSmu = mean(QNUOS);
QNUOSSigma = sqrt(var(QNUOS));

```

```

QNUOSUB = QNUOSmu + QNUOSsigma;
if QNUOSmu - QNUOSsigma > 0.001;
    QNUOSLB = QNUOSmu - QNUOSsigma;
else
    QNUOSLB = 0.001;
end
% -----

% Monte Carlo simulation of Q for NJHP and calculation
% to determine Q $\mu$ , QLB, and QUB.
% -----
QPNJHP = (RQD_NJHP./Jn_NJHP).*(Jr_NJHP./Ja_NJHP);
QNJHP = QPNJHP.*(Jw_NJHP./SRF_NJHP);
QNJHPmu = mean(QNJHP);
QNJHPsigma = sqrt(var(QNJHP));
QNJHPUB = QNJHPmu + QNJHPsigma;
if QNJHPmu - QNJHPsigma > 0.001;
    QNJHPLB = QNJHPmu - QNJHPsigma;
else
    QNJHPLB = 0.001;
end
% -----

% Histograms for statistical analysis of Q input parameters for NUOS.
% -----
figure(1)
histogram(RQD_NUOS,'FaceColor','w');
hold on;
set(gca,'FontSize',16);
xlabel('RQD','FontSize',16);
ylabel('Frequency','FontSize',16);

figure(2)
histogram(Jn_NUOS,'FaceColor','w');
set(gca,'FontSize',16);
xlabel('J_n','FontSize',16);
ylabel('Frequency','FontSize',16);

figure(3)
histogram(Jr_NUOS,'FaceColor','w');
set(gca,'FontSize',16);
xlabel('J_r','FontSize',16);
ylabel('Frequency','FontSize',16);

figure(4)
histogram(Ja_NUOS,'FaceColor','w');

```

```

set(gca,'FontSize',16);
xlabel('J_a','FontSize',16);
ylabel('Frequency','FontSize',16);

figure(5)
histogram(Jw_NUOS,'FaceColor','w');
set(gca,'FontSize',16);
xlabel('J_w','FontSize',16);
ylabel('Frequency','FontSize',16);

figure(6)
histogram(SRF_NUOS,'FaceColor','w');
set(gca,'FontSize',16);
xlabel('SRF','FontSize',16);
ylabel('Frequency','FontSize',16);
%-----

% PDF and CDF of Q from MCS of NUOS with point estimate values.
%-----
figure(7)
% Setting the color of both the left and right y-axis to black
left_color = [0 0 0];
right_color = [0 0 0];
set(figure(7),'defaultAxesColorOrder',[left_color; right_color]);
set(gca,'FontSize',14);

% Shading rock classification areas
hold on;
fill([0.1,1,1,0.1],[0,0,0.5,0.5],'r','FaceAlpha',0.3);
hold on;
fill([1,4,4,1],[0,0,0.5,0.5],'b','FaceAlpha',0.3);
hold on;
fill([4,10,10,4],[0,0,0.5,0.5],'y','FaceAlpha',0.3);
hold on;
fill([10,40,40,10],[0,0,0.5,0.5],'g','FaceAlpha',0.3);

% Developing the PDF curve for the Q-values
hold on;
pd = fitdist(QNUOS,'Lognormal');
x_values = 0:0.1:40;
y = pdf(pd,x_values);
plot(x_values,y,'LineWidth',2,'Color','k');
hold on;

% Labels for left axis and x-axis
xlabel('Q');

```

```

ylabel('PDF');

% Sets CDF and Statistical Value lines to second y-axis
yyaxis right;

% Developing CDF curve
hold on;
h = cdfplot(QNUOS);
set(h, 'LineWidth', 2, 'Color', 'b');

% Developing lines marking mu +/- sigma
hold on;
plot([QNUOSmu QNUOSmu],[0 1],':','Color','r','LineWidth',2)
hold on;
plot([QNUOSLB QNUOSLB],[0 1], '--','Color','r','LineWidth',2)
hold on;
plot([QNUOSUB QNUOSUB],[0 1], '--','Color','r','LineWidth',2)

% Setting right axis limits.
hold on;
axis([0 40 0 1]);
xlabel('Q', 'Color', 'k');
ylabel('CDF', 'Color', 'k');

% Label point estimate values
hold on;
strQNUOSmu = ['Q_μ = ' num2str(QNUOSmu)];
text(QNUOSmu,0.5,strQNUOSmu,'fontsize',12,'BackgroundColor','w');
hold on;
strQNUOSlb = ['Q_L_B = ' num2str(QNUOSLB)];
text(QNUOSLB,0.75,strQNUOSlb,'fontsize',12,'BackgroundColor','w');
hold on;
strQNUOSub = ['Q_U_B = ' num2str(QNUOSUB)];
text(QNUOSUB,0.25,strQNUOSub,'fontsize',12,'BackgroundColor','w');
% -----

% Histograms for statistical analysis of Q input parameters for NJHP.
% -----
figure(8)
histogram(RQD_NJHP,'FaceColor','w');
set(gca,'FontSize',16);
xlabel('RQD','FontSize',16);
ylabel('Frequency','FontSize',16);

figure(9)
histogram(Jn_NJHP,'FaceColor','w');

```

```

set(gca,'FontSize',16);
xlabel('J_n','FontSize',16);
ylabel('Frequency','FontSize',16);

```

```

figure(10)
histogram(Jr_NJHP,'FaceColor','w');
set(gca,'FontSize',16);
xlabel('J_r','FontSize',16);
ylabel('Frequency','FontSize',16);

```

```

figure(11)
histogram(Ja_NJHP,'FaceColor','w');
set(gca,'FontSize',16);
xlabel('J_a','FontSize',16);
ylabel('Frequency','FontSize',16);

```

```

figure(12)
histogram(Jw_NJHP,'FaceColor','w');
set(gca,'FontSize',16);
xlabel('J_w','FontSize',16);
ylabel('Frequency','FontSize',16);

```

```

figure(13)
histogram(SRF_NJHP,'FaceColor','w');
set(gca,'FontSize',16);
xlabel('SRF','FontSize',16);
ylabel('Frequency','FontSize',16);
%-----

```

```

% PDF and CDF of Q from MCS of NJHP with point estimate values.
%-----

```

```

figure(14)
% Setting the color of both the left and right y-axis to black
left_color = [0 0 0];
right_color = [0 0 0];
set(figure(14),'defaultAxesColorOrder',[left_color; right_color]);
set(gca,'FontSize',14);

```

```

% Shading rock classification areas
hold on;
fill([0.1,1,1,0.1],[0,0,0.5,0.5],'r','FaceAlpha',0.3);
hold on;
fill([1,4,4,1],[0,0,0.5,0.5],'b','FaceAlpha',0.3);
hold on;
fill([4,10,10,4],[0,0,0.5,0.5],'y','FaceAlpha',0.3);
hold on;

```

```

fill([10,40,40,10],[0,0,0.5,0.5],'g','FaceAlpha',0.3);

% Developing the PDF curve for the Q-values
hold on;
pd = fitdist(QNJHP,'Lognormal');
x_values = 0:0.1:40;
y = pdf(pd,x_values);
plot(x_values,y,'LineWidth',2,'Color','k');
hold on;

% Labels for left axis and x-axis
xlabel('Q');
ylabel('PDF');

% Sets CDF and Statistical Value lines to second y-axis
yyaxis right;

% Developing CDF curve
hold on;
h = cdfplot(QNJHP);
set(h,'LineWidth',2,'Color','b');

% Developing lines marking mu +/- sigma
hold on;
plot([QNJHPmu QNJHPmu],[0 1],':','Color','r','LineWidth',2)
hold on;
plot([QNJHPLB QNJHPLB],[0 1],'-','Color','r','LineWidth',2)
hold on;
plot([QNJHPUB QNJHPUB],[0 1],'-','Color','r','LineWidth',2)

% Settinng right axis limits.
hold on;
axis([0 40 0 1]);
xlabel('Q', 'Color', 'k');
ylabel('CDF', 'Color', 'k');

% Label point estimate values
hold on;
strQNJHPLB = ['Q_μ = ' num2str(QNJHPmu)];
text(QNJHPmu,0.5,strQNJHPLB,'fontsize',12,'BackgroundColor','w');
hold on;
strQNJHPLb = ['Q_L_B = ' num2str(QNJHPLB)];
text(QNJHPLB,0.75,strQNJHPLb,'fontsize',12,'BackgroundColor','w');
hold on;
strQNJHPub = ['Q_U_B = ' num2str(QNJHPUB)];
text(QNJHPUB,0.25,strQNJHPub,'fontsize',12,'BackgroundColor','w');

```



```

% -----
% NUOS PDF with QLB and  $Q\mu$ 
% -----
figure(15)
% Setting the color of both the left and right y-axis to black
left_color = [0 0 0];
right_color = [0 0 0];
set(figure(15),'defaultAxesColorOrder',[left_color; right_color]);
set(gca,'FontSize',12);

% Shading rock classification areas
hold on;
fill([0.1,1,1,0.1],[0,0,0.5,0.5],'r','FaceAlpha',0.3);
hold on;
fill([1,4,4,1],[0,0,0.5,0.5],'b','FaceAlpha',0.3);
hold on;
fill([4,10,10,4],[0,0,0.5,0.5],'y','FaceAlpha',0.3);
hold on;
fill([10,40,40,10],[0,0,0.5,0.5],'g','FaceAlpha',0.3);

% Developing the PDF curve for the NUOS Q-values
hold on;
pdNUOS = fitdist(QNUOS,'Lognormal');
x_valuesNUOS = 0:0.1:40;
yNUOS = pdf(pdNUOS,x_valuesNUOS);
plot(x_valuesNUOS,yNUOS,'LineWidth',2,'Color','k');

% Developing lines marking  $\mu \pm \sigma$ 
hold on;
plot([QNUOSmu QNUOSmu],[0 0.5],':','Color','r','LineWidth',4)
hold on;
plot([QNUOSLB QNUOSLB],[0 0.5], '--','Color','r','LineWidth',4)

% Labels for left axis and x-axis
xlabel('Q');
ylabel('PDF');

strQNUOSMU = ['Q_μ = ' num2str(QNUOSmu)];
strQNJHPLB = ['Q_L_B = ' num2str(QNUOSLB)];
text(QNUOSmu,0.45,strQNUOSMU,'fontsize',12,'BackgroundColor','w');
text(QNUOSLB,0.35,strQNJHPLB,'fontsize',12,'BackgroundColor','w');
% -----

% NJHP PDF with QLB and  $Q\mu$ 
% -----

```

```

figure(16)
% Setting the color of both the left and right y-axis to black
left_color = [0 0 0];
right_color = [0 0 0];
set(figure(16),'defaultAxesColorOrder',[left_color; right_color]);
set(gca,'FontSize',12);

% Shading rock classification areas
hold on;
fill([0.1,1,1,0.1],[0,0,0.5,0.5],'r','FaceAlpha',0.3);
hold on;
fill([1,4,4,1],[0,0,0.5,0.5],'b','FaceAlpha',0.3);
hold on;
fill([4,10,10,4],[0,0,0.5,0.5],'y','FaceAlpha',0.3);
hold on;
fill([10,40,40,10],[0,0,0.5,0.5],'g','FaceAlpha',0.3);

% Developing the PDF curve for the NJHP Q-values
hold on;
pdNJHP = fitdist(QNJHP,'Lognormal');
x_valuesNJHP = 0:0.1:40;
yNJHP = pdf(pdNJHP,x_valuesNJHP);
plot(x_valuesNJHP,yNJHP,'LineWidth',2,'Color','b');

% Developing lines marking LB
hold on;
plot([QNJHPmu QNJHPmu],[0 0.5],':','Color','r','LineWidth',4)
hold on;
plot([QNJHPLB QNJHPLB],[0 0.5], '--','Color','r','LineWidth',4)

% Labels for left axis and x-axis
xlabel('Q');
ylabel('PDF');

strQNJHPLB = ['Q_L_B = ' num2str(QNJHPLB)];
strQNJHPmu = ['Q_μ = ' num2str(QNJHPmu)];
text(QNJHPmu,0.45,strQNJHPmu,'fontsize',12,'BackgroundColor','w');
text(QNJHPLB,0.35,strQNJHPLB,'fontsize',12,'BackgroundColor','w');
% -----

% Data Dump NUOS
% -----
filename = 'QNUOS_data_dump1.xlsx';
xlswrite(filename,RQD_NUOS,1,'A1:A100000');
xlswrite(filename,Jn_NUOS,1,'B1:B100000');
xlswrite(filename,Jr_NUOS,1,'C1:C100000');

```

```
xlswrite(filename,Ja_NUOS,1,'D1:D100000');
xlswrite(filename,Jw_NUOS,1,'E1:E100000');
xlswrite(filename,SRF_NUOS,1,'F1:F100000');
xlswrite(filename,QNUOS,1,'G1:G100000');
% -----
```

```
% Data Dump NJHP
```

```
% -----
filename = 'QNJHP_data_dump1.xlsx';
xlswrite(filename,RQD_NJHP,1,'A1:A100000');
xlswrite(filename,Jn_NJHP,1,'B1:B100000');
xlswrite(filename,Jr_NJHP,1,'C1:C100000');
xlswrite(filename,Ja_NJHP,1,'D1:D100000');
xlswrite(filename,Jw_NJHP,1,'E1:E100000');
xlswrite(filename,SRF_NJHP,1,'F1:F100000');
xlswrite(filename,QNJHP,1,'G1:G100000');
```